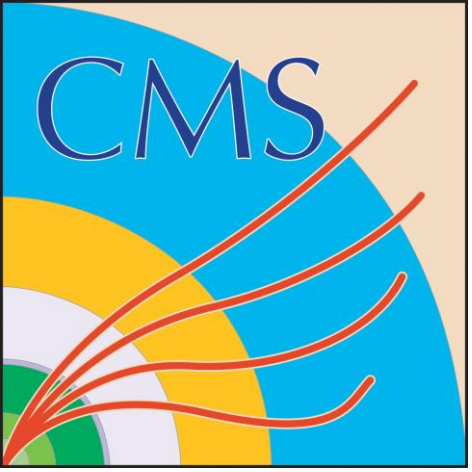

UC SANTA BARBARA

Probing BSM with the Higgs boson width

Ulascan Sarica
on behalf of
the CMS Collaboration

LPCC Seminar
30.11.2021

Width and lifetime

The ***width*** $\boldsymbol{\Gamma}$ of a particle quantifies how fast the particle decays into others:
= Simply a sum over the *partial widths* Γ_{dec} for each decay mode
→ *Branching ratio,* $\mathcal{B} = \Gamma_{\mathrm{dec}}/\Gamma$, is the proportion of each decay mode.

→ Stable particles: $\Gamma \to 0$.
→ Unstable particles: $\Gamma \gg 0$, many decay modes
Perhaps some involving BSM states!

e.g., Z bosons decay most of the time as $Z \to \ell\ell$, $Z \to \nu\nu$, $Z \to q\bar{q}$:

$\Gamma_{\mathrm{Z}\to\ell\ell} \approx 0.25$ GeV, $\Gamma_{\mathrm{Z}\to\nu\nu} \approx 0.50$ GeV, $\Gamma_{\mathrm{Z}\to q\bar{q}} \approx 1.74$ GeV
$\Rightarrow \Gamma_{\mathrm{Z}} \approx 2.5$ GeV

$\mathcal{B}(\mathrm{Z} \to \ell\ell) \approx 10\%$, $\mathcal{B}(\mathrm{Z} \to \nu\nu) \approx 20\%$, $\mathcal{B}(\mathrm{Z} \to q\bar{q}) \approx 70\%$

Width and lifetime

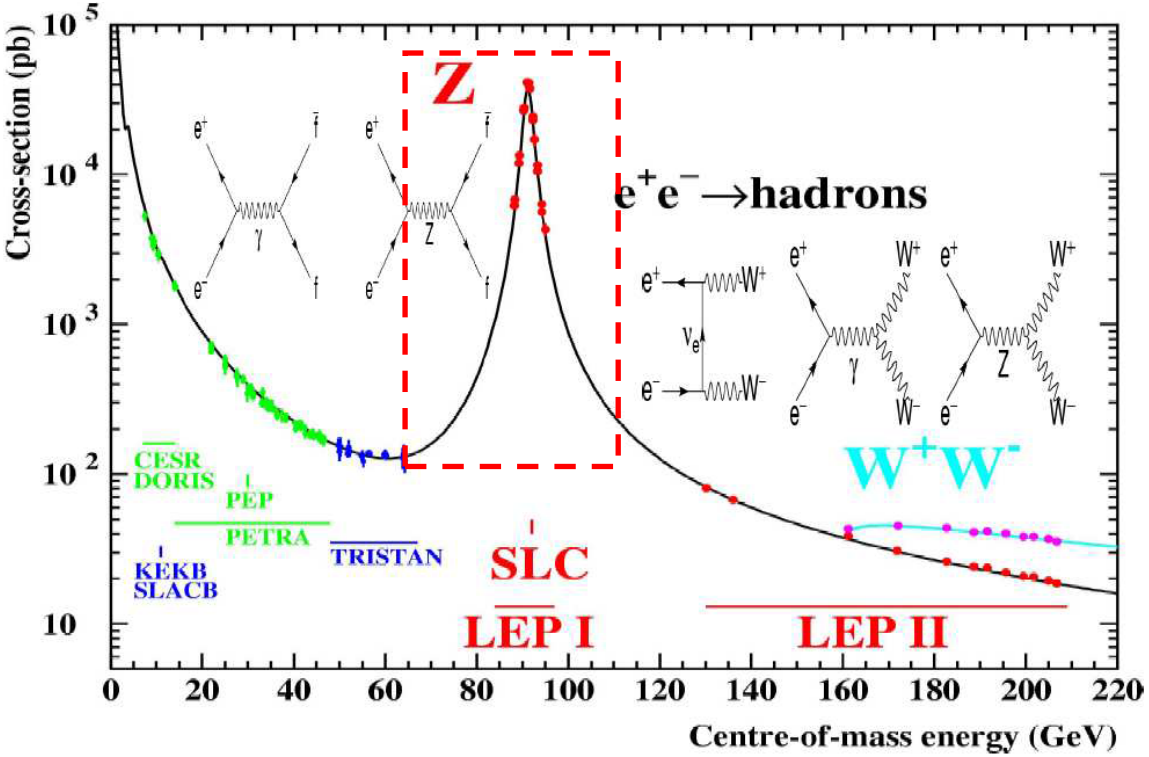

Inherent quantum mech. uncertainty on mass $\propto \Gamma$.

Resonance mass distribution usually describable with a relativistic Breit-Wigner distribution:

$$\frac{1}{(m_{obs}^2 - m^2)^2 + (m \times \Gamma)^2}$$

For the Z boson: 91 GeV 2.5 GeV

Width and lifetime

The ***lifetime*** $\boldsymbol{\tau}$ is related to Γ through the Heisenberg uncertainty principle: $\tau = \hbar/\Gamma$

"If you put a particle in a box, how long do you have to wait on average for it to decay?"

→ For the Z boson, you have to wait $\tau_Z \approx 6.58 \times 10^{-25}$ GeV.s /2.5 GeV $= 2.6 \times 10^{-25}$ s.

What affects the width?

Are there subdominant contributions to our current production and decay calculations we have not yet included?

Does this particle interact with known particles we cannot detect (e.g. neutrinos)?

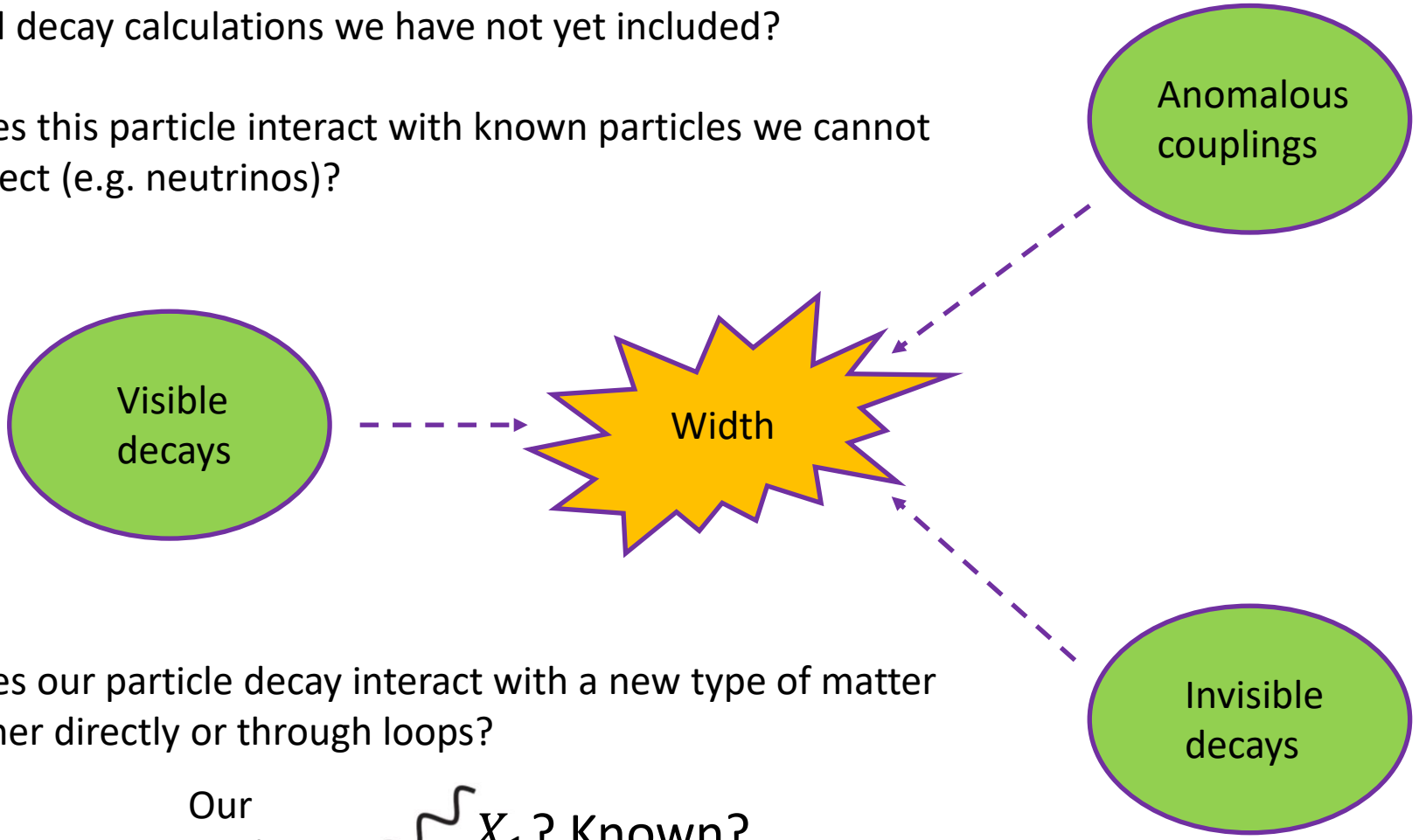

Does our particle decay interact with a new type of matter either directly or through loops?

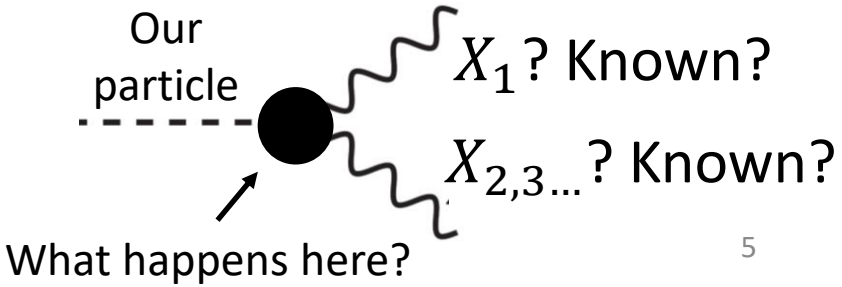

What affects the width?

Are there subdominant contributions to our current production and decay calculations we have not yet included?

Does this particle interact with known particles we cannot detect (e.g. neutrinos)?

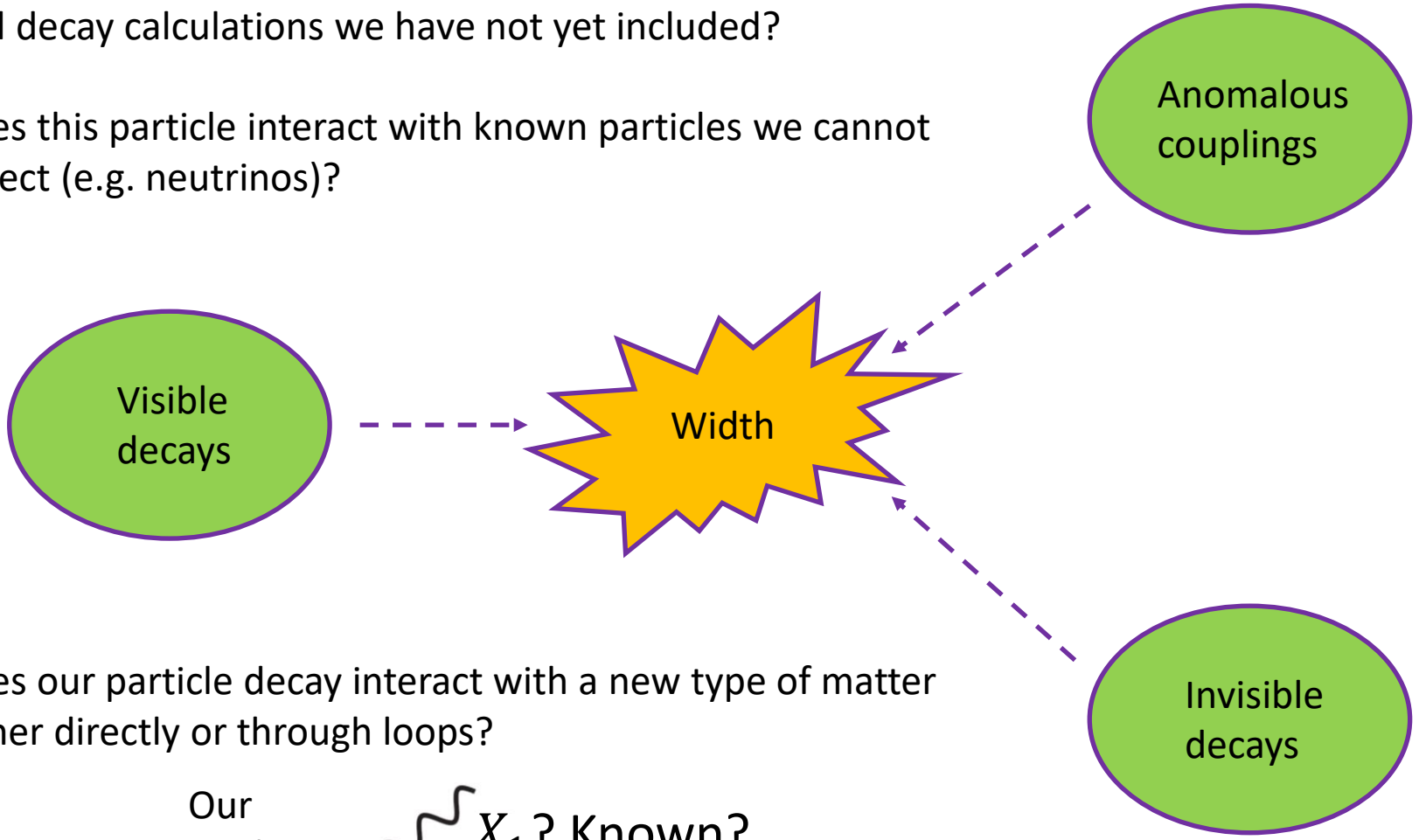

Does our particle decay interact with a new type of matter either directly or through loops?

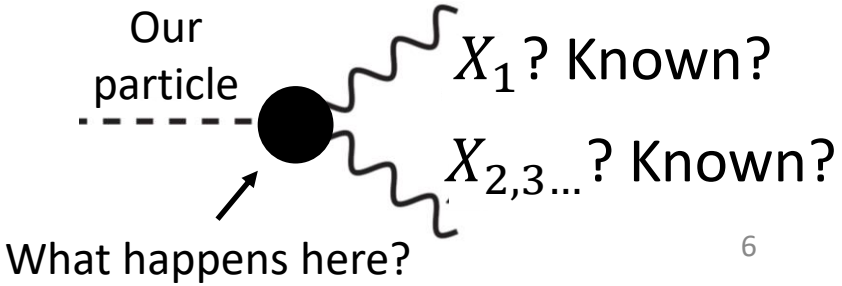

"So tell me... Which is the better story, the story with the animals or the story without animals?"

Pi Patel in *Life of Pi* by Yann Martel

The story of measuring the width...

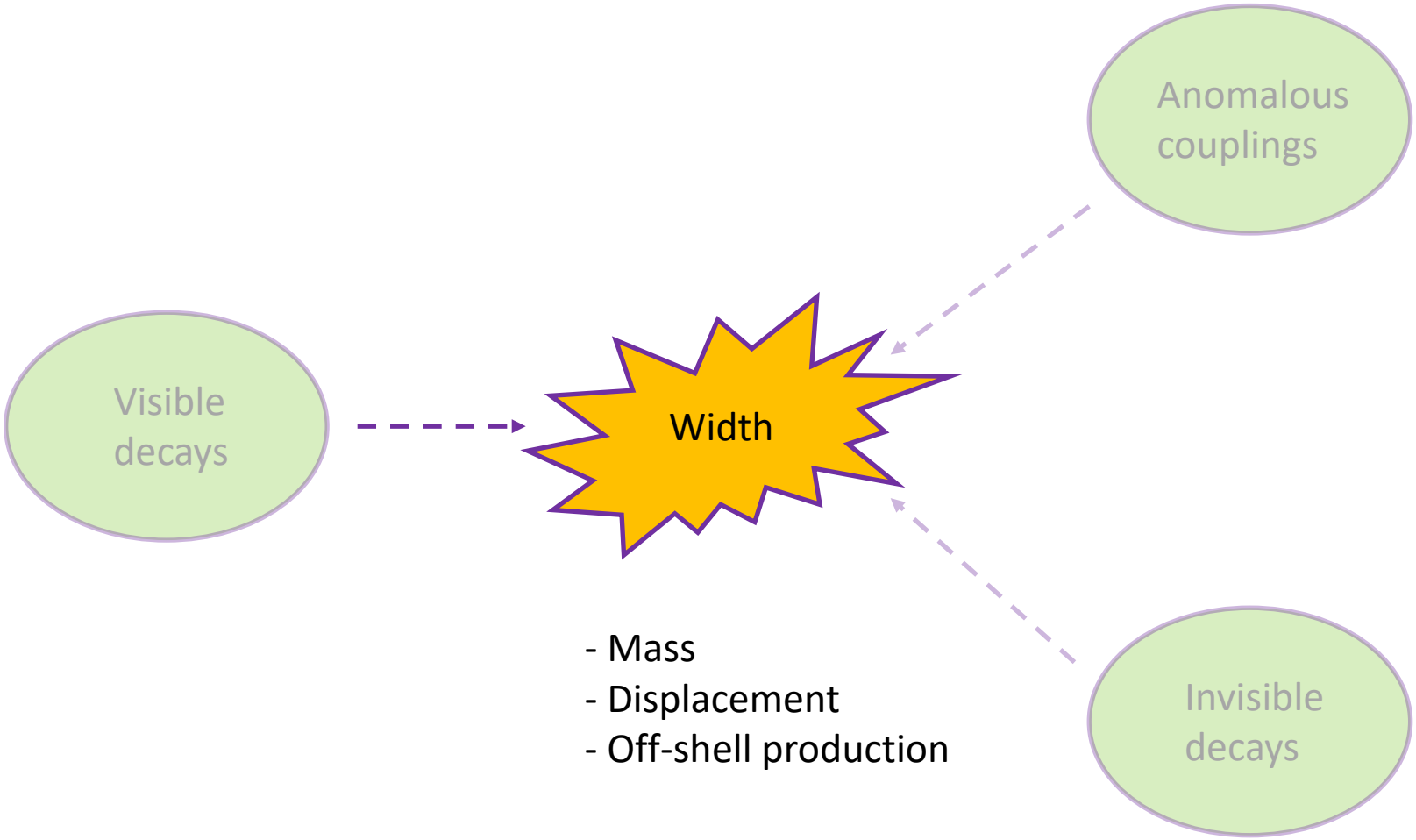

The story of measuring the width...

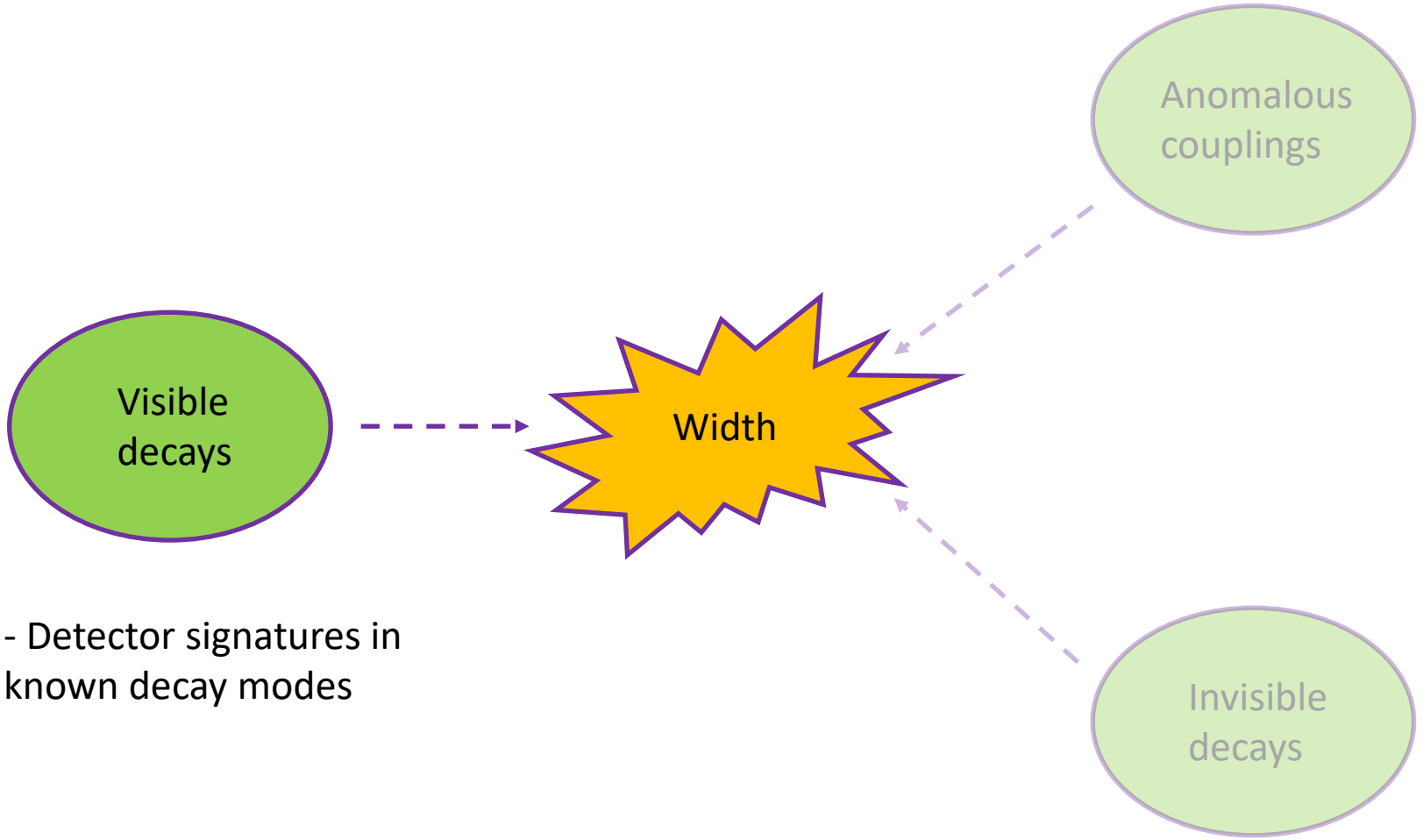

- Detector signatures in known decay modes

The story of measuring the width...

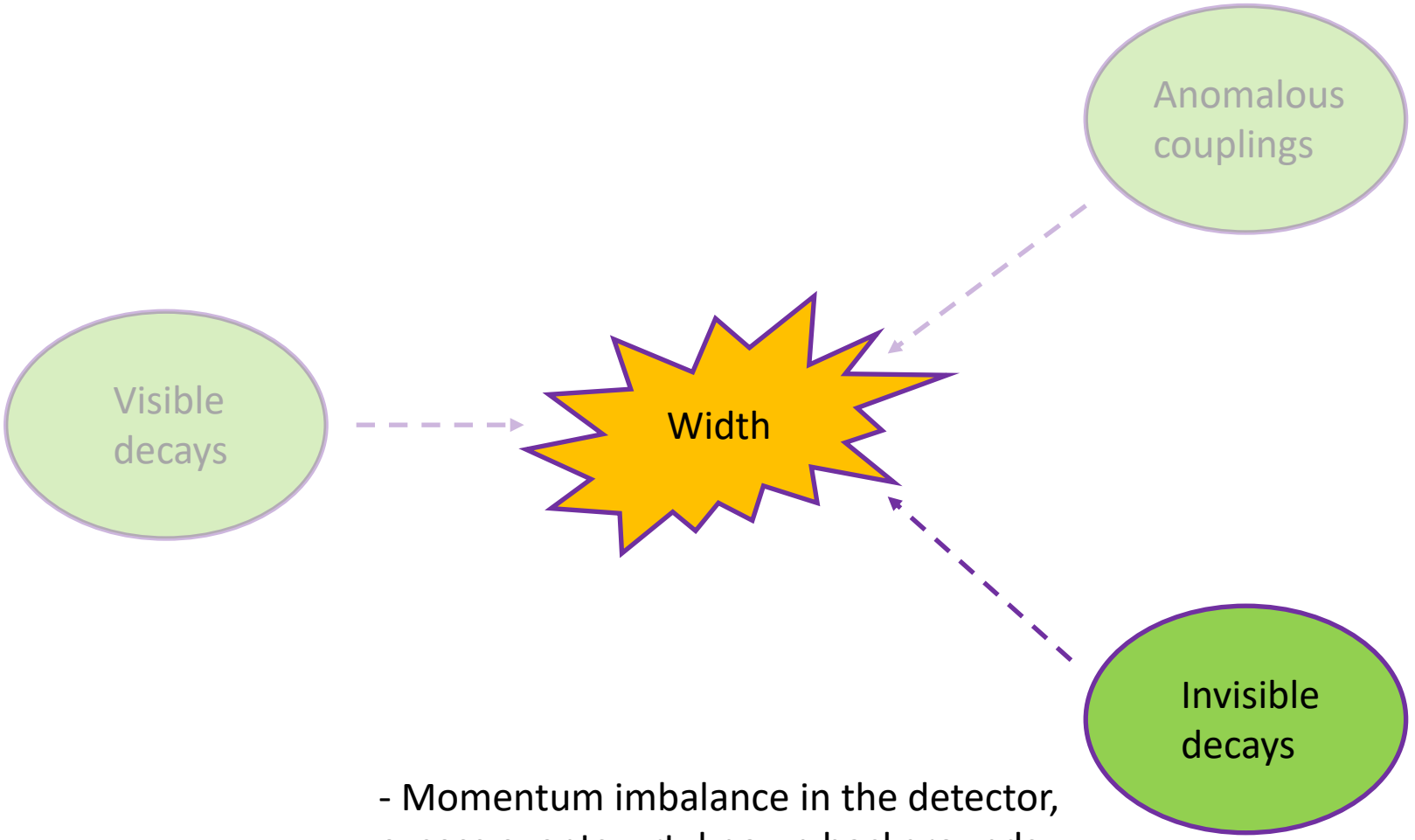

- Momentum imbalance in the detector, excess events wrt. known backgrounds

The story of measuring the width...

- Angular and mass observables
- Production and decay rate correlations

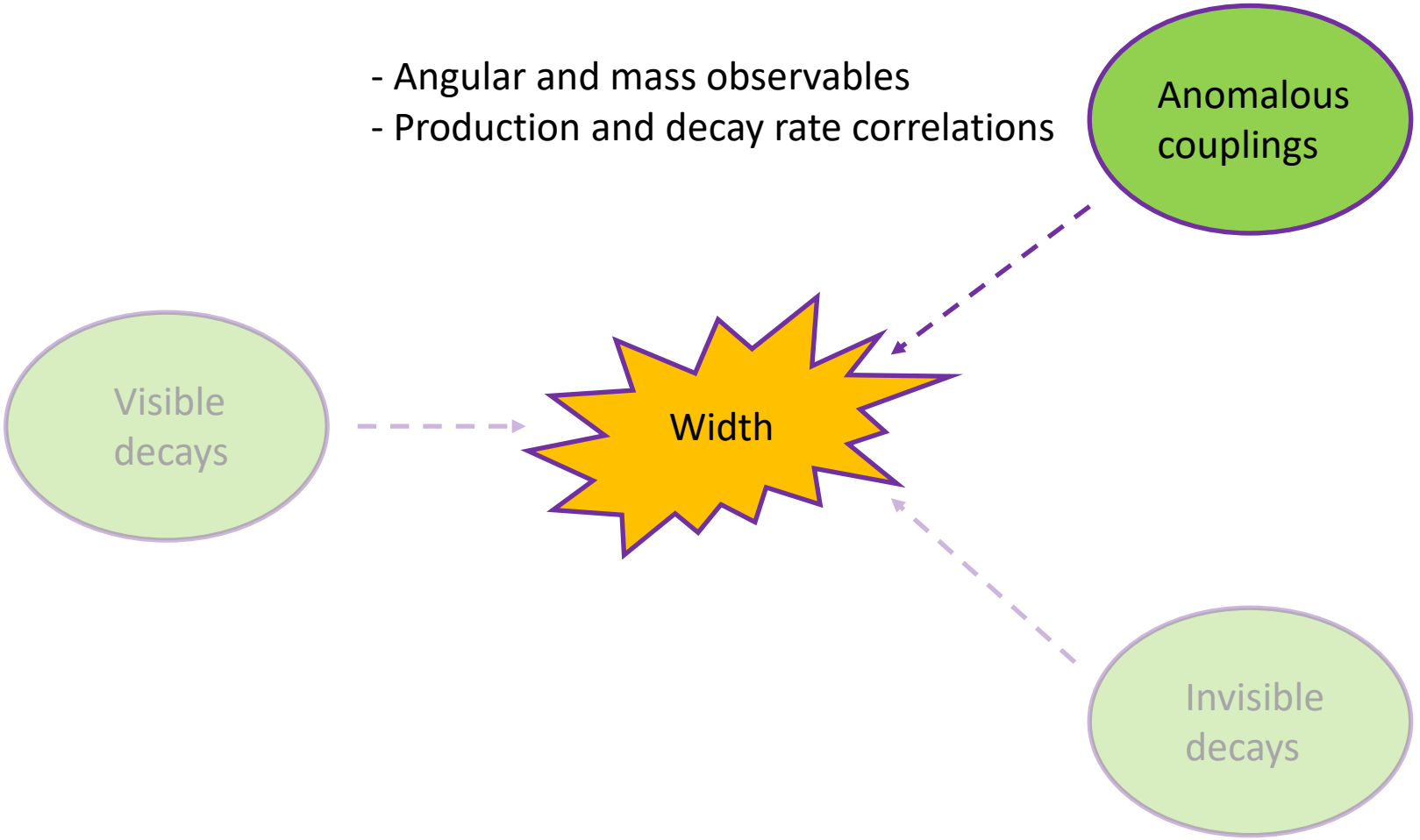

Putting the particle in a box:

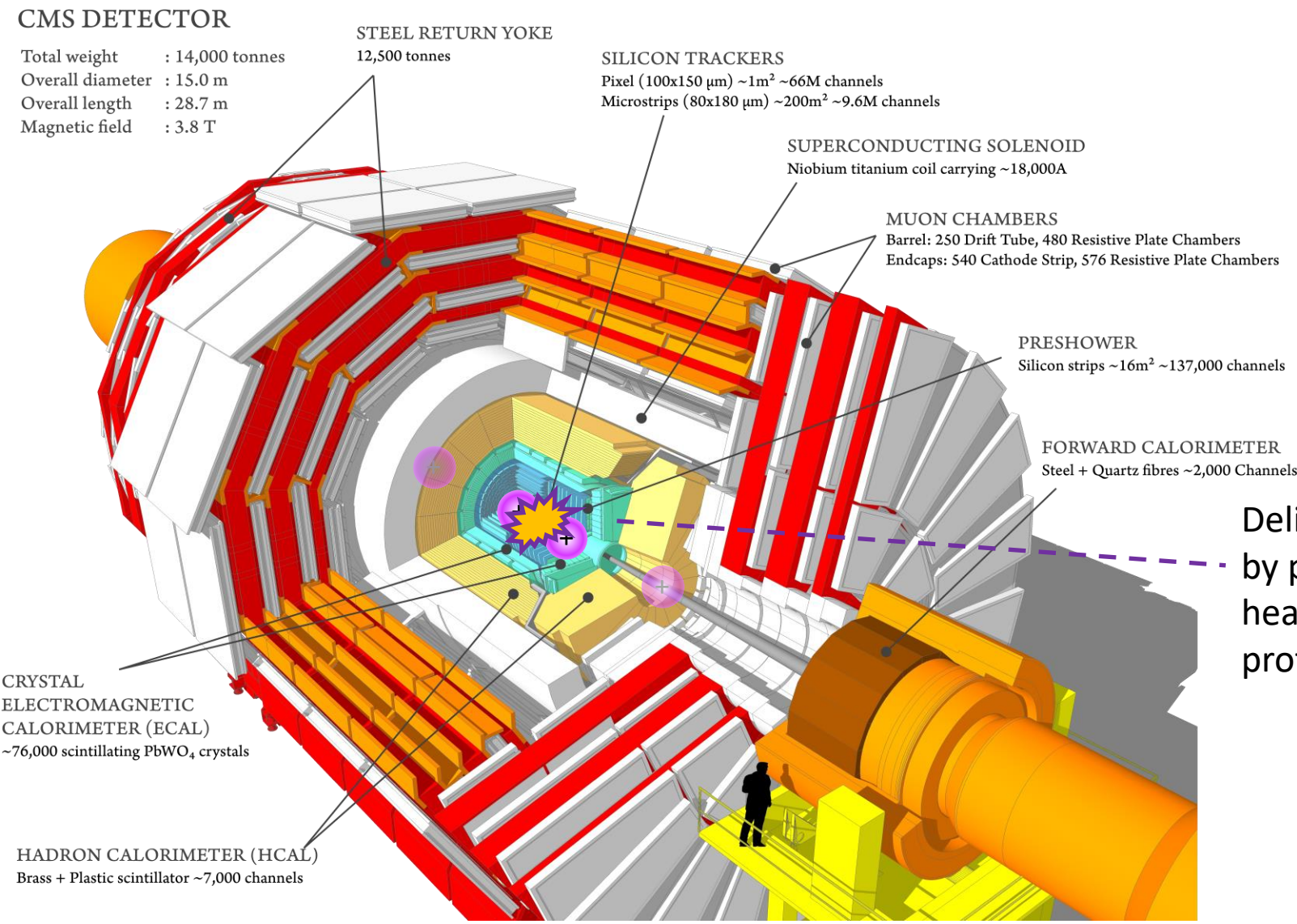

Deliver the particle by producing it via head-on proton-proton collisions

Putting the particle in a box:

Superconducting solenoid magnet at 3.8 T, helping to identify the charge and momentum of particles

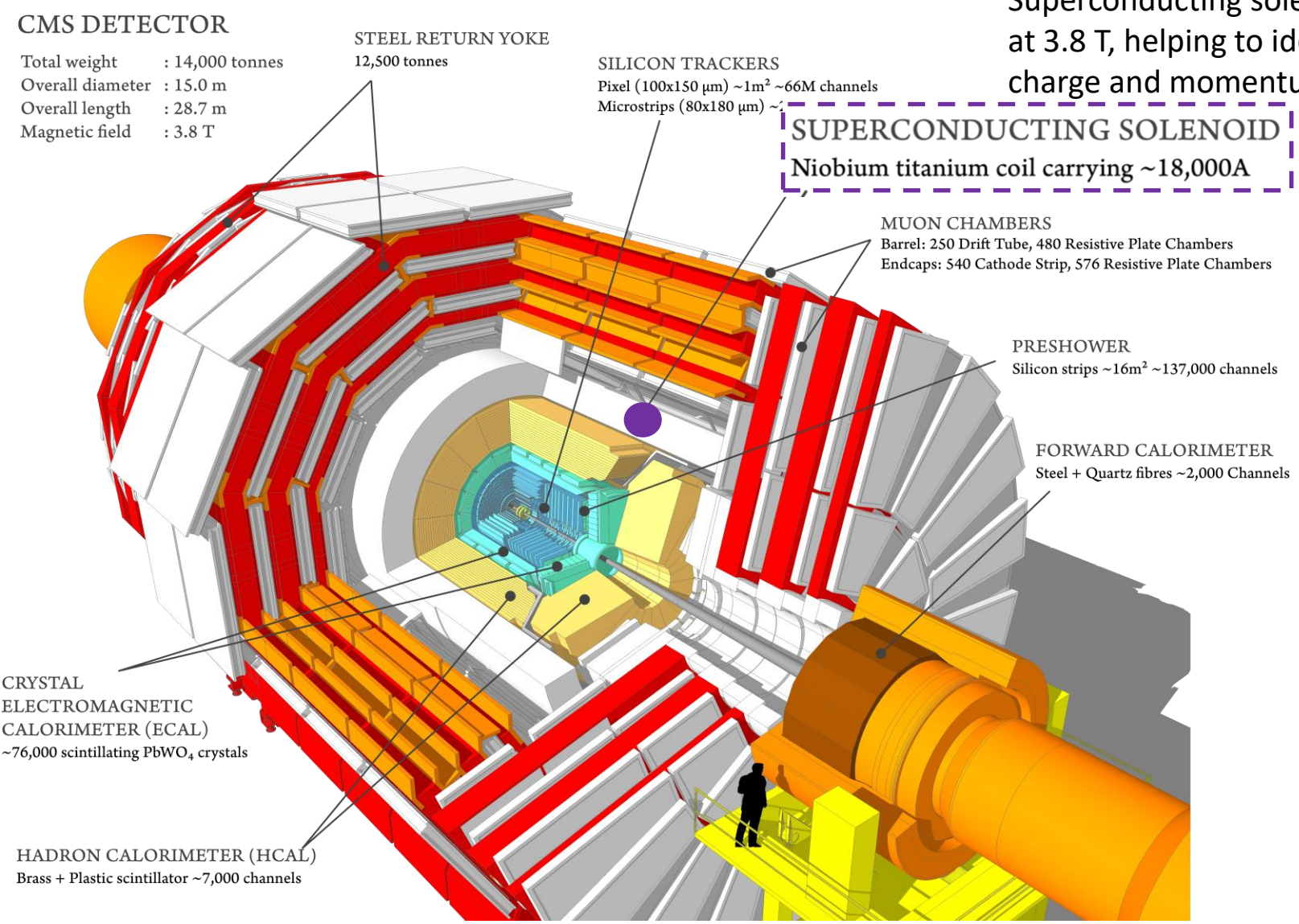

Putting the particle in a box:

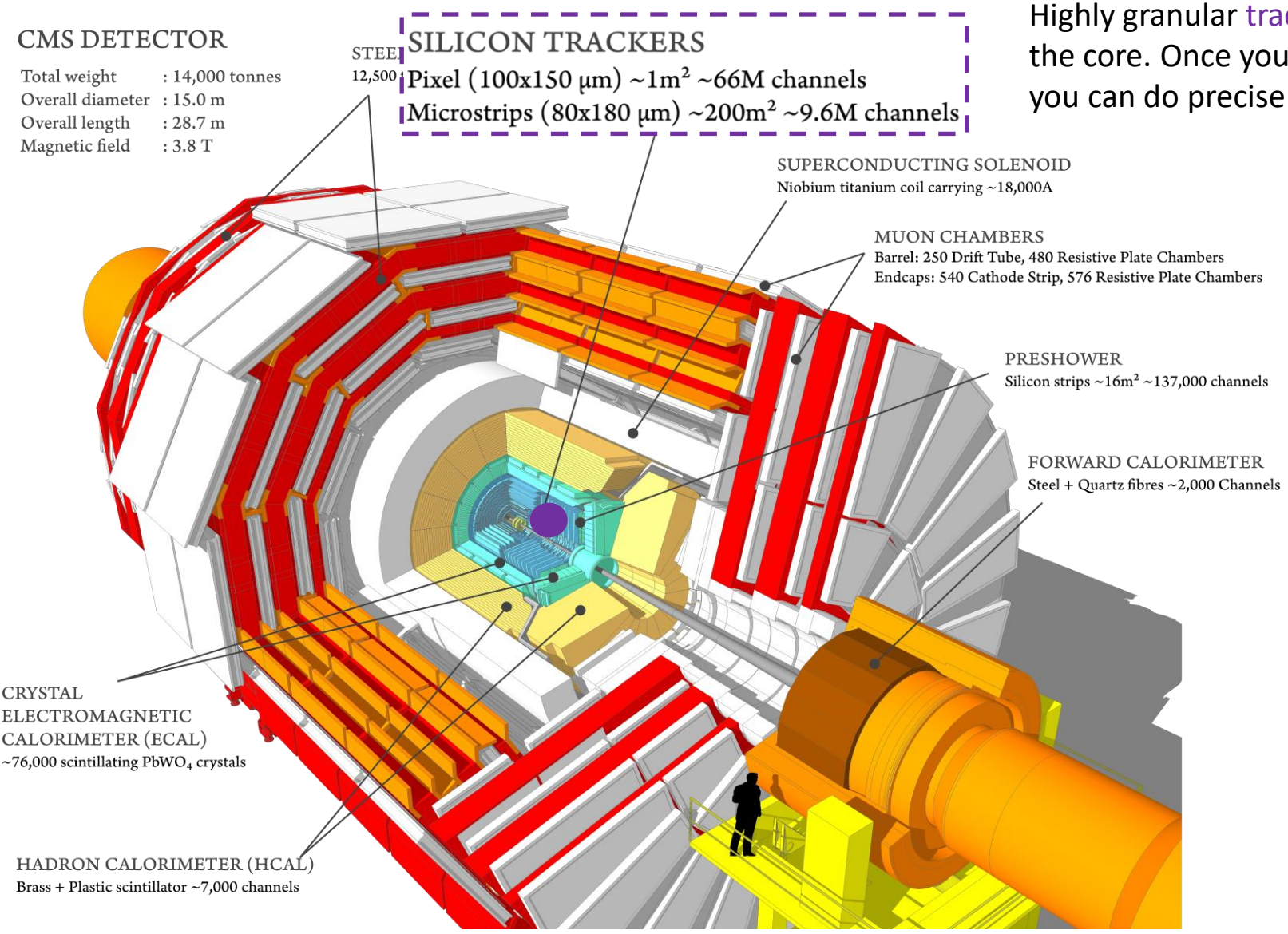

Highly granular tracking system at the core. Once you have tracks, you can do precise vertexing.

Putting the particle in a box:

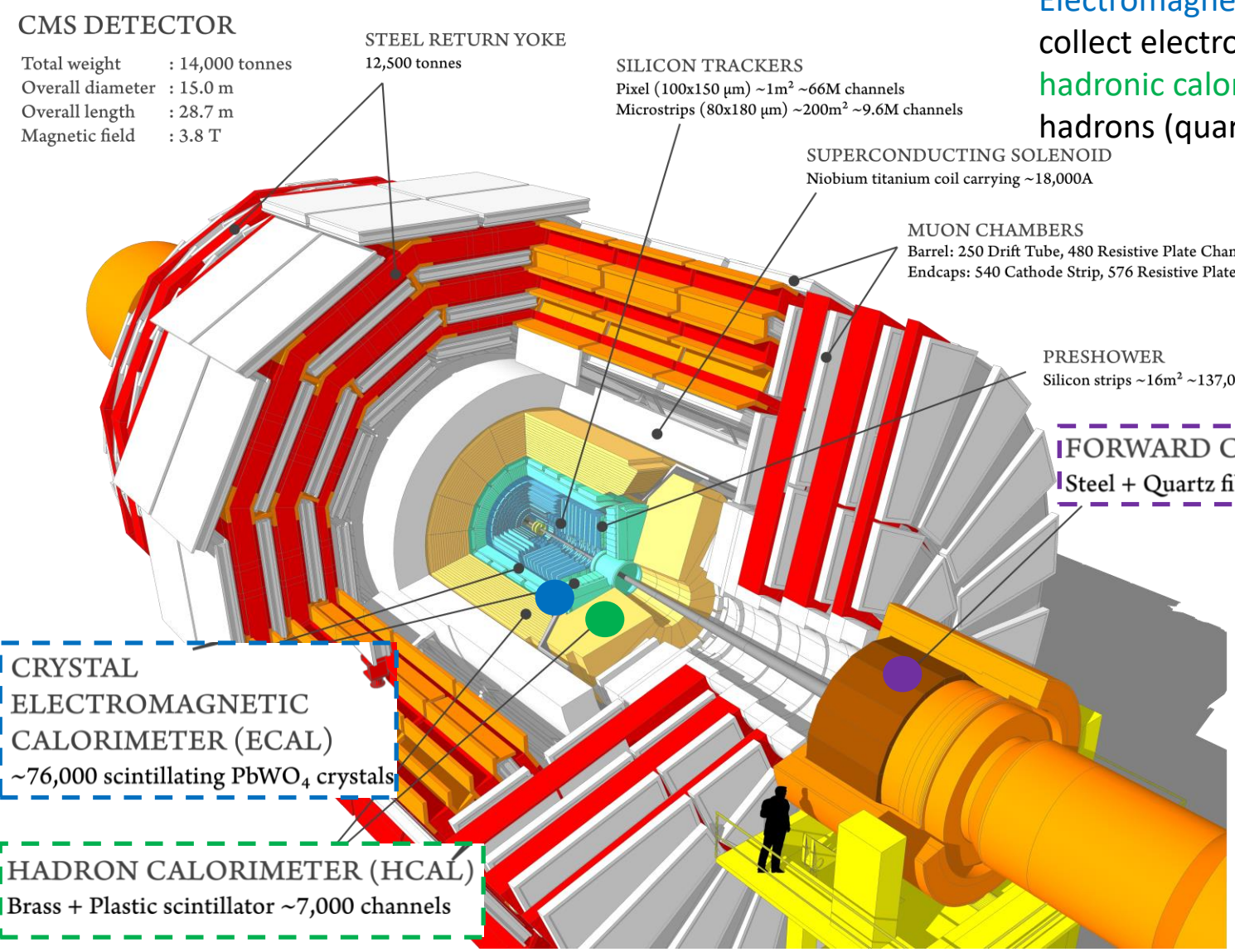

Electromagnetic calorimeter to collect electrons and photons, and hadronic calorimeter to collect hadrons (quarks and gluons)

Forward calorimeter increases detector reach, allows detection of forward jets

Putting the particle in a box:

A redundant system of muon chambers to collect muons, which otherwise traverses long distances without interacting.

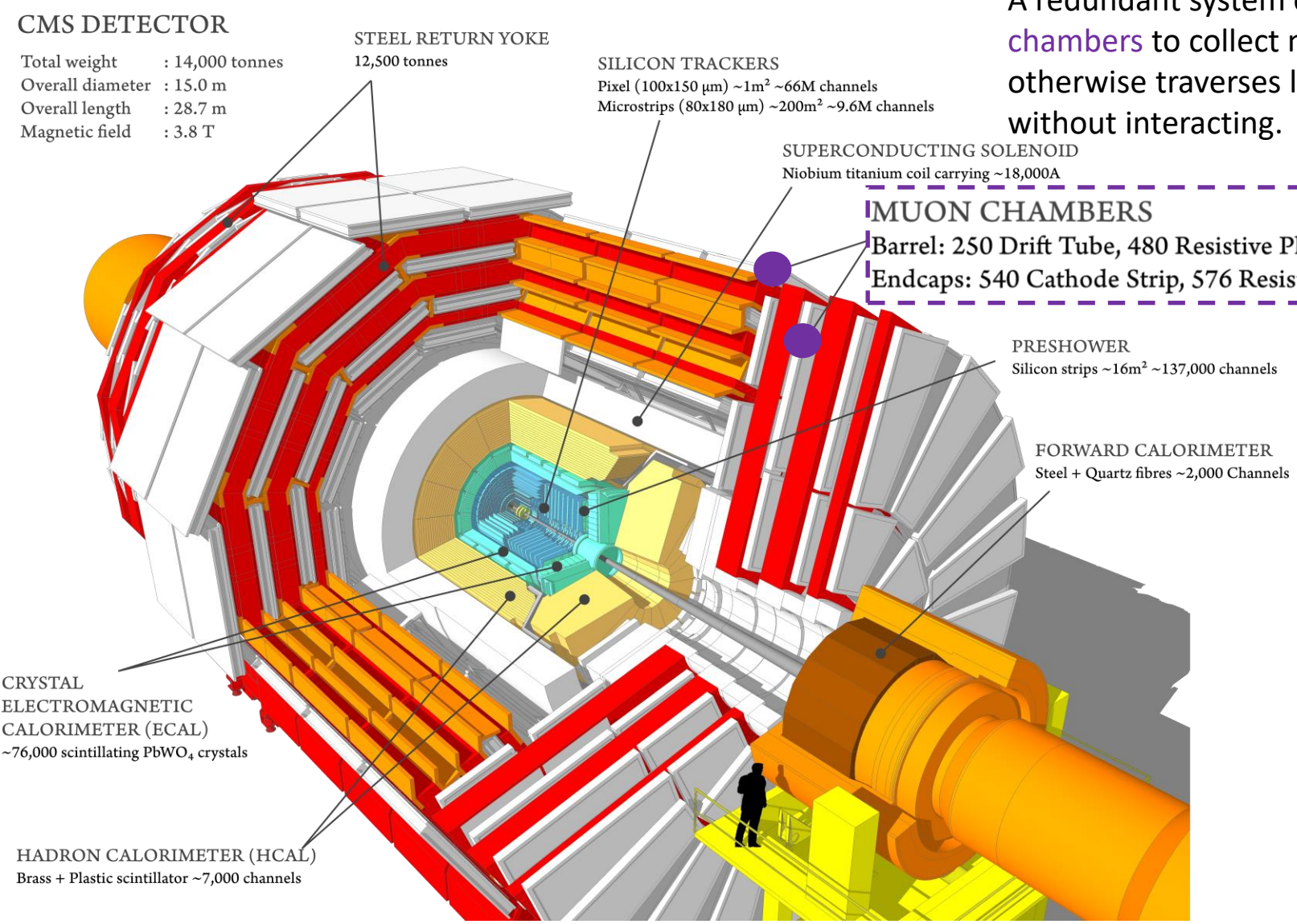

How to use this box effectively:

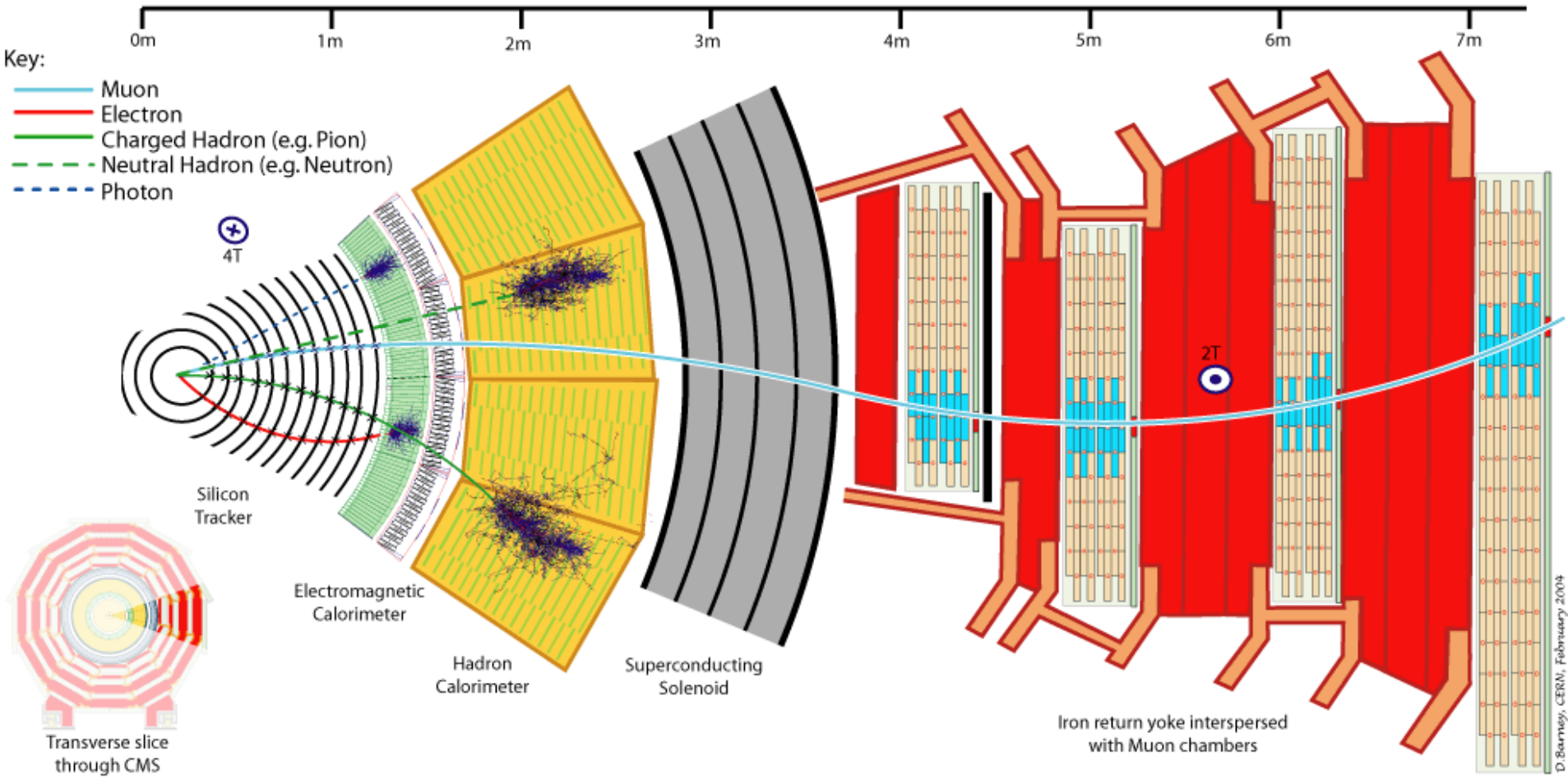

Use particle-flow algorithm [1,2,3]:

- Correlate basic detector info. from different layers to identify muons, electrons, photons, and charged and neutral hadrons

PF ID is the basis for particle identification before additional clustering or selection reqs.

How to use this box efficiently:

Detector is very efficient in reconstructing leptons.
→ Since several analyses we will mention use leptons, here are exemplary lepton selection efficiencies:

Muons: $\sim 85\% - 98\%$

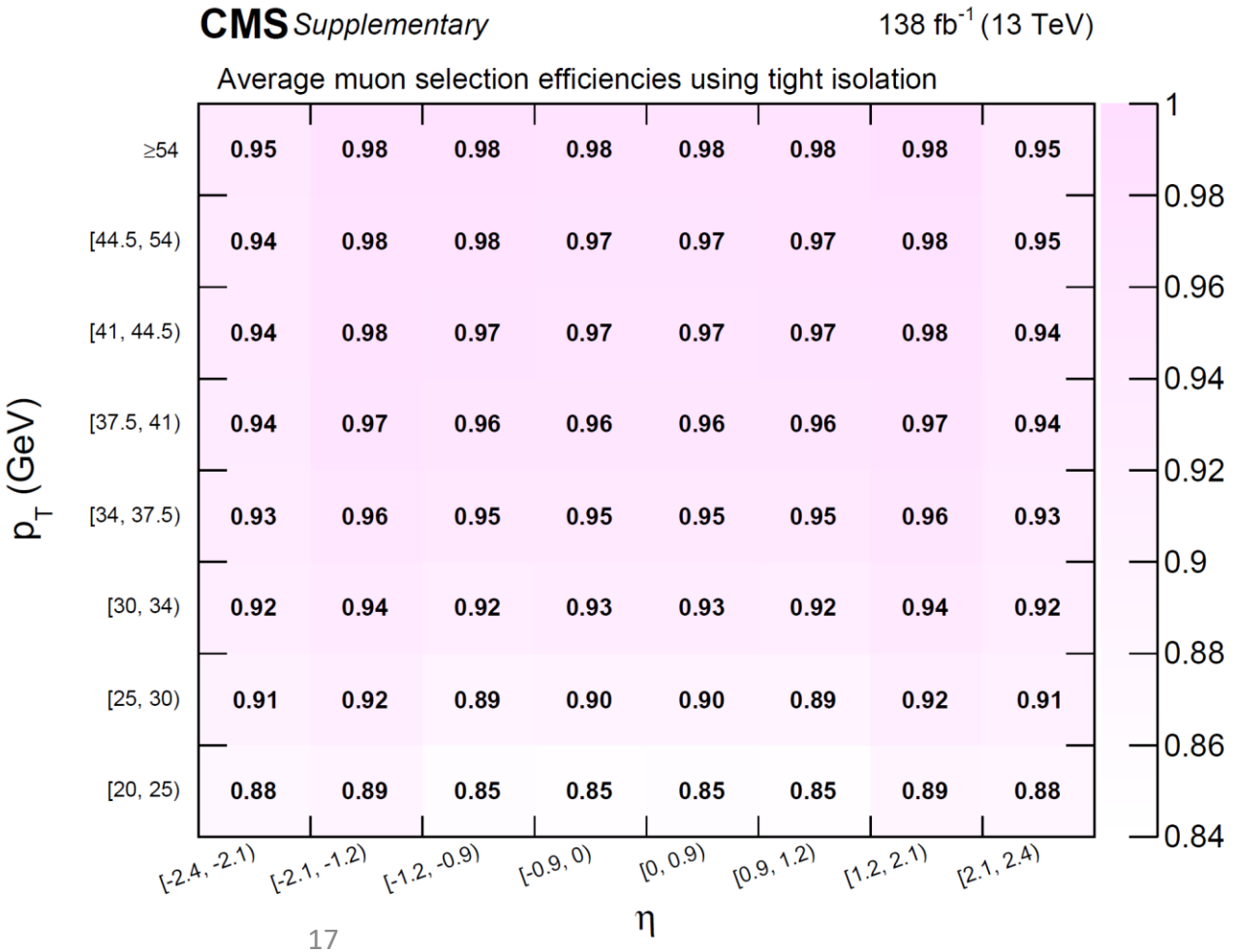

How to use this box efficiently:

Detector is very efficient in reconstructing leptons.
→ Since several analyses we will mention use leptons, here are exemplary lepton selection efficiencies:

Electrons: $\sim 48\% - 88\%$

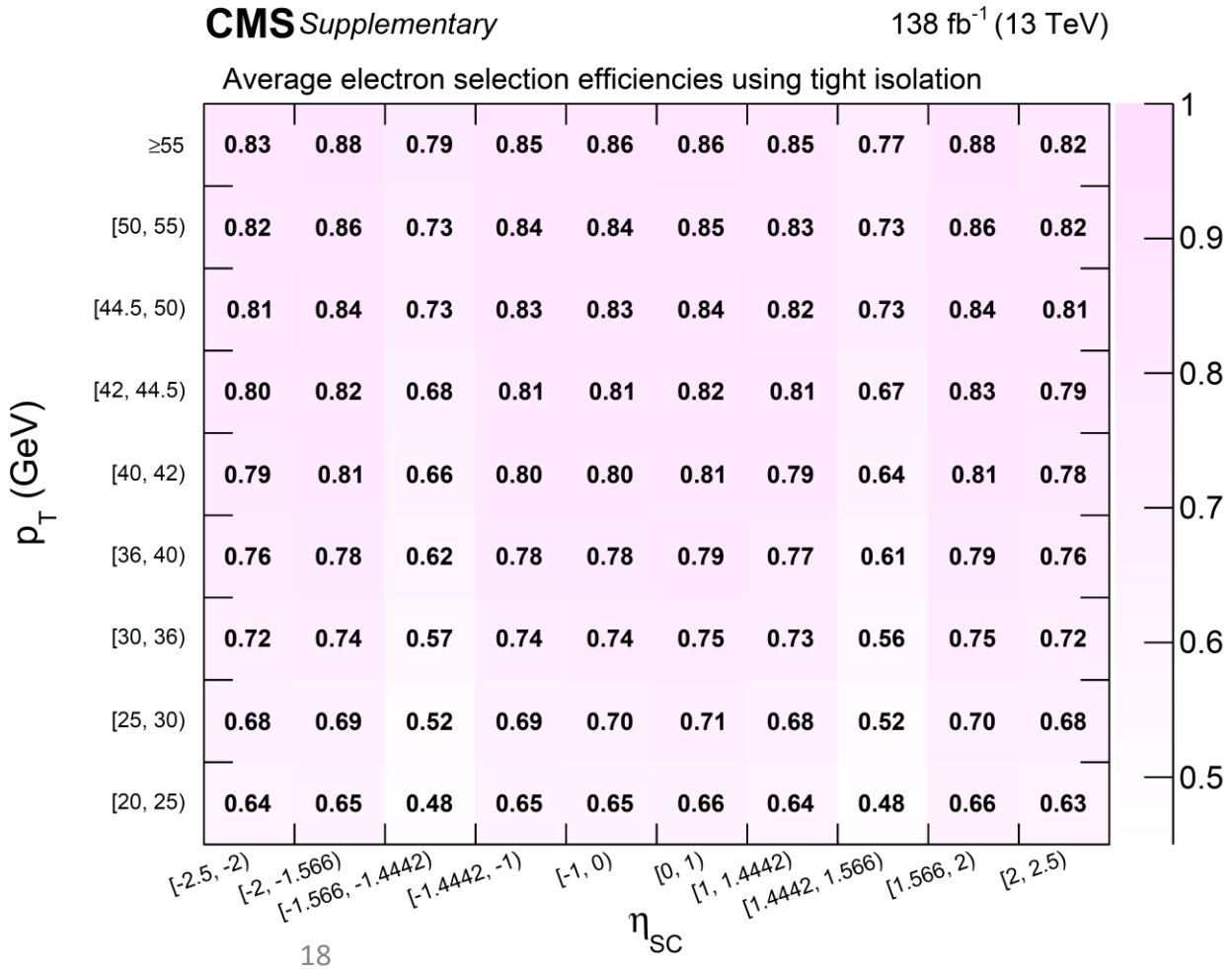

When you cannot detect...

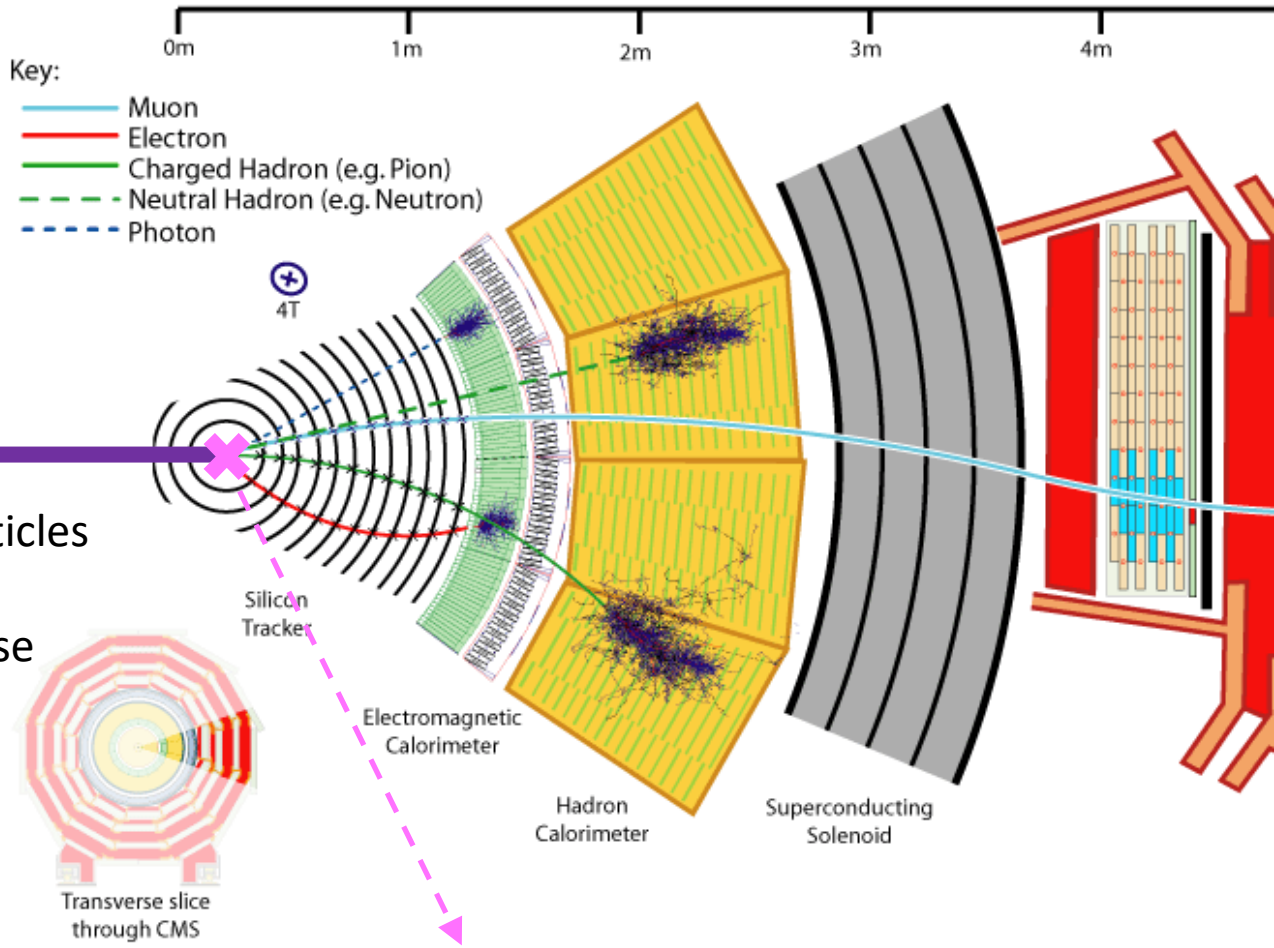

Assuming these are all the particles in an event, this arrow would represent the missing transverse momentum, $p_{\mathrm{T}}^{\mathrm{miss}}$.

Total transverse momentum from the collision should be 0.

Momentum should balance.

A few common analysis themes

How do you know the detector signature of the Higgs signal?

A few common analysis themes

How do you know the detector signature of the Higgs signal?
⇒ Use full detector simulation

A few common analysis themes

How do you know the detector signature of the Higgs signal?
⇒ Use full detector simulation
→ Preferably at next-to-leading order (NLO) in QCD
→ May apply parametrized NNLO/N^3LO corrections as needed
→ Study kinematic behavior and differences from backgrounds

A few common analysis themes

Possible backgrounds and ways to estimate them:

When the bkg. can be reproduced in a clean sample with more events...
→ Use data-driven estimate

A few common analysis themes

Possible backgrounds and ways to estimate them:

When the bkg. can be reproduced in a clean sample with more events...
→ Use data-driven estimate

Example:
→ Analysis examines $Z(\to \ell\ell)$ + large $p_{\mathrm{T}}^{\mathrm{miss}}$.
→ There are non-$Z(\to \ell\ell)$ contributions with a real $\ell\ell$ pair (fully leptonic $t\bar{t}, WW$ decays).

A few common analysis themes

Possible backgrounds and ways to estimate them:

When the bkg. can be reproduced in a clean sample with more events...
→ Use data-driven estimate

Example:
→ Analysis examines $Z(\rightarrow \ell\ell)$ + large $p_{\mathrm{T}}^{\mathrm{miss}}$.
→ There are non-$Z(\rightarrow \ell\ell)$ contributions with a real $\ell\ell$ pair (fully leptonic $t\bar{t}, WW$ decays).

Solution:
→ Pick $e\mu$ events with otherwise identical reqs.
→ Rate of $e\mu$ = 2 × rate of ee or $\mu\mu$
→ Reweight for lepton and trigger efficiencies to reproduce ee and $\mu\mu$ behavior

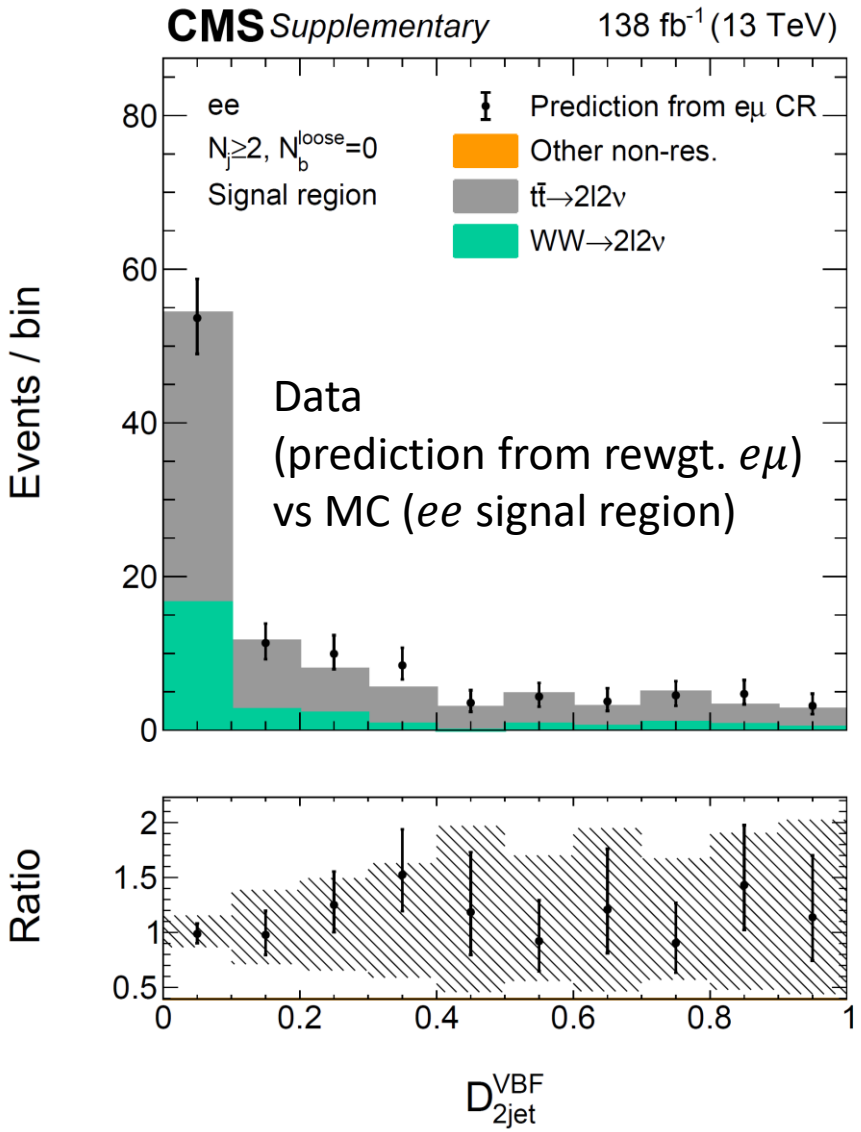

A few common analysis themes

Possible backgrounds and ways to estimate them:

When there is detector noise...
→ Simulation is approximate.
→ Use data-driven estimates

A few common analysis themes

Possible backgrounds and ways to estimate them:

When there is detector noise...
→ Simulation is approximate.
→ Use data-driven estimates

Example:
→ Analysis examines $Z(\rightarrow \ell\ell)$ + large $p_{\mathrm{T}}^{\mathrm{miss}}$.
→ $Z(\rightarrow \ell\ell)$+jets has large cross section.
→ Mismeasurements of jets, and unclustered energy produce *instrumental* $p_{\mathrm{T}}^{\mathrm{miss}}$ smearing.
→ Small smearing and tight selection, but event rate is high.

A few common analysis themes

Possible backgrounds and ways to estimate them:

When there is detector noise...
→ Simulation is approximate.
→ Use data-driven estimates

Example:
→ Analysis examines $Z(\rightarrow \ell\ell)$ + large $p_{\mathrm{T}}^{\mathrm{miss}}$.
→ $Z(\rightarrow \ell\ell)$+jets has large cross section.
→ Mismeasurements of jets, and unclustered energy produce *instrumental* $p_{\mathrm{T}}^{\mathrm{miss}}$ smearing.
→ Small smearing and tight selection, but event rate is high.

Solution:
→ Select γ+jets data to model $p_{\mathrm{T}}^{\mathrm{miss}}$ response
→ Calibrate γ kinematics to those for the Z
→ Subtract real-$p_{\mathrm{T}}^{\mathrm{miss}}$ processes (up to $Z(\rightarrow \nu\nu)\gamma$)

Need to know actual γ+jets in data

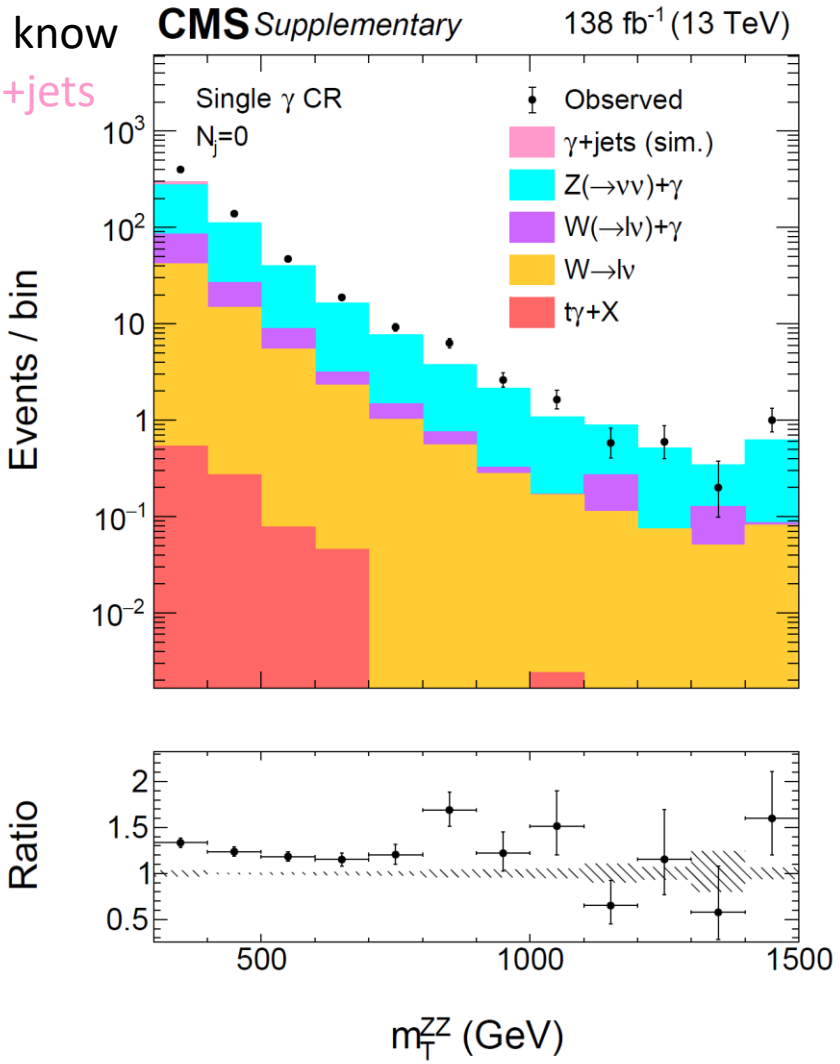

A few common analysis themes

Possible backgrounds and ways to estimate them:

When particles are not detected...
→ Simulation might still be approximate.
→ Use data-driven estimates guided by simulation

A few common analysis themes

Possible backgrounds and ways to estimate them:

When particles are not detected...
→ Simulation might still be approximate.
→ Use data-driven estimates guided by simulation

Example:
→ Analysis examines large $p_{\mathrm{T}}^{\mathrm{miss}}$ + jets.
→ $Z(\rightarrow \nu\nu)$+jets once again has large cross section and enters as a background.

A few common analysis themes

Possible backgrounds and ways to estimate them:

When particles are not detected...
→ Simulation might still be approximate.
→ Use data-driven estimates guided by simulation

Example:
→ Analysis examines large $p_{\mathrm{T}}^{\mathrm{miss}}$ + jets.
→ $Z(\rightarrow \nu\nu)$+jets once again has large cross section and enters as a background.

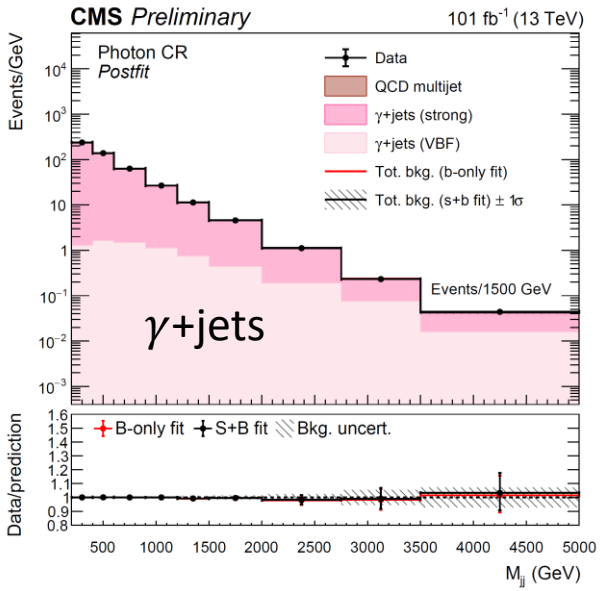

Solution:
→ Select $Z(\rightarrow \ell\ell)$+jets and γ+jets, similar data
→ $(Z(\rightarrow \ell\ell)$ or $\gamma) \Rightarrow Z(\rightarrow \nu\nu)$ transfer factors from sim.
→ Perform joint fit with analysis signal region

A few common analysis themes

Possible backgrounds and ways to estimate them:

When particles are not detected...
→ Simulation might still be approximate.
→ Use data-driven estimates guided by simulation

Example:
→ Analysis examines large $p_{\mathrm{T}}^{\mathrm{miss}}$ + jets.
→ $Z(\rightarrow \nu\nu)$+jets once again has large cross section and enters as a background.

Solution:
→ Select $Z(\rightarrow \ell\ell)$+jets and γ+jets, similar data
→ $(Z(\rightarrow \ell\ell)$ or $\gamma) \Rightarrow Z(\rightarrow \nu\nu)$ transfer factors from sim.
→ Perform joint fit with analysis signal region

Similar idea for a lost-lepton background from $W(\rightarrow \ell\nu)$+jets. Select a $W(\rightarrow \ell\nu)$+jets sample with visible leptons, and then apply the next two steps.

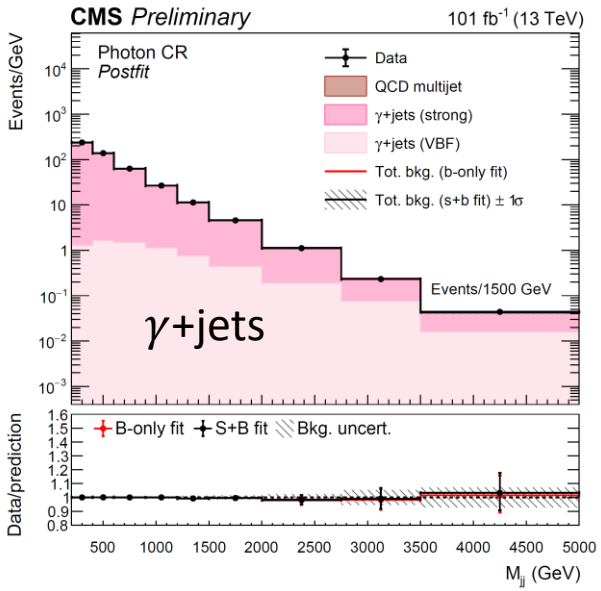

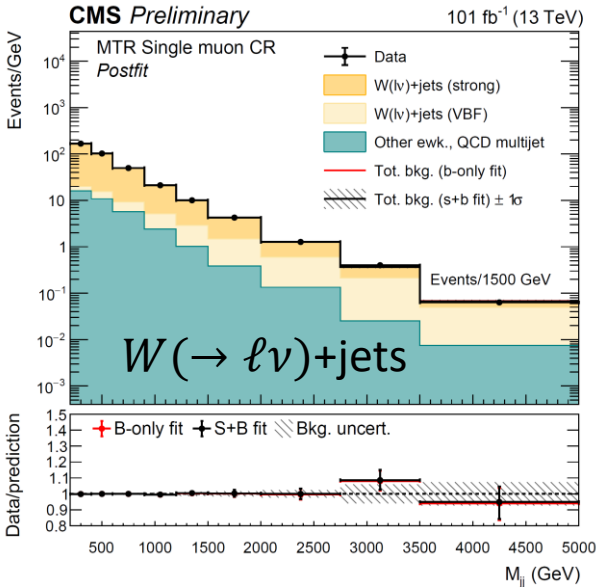

A few common analysis themes

Possible backgrounds and ways to estimate them:

When background signature is about the same as the signal...
→ Rely on simulation and initial prediction
→ Calibrate simulation
→ Use data-driven calibration whenever possible

A few common analysis themes

Possible backgrounds and ways to estimate them:

When background signature is about the same as the signal...
→ Rely on simulation and initial prediction
→ Calibrate simulation
→ Use data-driven calibration whenever possible

Example:
→ Analysis examines high ZZ invariant mass.
→ To first order, $q\bar{q} \rightarrow ZZ$ looks like $H \rightarrow ZZ$.
→ Cannot select for a relevant $q\bar{q} \rightarrow ZZ$ – rich sample without $H \rightarrow ZZ$ contamination

A few common analysis themes

Possible backgrounds and ways to estimate them:

When background signature is about the same as the signal...
→ Rely on simulation and initial prediction
→ Calibrate simulation
→ Use data-driven calibration whenever possible

Example:
→ Analysis examines high ZZ invariant mass.
→ To first order, $q\bar{q} \to ZZ$ looks like $H \to ZZ$.
→ Cannot select for a relevant $q\bar{q} \to ZZ$ – rich sample without $H \to ZZ$ contamination

Solution:
→ Use a sample of $q\bar{q}' \to WZ$ instead.
→ Minimal Higgs contribution
→ Kinematic behavior similar to $q\bar{q} \to ZZ$
→ Shapes and common uncertainties from simulation, perform joint fit with the signal sample.

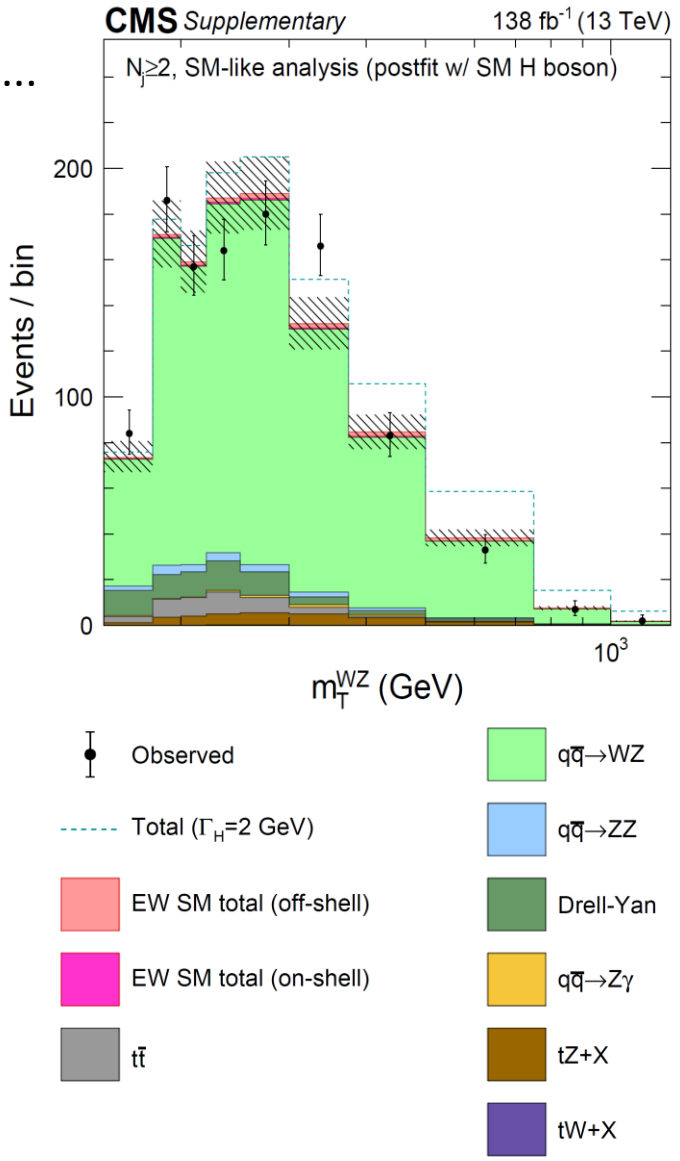

What do visible decay measurements tell us?

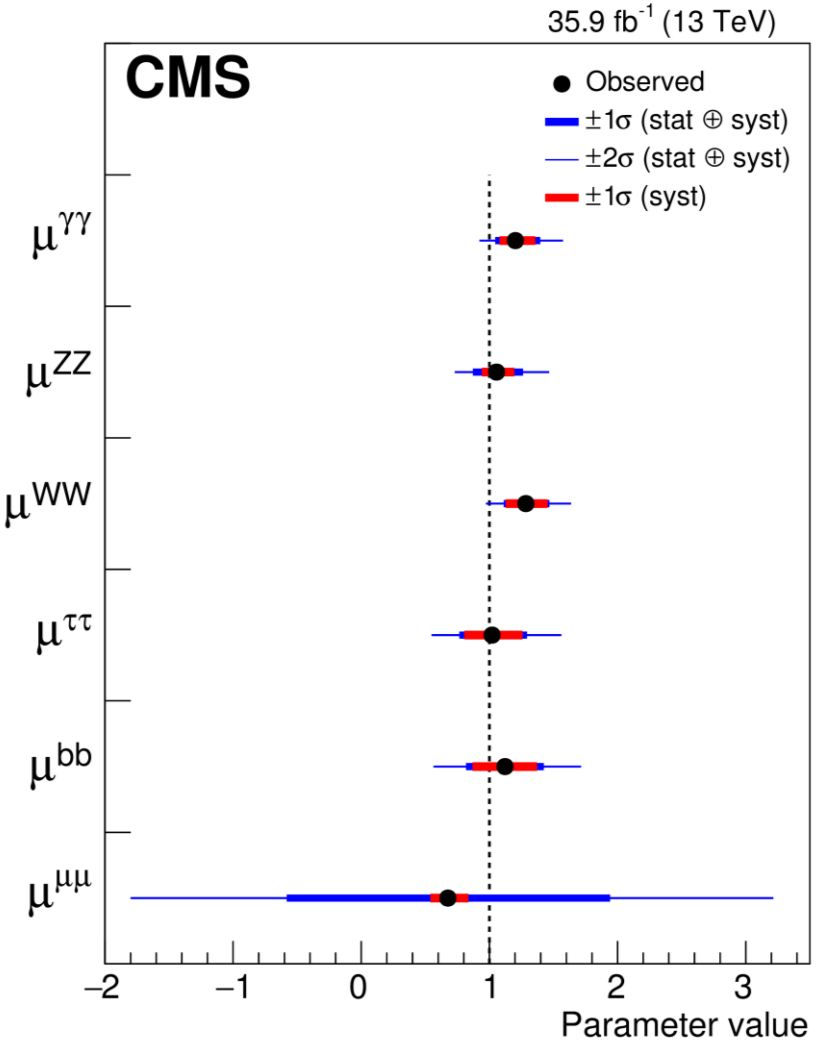

CMS-HIG-17-031

→ Combined analysis of signal strengths for individual Higgs decay channels

→ 2016 data only

→ More updates in some of the individual final states, but this plot represents our current knowledge.

$\mathcal{B}$ for major decay modes [1]

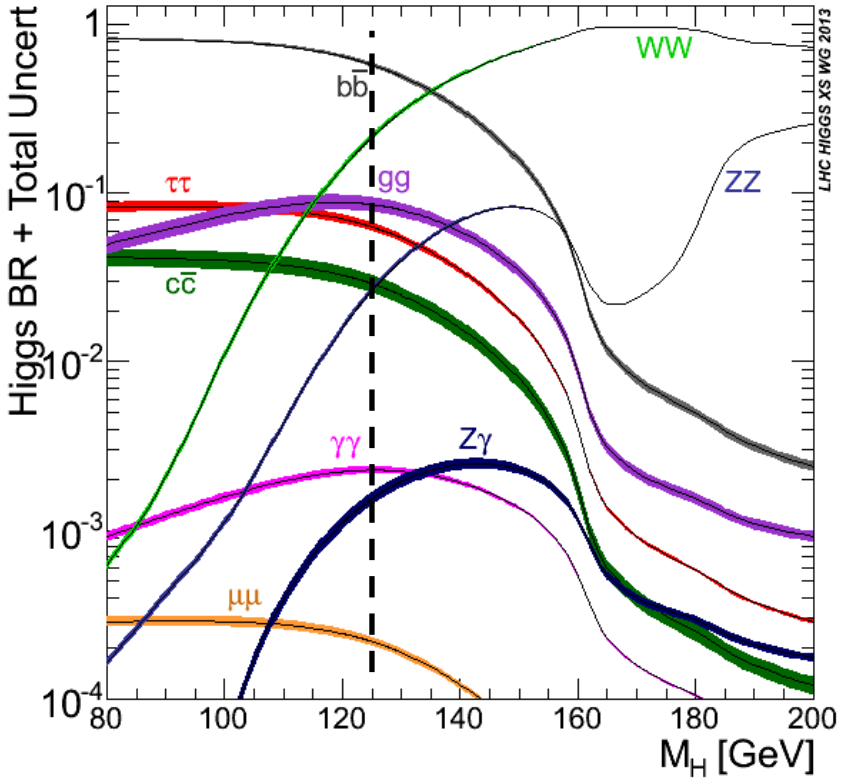

What do visible decay measurements tell us?

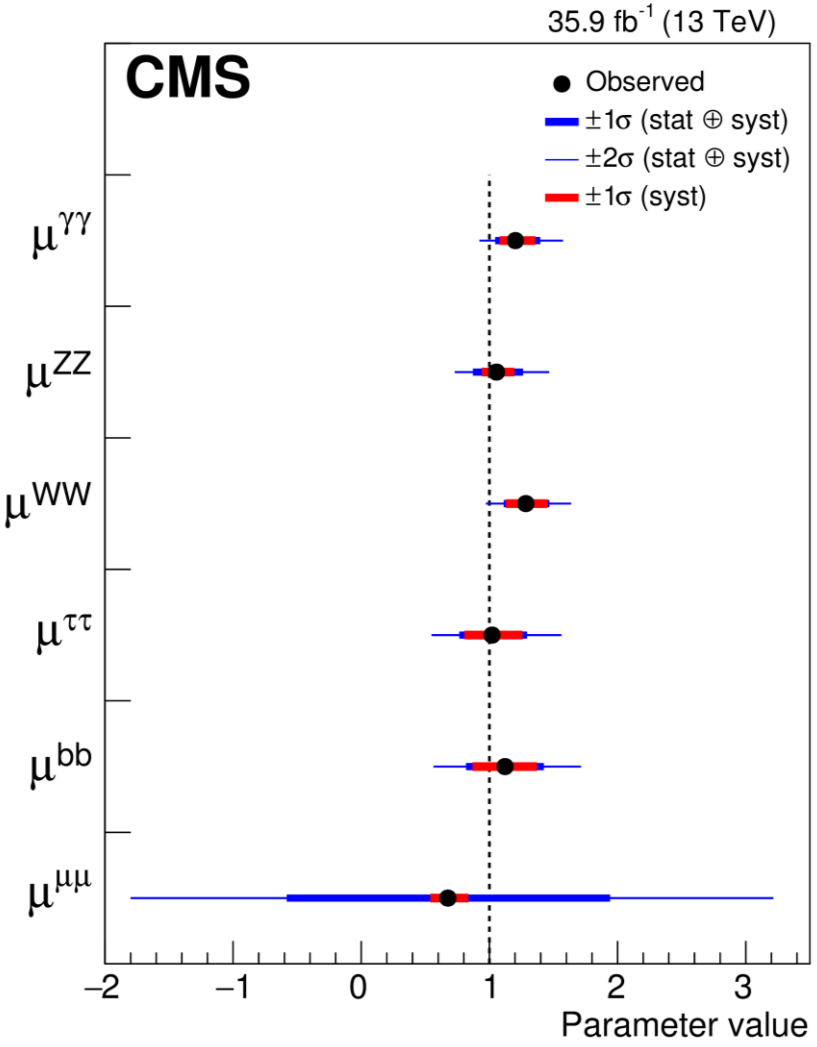

CMS-HIG-17-031

→ Combined analysis of signal strengths for individual Higgs decay channels

→ 2016 data only

→ More updates in some of the individual final states, but this plot represents our current knowledge.

$\mathcal{B}$ for major decay modes [1]

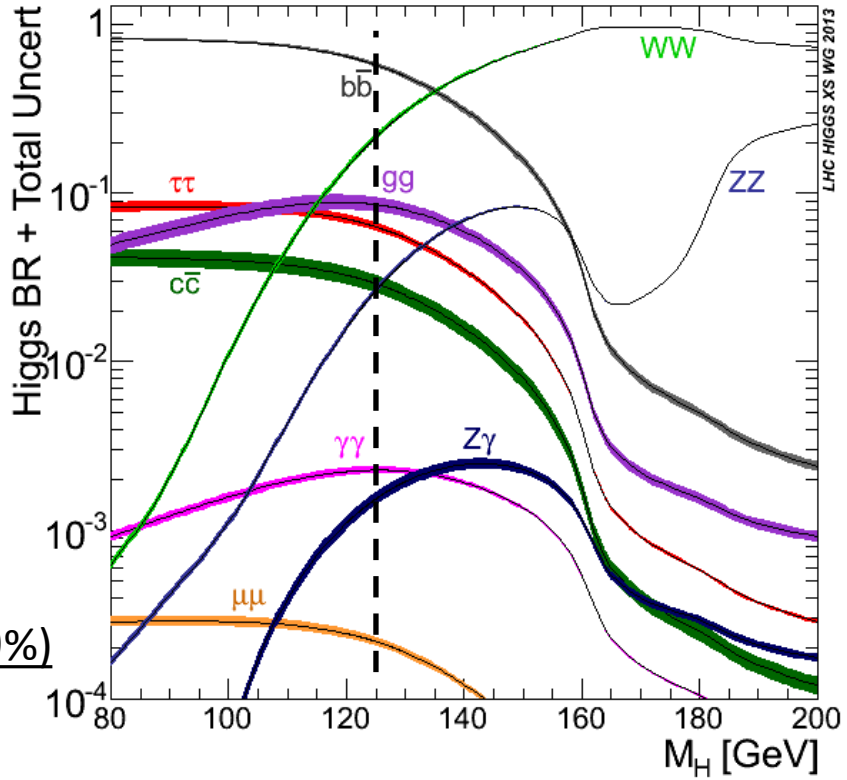

Constraints from couplings and signal strengths O(10%)

How about measuring width/lifetime directly?

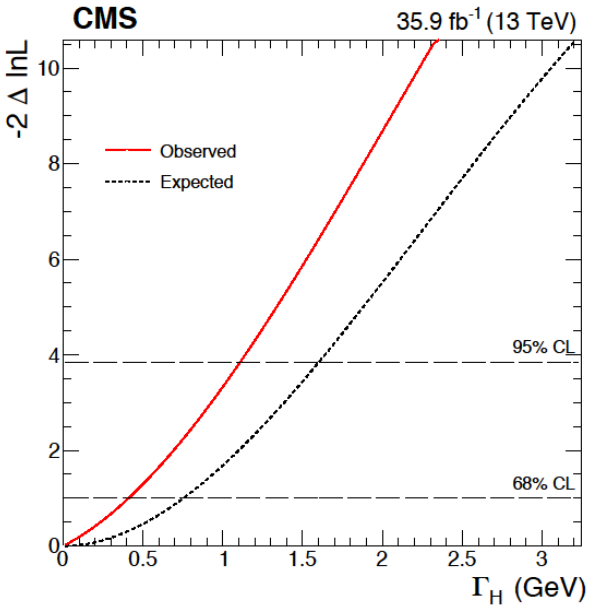

Using 4ℓ events with $\ell = e, \mu$:

Best width upper bound from on-shell mass spectrum:
$\Gamma_H < 1.1$ GeV
($\tau_H > 6.0 \times 10^{-25}$ s)

CMS-HIG-16-041

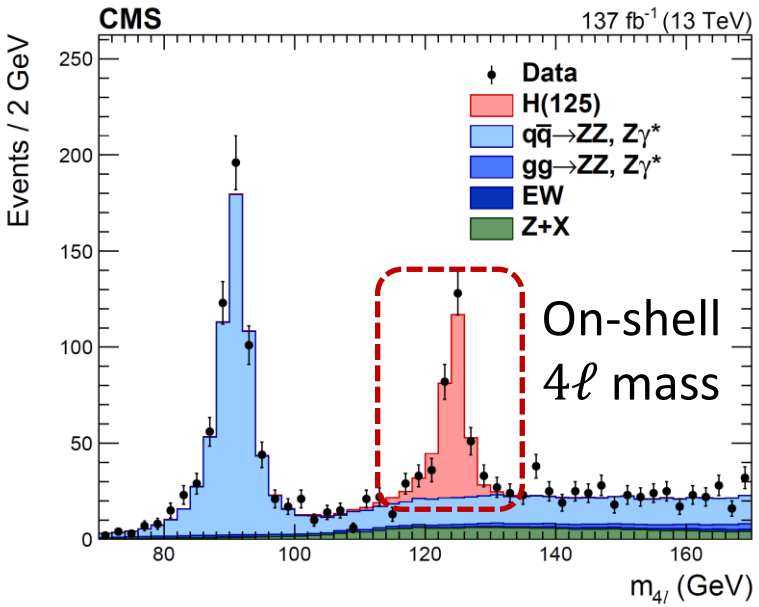

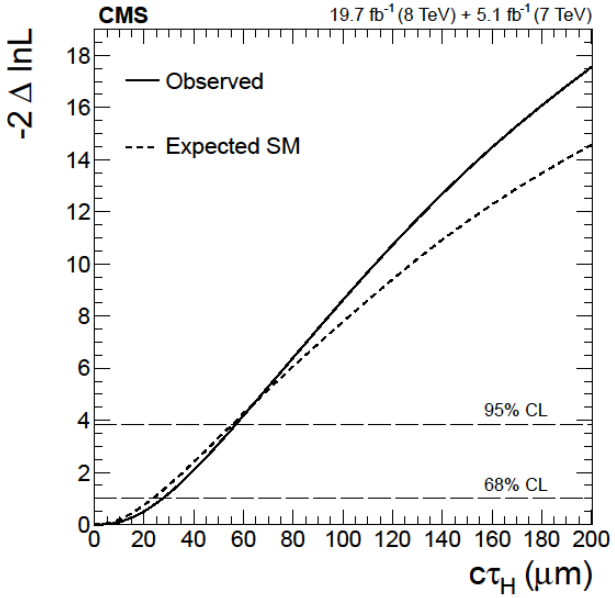

Best lifetime upper bound from on-shell 4ℓ displacement:
$\tau_H < 1.9 \times 10^{-13}$ s
($\Gamma_H > 3.5 \times 10^{-12}$ GeV)

CMS-HIG-14-036

How about measuring width/lifetime directly?

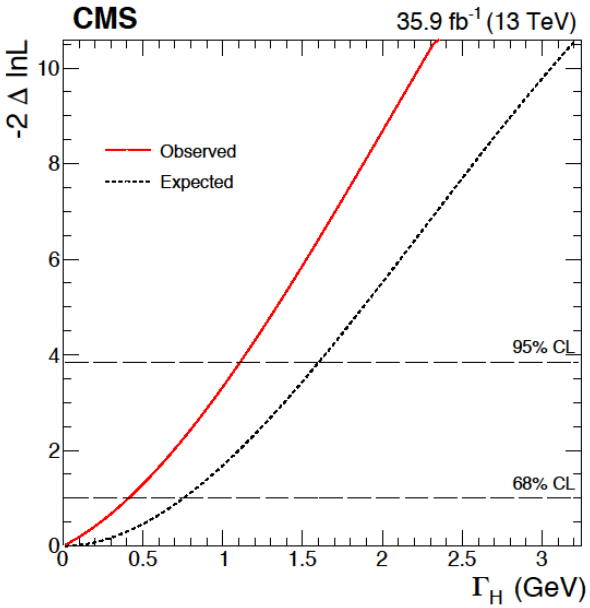

Using 4ℓ events with $\ell = e, \mu$:

Best width upper bound from on-shell mass spectrum:
$\Gamma_H < 1.1$ GeV
($\tau_H > 6.0 \times 10^{-25}$ s)

CMS-HIG-16-041

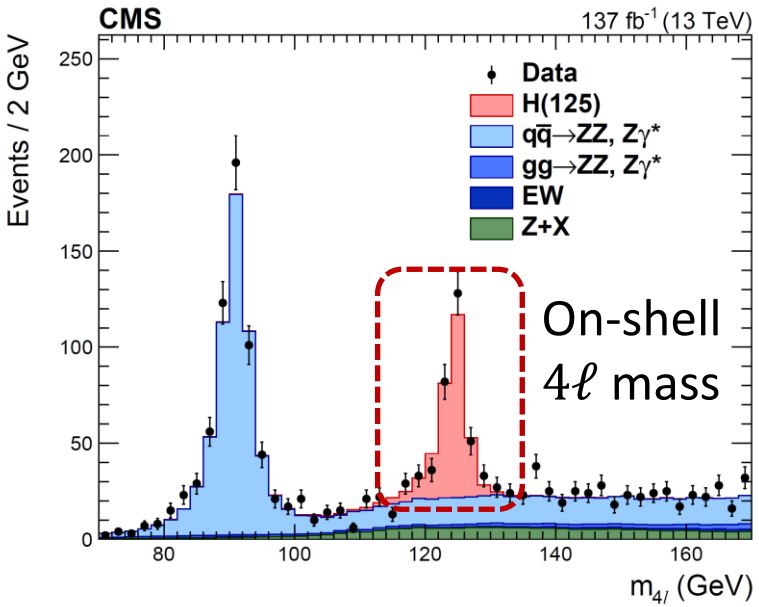

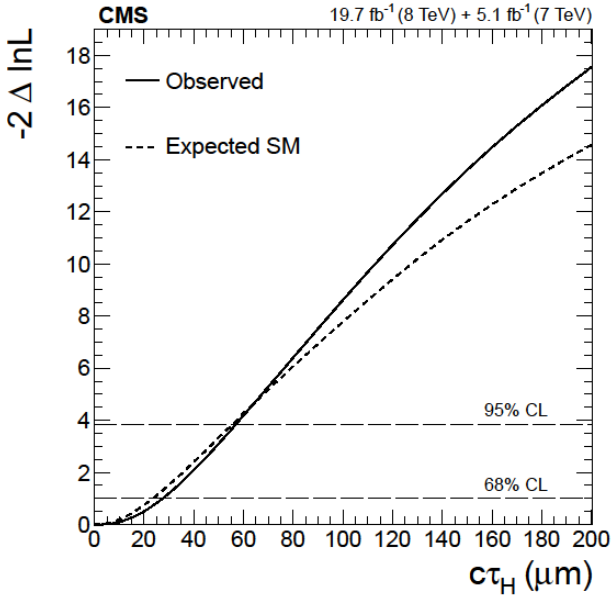

Best lifetime upper bound from on-shell 4ℓ displacement:
$\tau_H < 1.9 \times 10^{-13}$ s
($\Gamma_H > 3.5 \times 10^{-12}$ GeV)

CMS-HIG-14-036

SM value:
$\tau_H = 1.6 \times 10^{-22}$ s
$\Gamma_H = 4.1$ MeV

Out of reach of either method in precision!

Off-shell Higgs production

In $H \to VV$ $(V = Z, W)$

→ $m_V < m_{\mathrm{H}} < 2m_V$:

Either H is on-shell and one V is off-shell, or H is off-shell and both Vs are on-shell

→ Both Vs going on-shell allows ~10% of events in the SM to produce an off-shell Higgs boson [1,2]

Possible to measure two off-shell production mechanisms:

- $\mu_F^{off-shell}$ (gg)
- $\mu_V^{off-shell}$ (EW H + 2 jets), or
- Can also measure overall $\mu^{off-shell}$

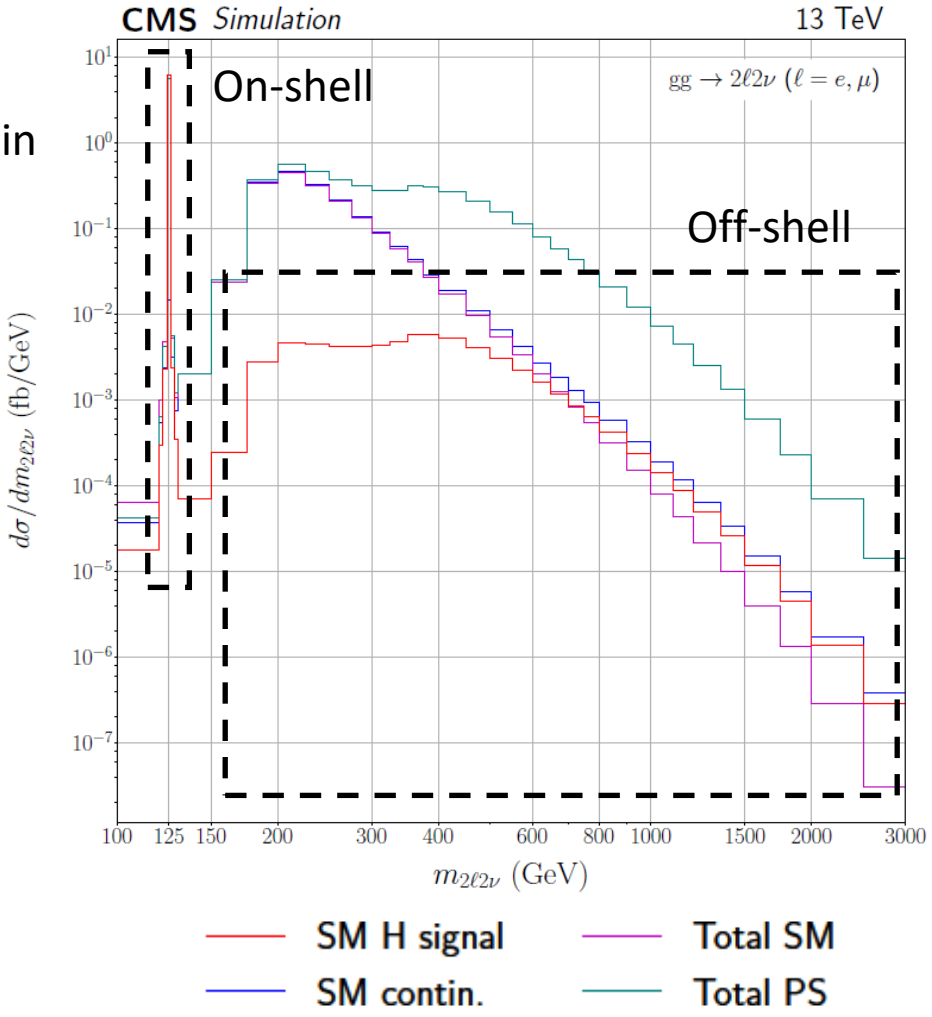

Off-shell Higgs production

In $H \to VV$ $(V = Z, W)$

→ $m_V < m_{\mathrm{H}} < 2m_V$:

Either H is on-shell and one V is off-shell, or H is off-shell and both Vs are on-shell

→ Both Vs going on-shell allows ~10% of events in the SM to produce an off-shell Higgs boson [1,2]

Possible to measure two off-shell production mechanisms:

- $\mu_F^{off-shell}$ (gg)
- $\mu_V^{off-shell}$ (EW H + 2 jets), or
- Can also measure overall $\mu^{off-shell}$

Higgs-mediated diagrams interfere destructively with continuum VV production at off-shell:

→ Large in magnitude

→ ~ Twice the size of the Higgs signal

→ Necessary in the SM to ensure unitarity

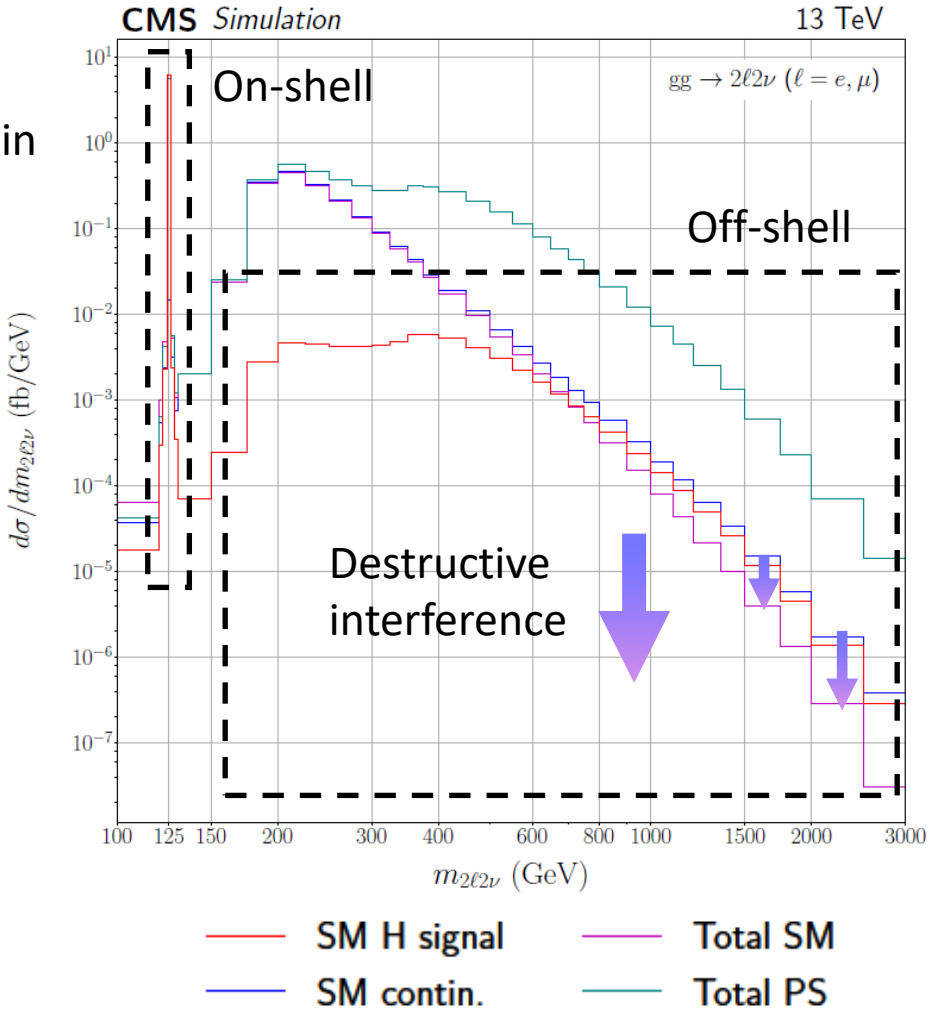

Diagrams of off-shell Higgs production

$gg \to H \to ZZ$:

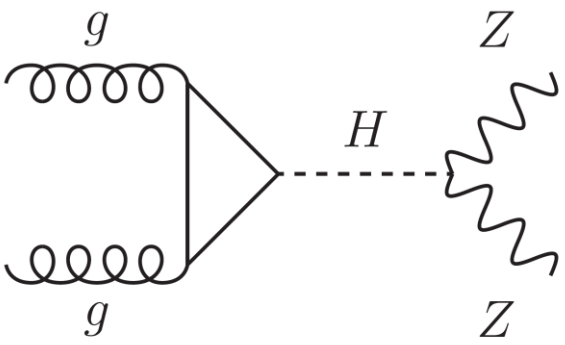

$gg \to H$ production dominant at lower masses in the off-shell region

VBF (s-channel):

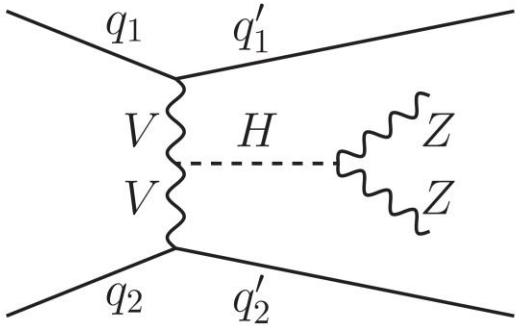

VBF (t-channel):

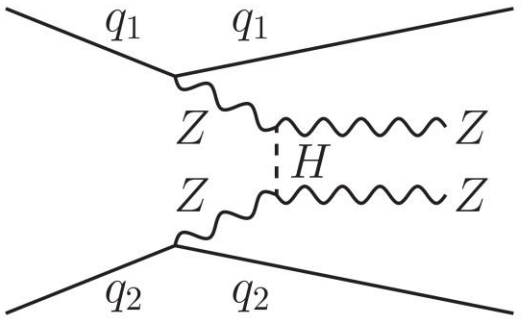

ZH (s-, t-, u-channels):

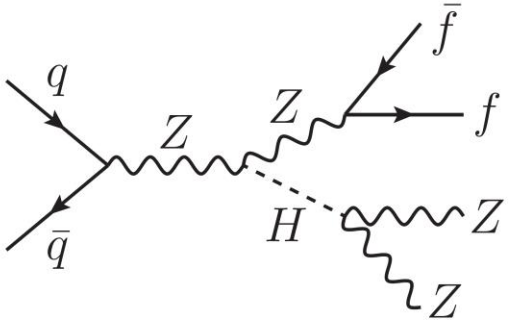

WH:

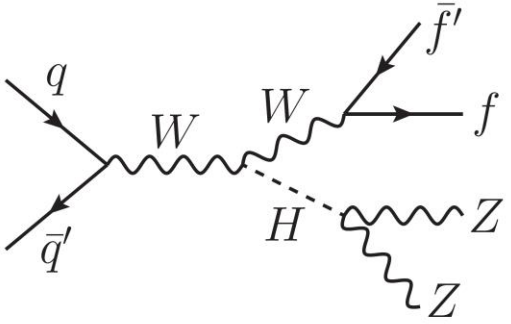

EW production more dominant at higher masses in the off-shell region (mostly VBF in the SM)

The off-shell method for the width

Combine with on-shell signal strength measurement to extract Γ_H [1]:

$$\sigma = \int \frac{g_{prod}^2 g_{dec}^2}{(m^2 - m_H^2)^2 + m_H^2 \Gamma_H^2} \dots dm^2$$

On-shell

$$\sigma \propto \frac{g_{prod}^2 g_{dec}^2}{\Gamma_H} \propto \mu_{prod}$$

Take on-shell signal strength from final states ZZ or WW

The off-shell method for the width

Combine with on-shell signal strength measurement to extract Γ_H [1]:

$$\sigma = \int \frac{g_{prod}^2 g_{dec}^2}{(m^2 - m_H^2)^2 + m_H^2 \Gamma_H^2} \dots dm^2$$

On-shell

$$\sigma \propto \frac{g_{prod}^2 g_{dec}^2}{\Gamma_H} \propto \mu_{prod}$$

Off-shell

$$\sigma \sim \int \frac{g_{prod}^2 g_{dec}^2}{(m^2 - m_H^2)^2} \dots dm^2 \propto \underbrace{\mu_{prod} \cdot \Gamma_H}_{\mu_{prod}^{off-shell}}$$

Take on-shell signal strength from final states ZZ or WW

The off-shell method for the width

Combine with on-shell signal strength measurement to extract Γ_H [1]:

$$\sigma = \int \frac{g_{prod}^2 g_{dec}^2}{(m^2 - m_H^2)^2 + m_H^2 \Gamma_H^2} \dots dm^2$$

On-shell

$$\sigma \propto \frac{g_{prod}^2 g_{dec}^2}{\Gamma_H} \propto \mu_{prod}$$

Take on-shell signal strength from final states ZZ or WW

Off-shell

$$\sigma \sim \int \frac{g_{prod}^2 g_{dec}^2}{(m^2 - m_H^2)^2} \dots dm^2 \propto \underbrace{\mu_{prod} \cdot \Gamma_H}_{\mu_{prod}^{off-shell}}$$

Ratio of off-shell to on-shell signal strengths for each production mode gives Γ_H

Off-shell & BSM HVV couplings

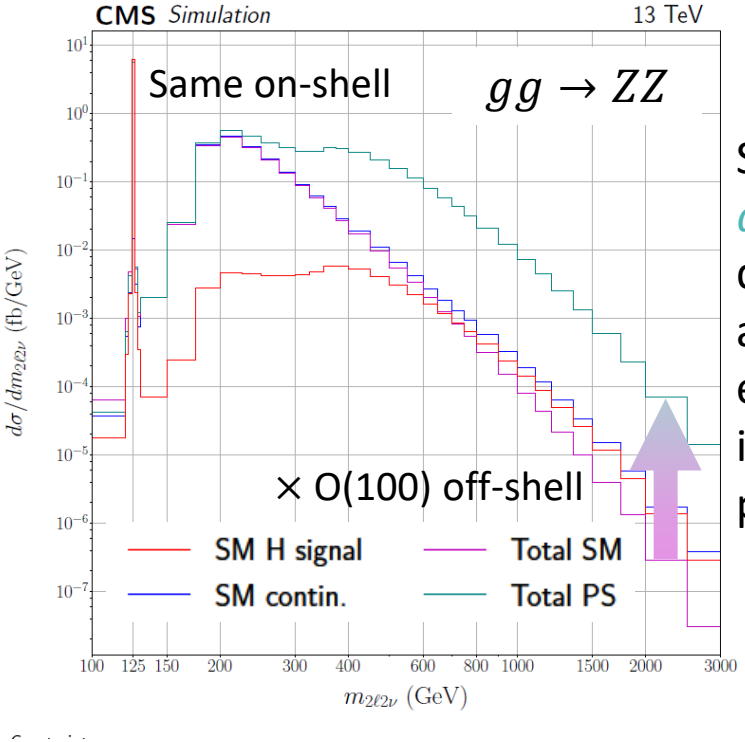

Same a_1 (SM) or a_3 (PS) couplings, different on-shell and off-shell enhancements in gg and EW production modes

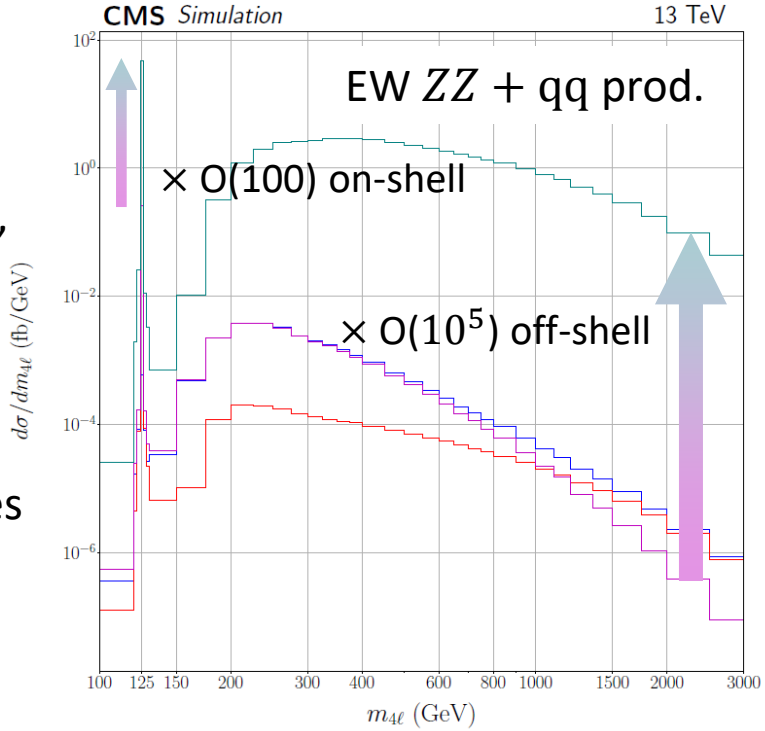

$$A(HVV) \sim \left[a_1 - e^{i\phi_{\Lambda 1}} \frac{(q_{V1}^2 + q_{V2}^2)}{\Lambda_1^2} + \cdots \right] m_V^2 \epsilon_{V1}^* \epsilon_{V2}^*$$
$$+ |a_2| e^{i\phi_{a2}} f_{\mu\nu}^{*(1)} f^{*(2),\mu\nu} + |a_3| e^{i\phi_{a3}} f_{\mu\nu}^{*(1)} \tilde{f}^{*(2),\mu\nu}$$

HVV amplitude
$\propto \Lambda_1, a_2, a_3$ BSM contributions
+ SM-like a_1 term.

Off-shell & BSM HVV couplings

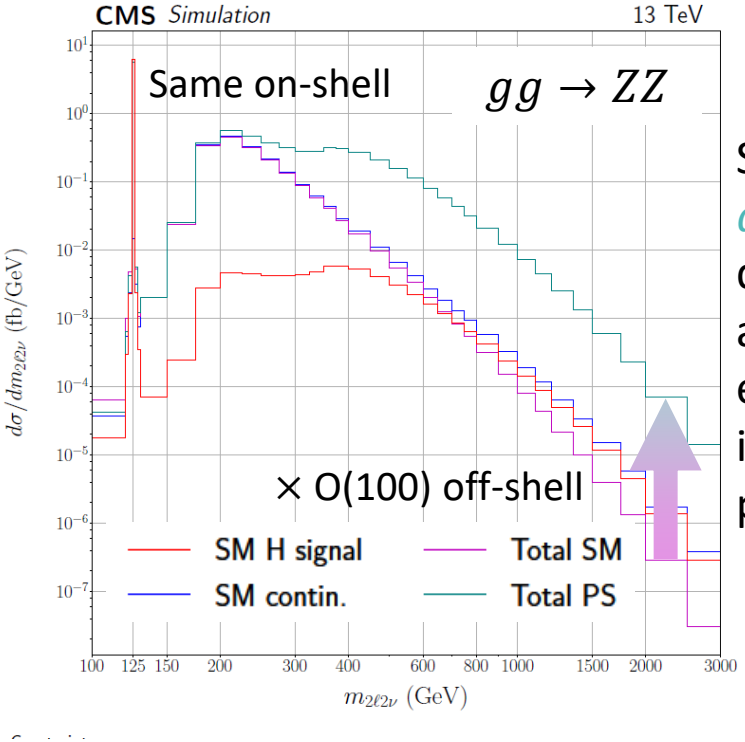

Same a_1 (SM) or a_3 (PS) couplings, different on-shell and off-shell enhancements in gg and EW production modes

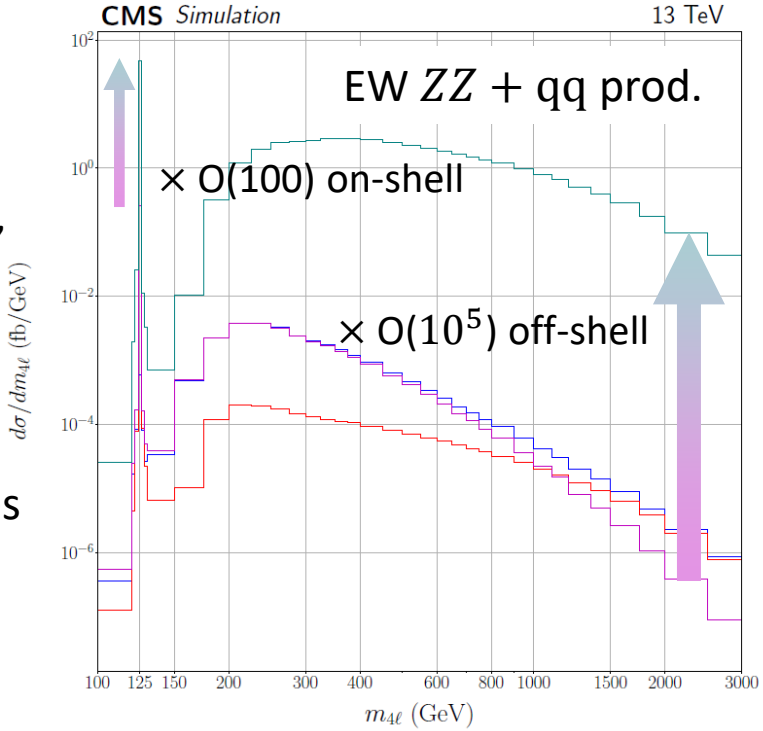

$$A(HVV) \sim \left[a_1 - e^{i\phi_{\Lambda 1}} \frac{(q_{V1}^2 + q_{V2}^2)}{\Lambda_1^2} + \cdots \right] m_V^2 \epsilon_{V1}^* \epsilon_{V2}^*$$
$$+ |a_2| e^{i\phi_{a2}} f_{\mu\nu}^{*(1)} f^{*(2),\mu\nu} + |a_3| e^{i\phi_{a3}} f_{\mu\nu}^{*(1)} \tilde{f}^{*(2),\mu\nu}$$

HVV amplitude
$\propto \Lambda_1, a_2, a_3$ BSM contributions
+ SM-like a_1 term.

Off-shell analyses can combine with on-shell information.
→ Allows testing for Γ_H + BSM HVV couplings at the same time

Off-shell 4ℓ: Analysis strategy

CMS-HIG-18-002: Analysis of off-shell ($m_{4l} > 220$ GeV) 2016+2017 data

→ All momenta are known in 4ℓ ⇒ Use MELA matrix element discriminants

→ Can compute for Higgs production, decay, or both; or backgrounds

$$\mathcal{D}_{\text{alt}}(\boldsymbol{\Omega}) = \frac{\mathcal{P}_{\text{sig}}(\boldsymbol{\Omega})}{\mathcal{P}_{\text{sig}}(\boldsymbol{\Omega}) + \mathcal{P}_{\text{alt}}(\boldsymbol{\Omega})}$$

sig. vs alt.

$$\mathcal{D}_{\text{int}}(\boldsymbol{\Omega}) = \frac{\mathcal{P}_{\text{int}}(\boldsymbol{\Omega})}{2\sqrt{\mathcal{P}_{\text{sig}}(\boldsymbol{\Omega})\ \mathcal{P}_{\text{alt}}(\boldsymbol{\Omega})}}$$

sig.-alt. interference

Off-shell 4ℓ: Analysis strategy

CMS-HIG-18-002: Analysis of off-shell ($m_{4l} > 220$ GeV) 2016+2017 data

→ All momenta are known in 4ℓ ⇒ Use MELA matrix element discriminants

→ Can compute for Higgs production, decay, or both; or backgrounds

$$\mathcal{D}_{\text{alt}}(\boldsymbol{\Omega}) = \frac{\mathcal{P}_{\text{sig}}(\boldsymbol{\Omega})}{\mathcal{P}_{\text{sig}}(\boldsymbol{\Omega}) + \mathcal{P}_{\text{alt}}(\boldsymbol{\Omega})}$$

sig. vs alt.

$$\mathcal{D}_{\text{int}}(\boldsymbol{\Omega}) = \frac{\mathcal{P}_{\text{int}}(\boldsymbol{\Omega})}{2\sqrt{\mathcal{P}_{\text{sig}}(\boldsymbol{\Omega})\ \mathcal{P}_{\text{alt}}(\boldsymbol{\Omega})}}$$

sig.-alt. interference

Category	VBF-tagged	VH-tagged	Untagged
Selection	$\mathcal{D}_{\text{2jet}}^{\text{VBF}}$ or $\mathcal{D}_{\text{2jet}}^{\text{VBF,BSM}} > 0.5$	$\mathcal{D}_{\text{2jet}}^{\text{WH}}$ or $\mathcal{D}_{\text{2jet}}^{\text{WH,BSM}}$, or $\mathcal{D}_{\text{2jet}}^{\text{ZH}}$ or $\mathcal{D}_{\text{2jet}}^{\text{ZH,BSM}} > 0.5$	Rest of events
SM obs.	$m_{4\ell}$, $\mathcal{D}_{\text{bkg}}^{\text{VBF+dec}}$, $\mathcal{D}_{\text{bsi}}^{\text{VBF+dec}}$	$m_{4\ell}$, $\mathcal{D}_{\text{bkg}}^{\text{VH+dec}}$, $\mathcal{D}_{\text{bsi}}^{\text{VH+dec}}$	$m_{4\ell}$, $\mathcal{D}_{\text{bkg}}^{\text{kin}}$ $\mathcal{D}_{\text{bsi}}^{\text{gg,dec}}$

Mass shape is the most sensitive to off-shell production

→ Any off-shell analysis uses some form of it

Off-shell 4ℓ: Analysis strategy

CMS-HIG-18-002: Analysis of off-shell ($m_{4l} > 220$ GeV) 2016+2017 data

→ All momenta are known in 4ℓ ⇒ Use MELA matrix element discriminants

→ Can compute for Higgs production, decay, or both; or backgrounds

$$\mathcal{D}_{\text{alt}}(\boldsymbol{\Omega}) = \frac{\mathcal{P}_{\text{sig}}(\boldsymbol{\Omega})}{\mathcal{P}_{\text{sig}}(\boldsymbol{\Omega}) + \mathcal{P}_{\text{alt}}(\boldsymbol{\Omega})}$$

sig. vs alt.

$$\mathcal{D}_{\text{int}}(\boldsymbol{\Omega}) = \frac{\mathcal{P}_{\text{int}}(\boldsymbol{\Omega})}{2\sqrt{\mathcal{P}_{\text{sig}}(\boldsymbol{\Omega})\ \mathcal{P}_{\text{alt}}(\boldsymbol{\Omega})}}$$

sig.-alt. interference

Category	VBF-tagged	VH-tagged	Untagged
Selection	$\mathcal{D}_{\text{2jet}}^{\text{VBF}}$ or $\mathcal{D}_{\text{2jet}}^{\text{VBF,BSM}} > 0.5$	$\mathcal{D}_{\text{2jet}}^{\text{WH}}$ or $\mathcal{D}_{\text{2jet}}^{\text{WH,BSM}}$, or $\mathcal{D}_{\text{2jet}}^{\text{ZH}}$ or $\mathcal{D}_{\text{2jet}}^{\text{ZH,BSM}} > 0.5$	Rest of events
SM obs.	$m_{4\ell}$, $\mathcal{D}_{\text{bkg}}^{\text{VBF+dec}}$, $\mathcal{D}_{\text{bsi}}^{\text{VBF+dec}}$	$m_{4\ell}$, $\mathcal{D}_{\text{bkg}}^{\text{VH+dec}}$, $\mathcal{D}_{\text{bsi}}^{\text{VH+dec}}$	$m_{4\ell}$, $\mathcal{D}_{\text{bkg}}^{\text{kin}}$ $\mathcal{D}_{\text{bsi}}^{\text{gg,dec}}$

Mass shape is the most sensitive to off-shell production

→ Any off-shell analysis uses some form of it

+ Discriminant for signal vs bkg

+ Discriminant for Higgs-continuum ZZ interference

(or SM vs BSM if constraining anomalous couplings)

Off-shell 4ℓ: Event distributions

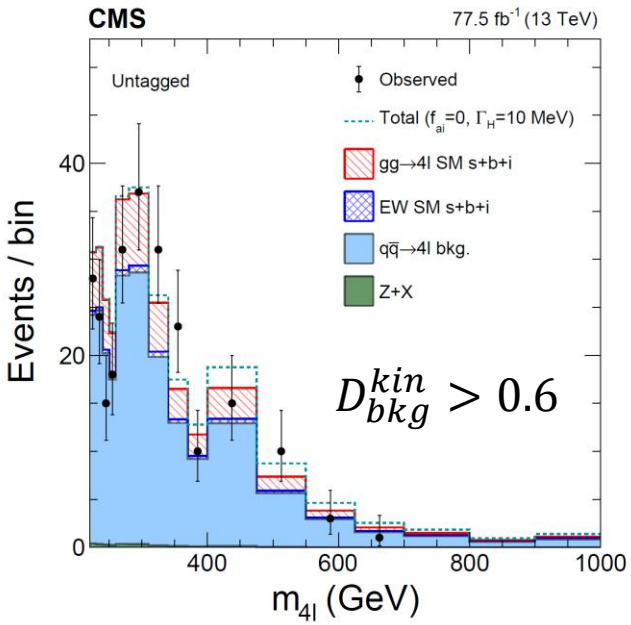

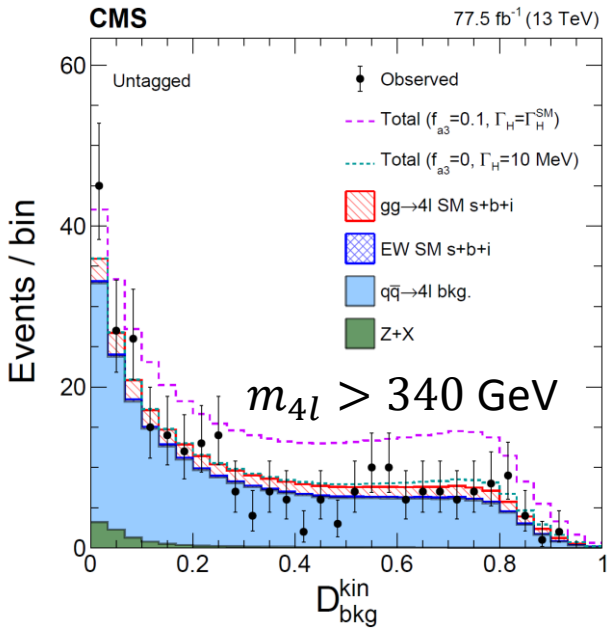

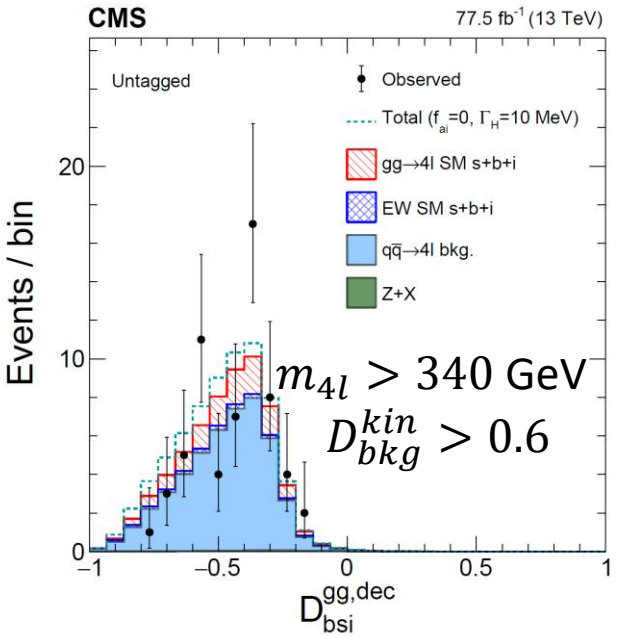

Example distributions from the untagged category

Selection requirements applied to enhance Higgs contributions

Stacked histograms for prefit SM distributions ($\Gamma_H = 4.1$ MeV),
cyan for $\Gamma_H = 10$ MeV, magenta for an on-shell 10% PS (a_3) mixture

On-shell 4ℓ: Analysis strategy

CMS-HIG-19-009: Analysis of on-shell 4ℓ 2016-2018 data

→ Utilizes a finer categorization and more discriminants as observables

→ Same categorization and observables for all couplings

→ Example from untagged category:

$$\mathcal{D}_{\text{bkg}}, \underbrace{\mathcal{D}^{\text{dec}}_{0\text{h}+}, \mathcal{D}^{\text{dec}}_{0-}, \mathcal{D}^{\text{dec}}_{\Lambda 1}, \mathcal{D}^{\text{Z}\gamma,\text{dec}}_{\Lambda 1}}_{\text{SM vs BSM}}, \underbrace{\mathcal{D}^{\text{dec}}_{\text{int}}, \mathcal{D}^{\text{dec}}_{CP}}_{\text{SM-BSM interf.}}$$

Provides extensive set of results

→ Provides the following input to off-shell analysis:

on-shell μ_F and μ_V

on-shell BSM HVV contribution fractions f_{ai}

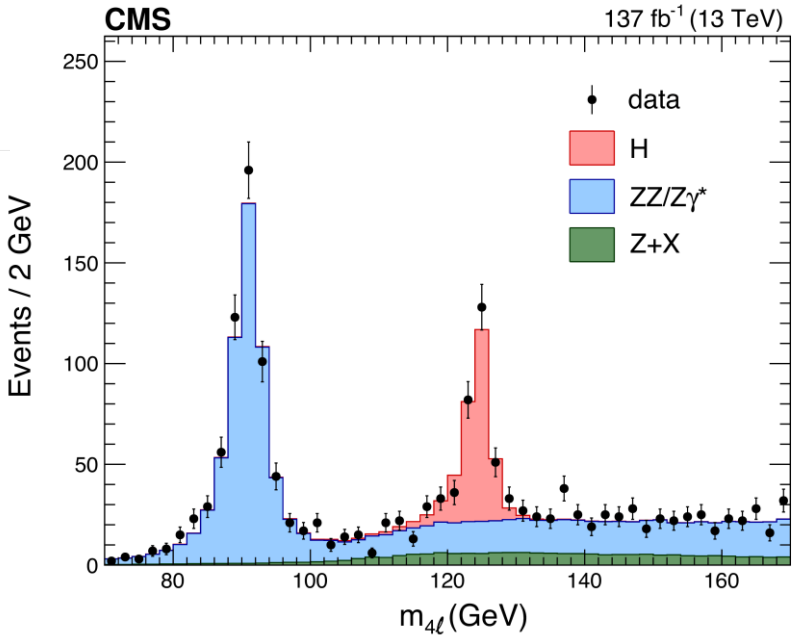

On-shell 4ℓ: Analysis strategy

CMS-HIG-19-009: Analysis of on-shell 4ℓ 2016-2018 data

→ Utilizes a finer categorization and more discriminants as observables

→ Same categorization and observables for all couplings

→ Example from untagged category:

$$\mathcal{D}_{\text{bkg}}, \underbrace{\mathcal{D}^{\text{dec}}_{0\text{h}+}, \mathcal{D}^{\text{dec}}_{0-}, \mathcal{D}^{\text{dec}}_{\Lambda 1}, \mathcal{D}^{\text{Z}\gamma,\text{dec}}_{\Lambda 1}}_{\text{SM vs BSM}}, \underbrace{\mathcal{D}^{\text{dec}}_{\text{int}}, \mathcal{D}^{\text{dec}}_{CP}}_{\text{SM-BSM interf.}}$$

Provides extensive set of results

→ Provides the following input to off-shell analysis:
on-shell μ_F and μ_V
on-shell BSM HVV contribution fractions f_{ai}

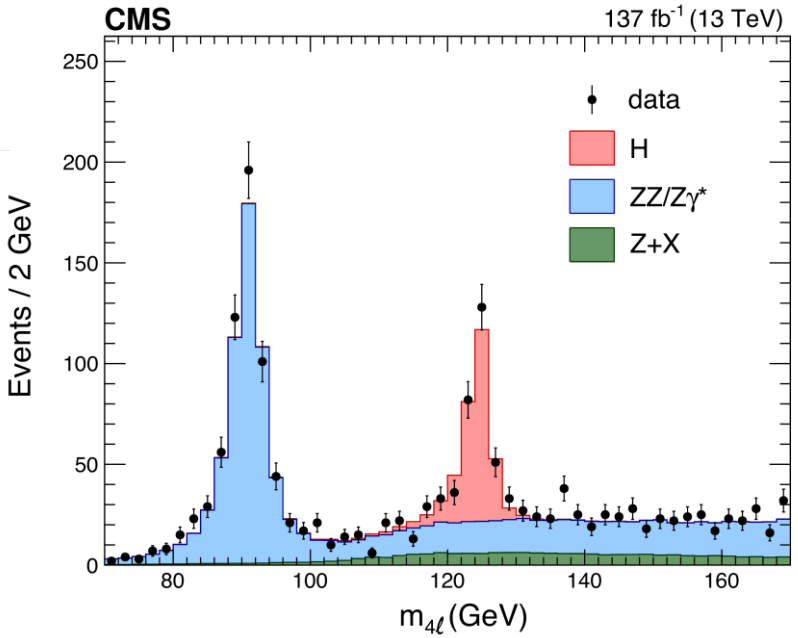

CMS-HIG-17-011: Analysis of on-shell 4ℓ 2015 data

→ Inclusive in categorization

→ Observables: $D_{bkg}, D^{dec}_{BSM}, D^{dec}_{int}$ as in the untagged category above.

→ The BSM discriminant depends on the analyzed coupling.

Off-shell $2\ell 2\nu$: Analysis strategy

CMS-PAS-HIG-21-013: ∗NEW∗ analysis of off-shell ZZ → $2\ell 2\nu$ 2016-2018 data

→ Main observable: Transverse ZZ mass defined through

$$m_{\mathrm{T}}^{\mathrm{ZZ}\,2} = \left[\sqrt{p_{\mathrm{T}}^{\ell\ell\,2} + m_{\ell\ell}{}^{2}} + \sqrt{p_{\mathrm{T}}^{\mathrm{miss}\,2} + m_{\mathrm{Z}}{}^{2}}\right]^{2} - \left|\vec{p}_{\mathrm{T}}^{\,\ell\ell} + \vec{p}_{\mathrm{T}}^{\,\mathrm{miss}}\right|^{2}$$

→ $p_{\mathrm{T}}^{\mathrm{miss}}$ also used as an observable since it is sensitive to backgrounds

Off-shell $2\ell 2\nu$: Analysis strategy

CMS-PAS-HIG-21-013: ∗NEW∗ analysis of off-shell ZZ → $2\ell 2\nu$ 2016-2018 data

→ Main observable: Transverse ZZ mass defined through

$$m_{\mathrm{T}}^{\mathrm{ZZ}\,2} = \left[\sqrt{p_{\mathrm{T}}^{\ell\ell\,2} + m_{\ell\ell}{}^2} + \sqrt{p_{\mathrm{T}}^{\mathrm{miss}\,2} + m_{\mathrm{Z}}{}^2}\right]^2 - \left|\vec{p}_{\mathrm{T}}^{\,\ell\ell} + \vec{p}_{\mathrm{T}}^{\,\mathrm{miss}}\right|^2$$

→ $p_{\mathrm{T}}^{\mathrm{miss}}$ also used as an observable since it is sensitive to backgrounds

→ Categorization in bins of the number of jets: $N_j = 0, 1, \geq 2$

→ Also uses the MELA discriminants $D_{2jet}^{VBF(,BSM)}$ when $N_j \geq 2$ by assuming $\eta_{\nu\nu} = \eta_{\ell\ell}$

Off-shell $2\ell 2\nu$: Analysis strategy

CMS-PAS-HIG-21-013: ∗NEW∗ analysis of off-shell ZZ → $2\ell 2\nu$ 2016-2018 data

→ Main observable: Transverse ZZ mass defined through

$$m_{\mathrm{T}}^{\mathrm{ZZ}\,2} = \left[\sqrt{{p_{\mathrm{T}}^{\ell\ell}}^2 + {m_{\ell\ell}}^2} + \sqrt{{p_{\mathrm{T}}^{\mathrm{miss}}}^2 + {m_{\mathrm{Z}}}^2}\right]^2 - \left|\vec{p}_{\mathrm{T}}^{\,\ell\ell} + \vec{p}_{\mathrm{T}}^{\,\mathrm{miss}}\right|^2$$

→ $p_{\mathrm{T}}^{\mathrm{miss}}$ also used as an observable since it is sensitive to backgrounds

→ Categorization in bins of the number of jets: $N_j = 0, 1, \geq 2$

→ Also uses the MELA discriminants $D_{2jet}^{VBF(,BSM)}$ when $N_j \geq 2$ by assuming $\eta_{\nu\nu} = \eta_{\ell\ell}$

Interpretation parameters	$N_j < 2$	$N_j \geq 2$
$\mu_F^{off-shell}, \mu_V^{off-shell}, \mu^{off-shell}$	$m_{\mathrm{T}}^{ZZ}, p_{\mathrm{T}}^{\mathrm{miss}}$	$m_{\mathrm{T}}^{ZZ}, p_{\mathrm{T}}^{\mathrm{miss}}, D_{2jet}^{VBF}, D_{2jet}^{VBF,a2}$
$\Gamma_{\mathrm{H}}\ (\mathrm{f_{ai}} = 0)$	$m_{\mathrm{T}}^{ZZ}, p_{\mathrm{T}}^{\mathrm{miss}}$	$m_{\mathrm{T}}^{ZZ}, p_{\mathrm{T}}^{\mathrm{miss}}, D_{2jet}^{VBF}, D_{2jet}^{VBF,a2}$
$\Gamma_{\mathrm{H}}, \mathrm{f_{a2}}$	$m_{\mathrm{T}}^{ZZ}, p_{\mathrm{T}}^{\mathrm{miss}}$	$m_{\mathrm{T}}^{ZZ}, p_{\mathrm{T}}^{\mathrm{miss}}, D_{2jet}^{VBF}, D_{2jet}^{VBF,\mathrm{a2}}$
$\Gamma_{\mathrm{H}}, \mathrm{f_{a3}}$	$m_{\mathrm{T}}^{ZZ}, p_{\mathrm{T}}^{\mathrm{miss}}$	$m_{\mathrm{T}}^{ZZ}, p_{\mathrm{T}}^{\mathrm{miss}}, D_{2jet}^{VBF}, D_{2jet}^{VBF,\mathrm{a3}}$
$\Gamma_{\mathrm{H}}, \mathrm{f_{\Lambda 1}}$	$m_{\mathrm{T}}^{ZZ}, p_{\mathrm{T}}^{\mathrm{miss}}$	$m_{\mathrm{T}}^{ZZ}, p_{\mathrm{T}}^{\mathrm{miss}}, D_{2jet}^{VBF}, D_{2jet}^{VBF,\Lambda 1}$

Off-shell $2\ell 2\nu$: Noninterfering backgrounds

$q\bar{q} \to ZZ, WZ$:

→ Dominant backgrounds at high m_{T}^{ZZ}

→ Shapes and normalizations taken from all possible variations of the simulation

→ Final estimate performed with a joint fit to a 3ℓ WZ CR

Off-shell $2\ell 2\nu$: Noninterfering backgrounds

$q\bar{q} \to ZZ, WZ$:
→ Dominant backgrounds at high m_{T}^{ZZ}
→ Shapes and normalizations taken from all possible variations of the simulation
→ Final estimate performed with a joint fit to a 3ℓ WZ CR

Instrumental $p_{\mathrm{T}}^{\mathrm{miss}}$:
→ Comes primarily from the $p_{\mathrm{T}}^{\mathrm{miss}}$ tail of Z+jets
→ Estimated from the single-photon CR by reweighting photons to $Z \to \ell\ell$

Off-shell $2\ell 2\nu$: Noninterfering backgrounds

$q\bar{q} \to ZZ, WZ$:
→ Dominant backgrounds at high m_{T}^{ZZ}
→ Shapes and normalizations taken from all possible variations of the simulation
→ Final estimate performed with a joint fit to a 3ℓ WZ CR

Instrumental $p_{\mathrm{T}}^{\mathrm{miss}}$:
→ Comes primarily from the $p_{\mathrm{T}}^{\mathrm{miss}}$ tail of Z+jets
→ Estimated from the single-photon CR by reweighting photons to $Z \to \ell\ell$

Nonresonant ($t\bar{t}, WW$):
→ Estimated from reweighting $e\mu$ events for trigger and lepton efficiencies

Off-shell $2\ell 2\nu$: Noninterfering backgrounds

$q\bar{q} \to ZZ, WZ$:
→ Dominant backgrounds at high m_{T}^{ZZ}
→ Shapes and normalizations taken from all possible variations of the simulation
→ Final estimate performed with a joint fit to a 3ℓ WZ CR

Instrumental $p_{\mathrm{T}}^{\mathrm{miss}}$:
→ Comes primarily from the $p_{\mathrm{T}}^{\mathrm{miss}}$ tail of Z+jets
→ Estimated from the single-photon CR by reweighting photons to $Z \to \ell\ell$

Nonresonant ($t\bar{t}, WW$):
→ Estimated from reweighting $e\mu$ events for trigger and lepton efficiencies

$tZ + X$:
→ Minor contribution
→ Estimated fully from simulation

Off-shell $2\ell 2\nu$: Event distributions

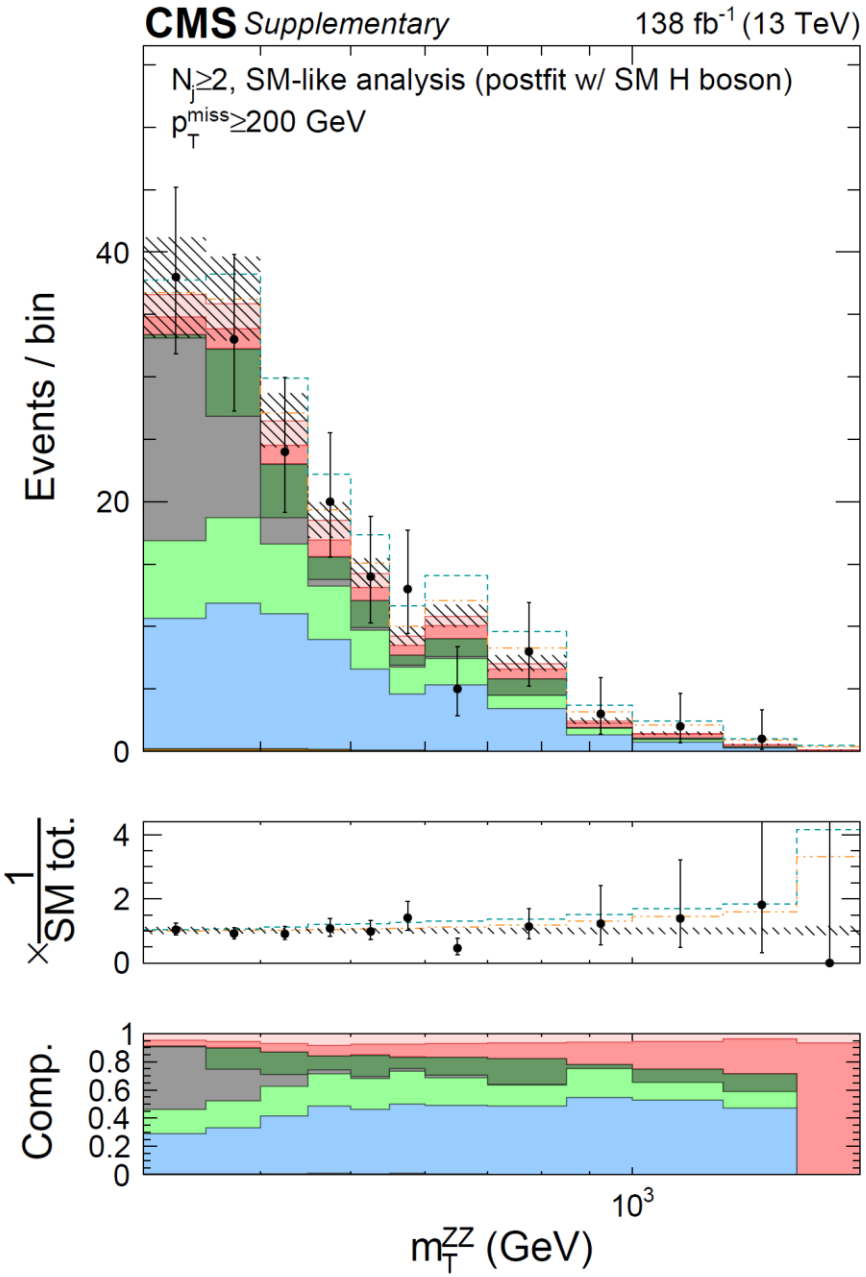

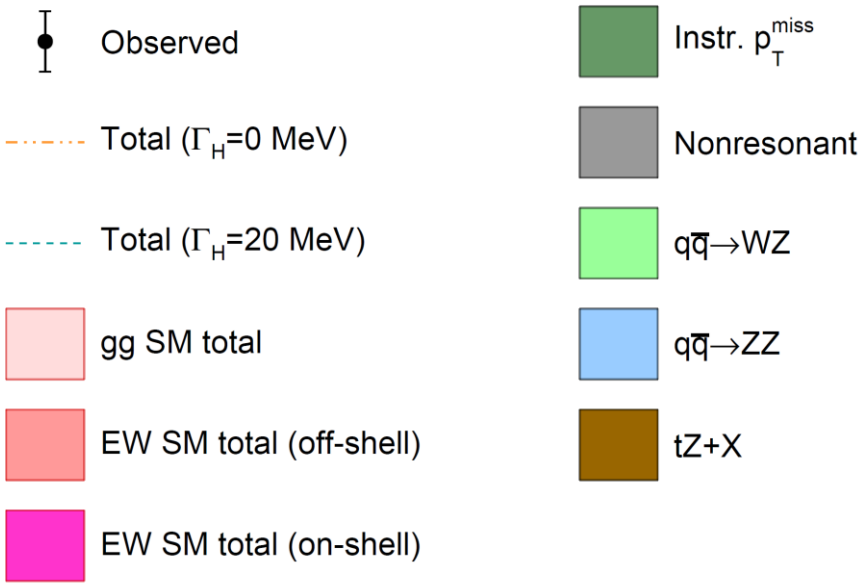

Example from $N_j \geq 2$, $p_{\mathrm{T}}^{\mathrm{miss}} > 200$ GeV

Off-shell $2\ell 2\nu$: Event distributions

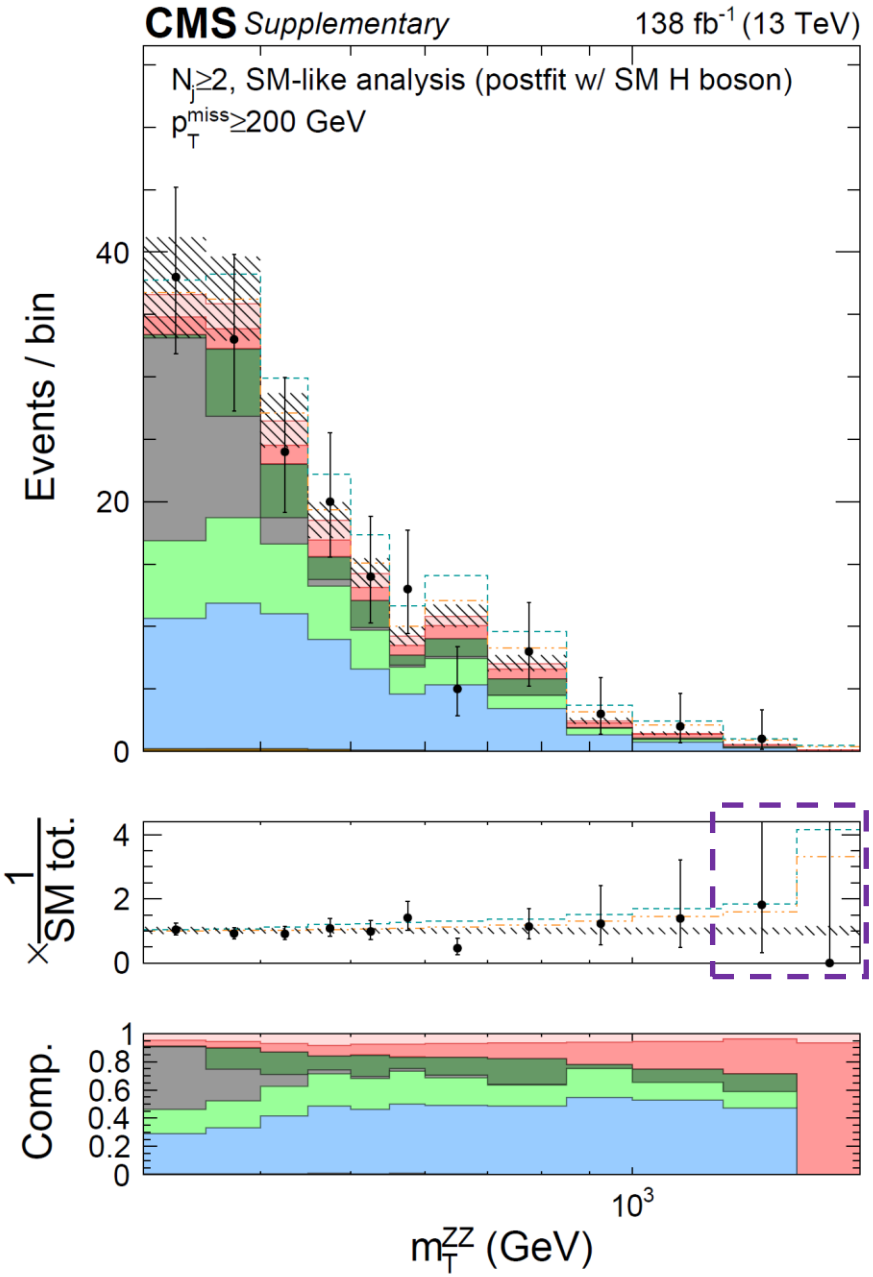

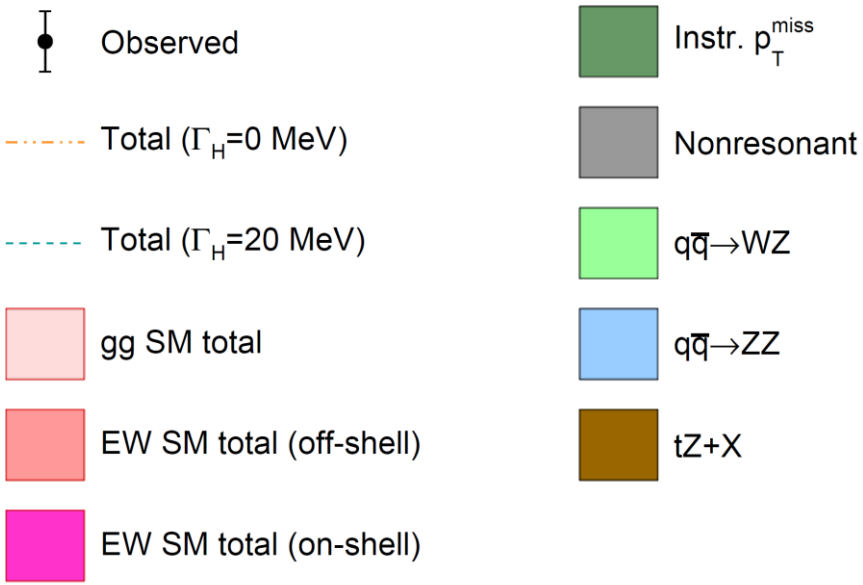

Example from $N_j \geq 2$, $p_{\mathrm{T}}^{\mathrm{miss}} > 200$ GeV

No – off-shell ($\Gamma_{\mathrm{H}} = 0$ MeV) hypothesis inconsistent with observed data
→ Visible at high m_{T}^{ZZ}

Off-shell $2\ell 2\nu$: Golden VBF/VBS event

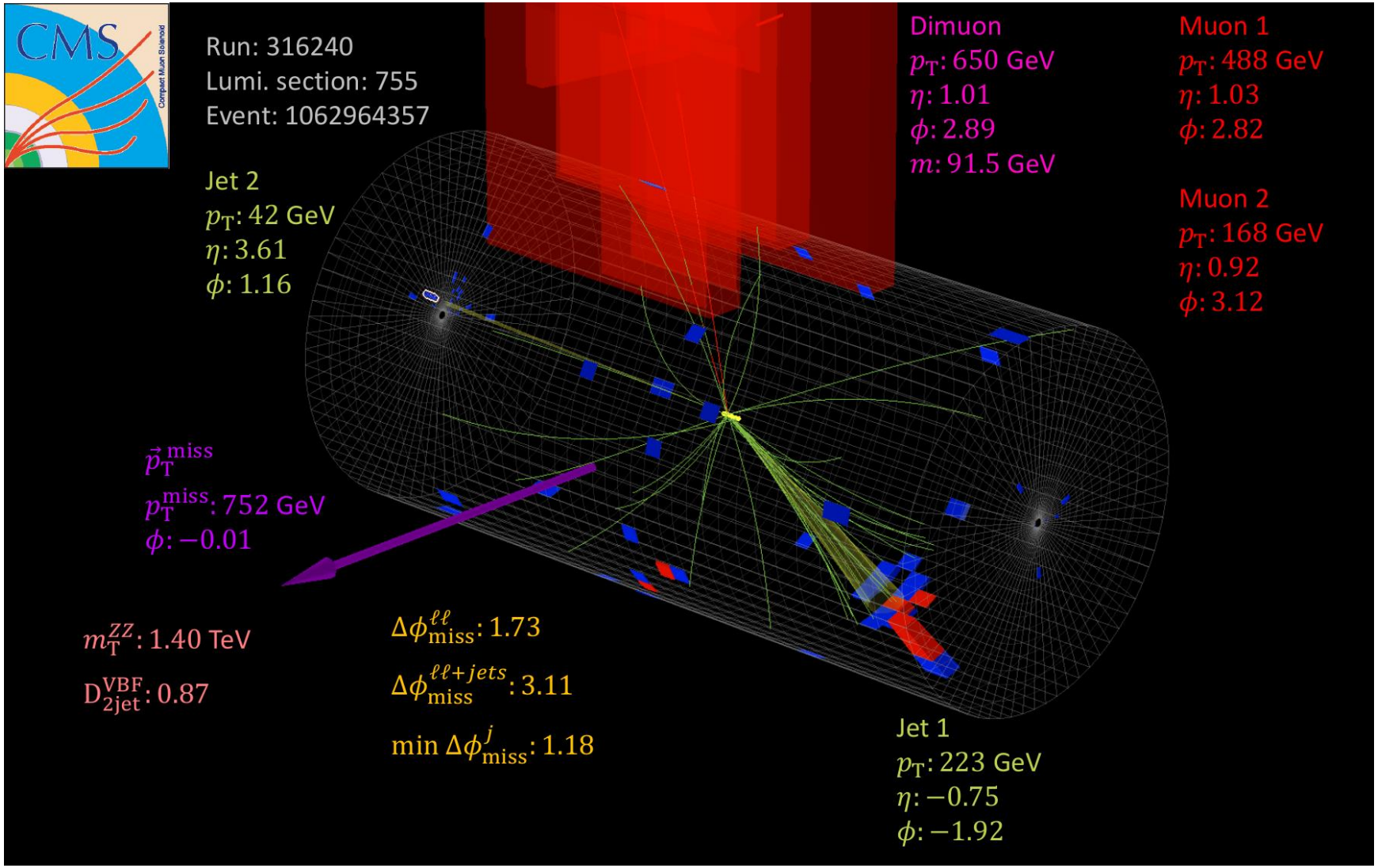

Here is a clean VBF/VBS $ZZ(\rightarrow 2\mu 2\nu)$+2 jets candidate at high mass with large D_{2jet}^{VBF} value, as also evident from the two high-rapidity jets at opposite hemispheres.

Evidence for off-shell from $2\ell 2\nu + 4\ell$

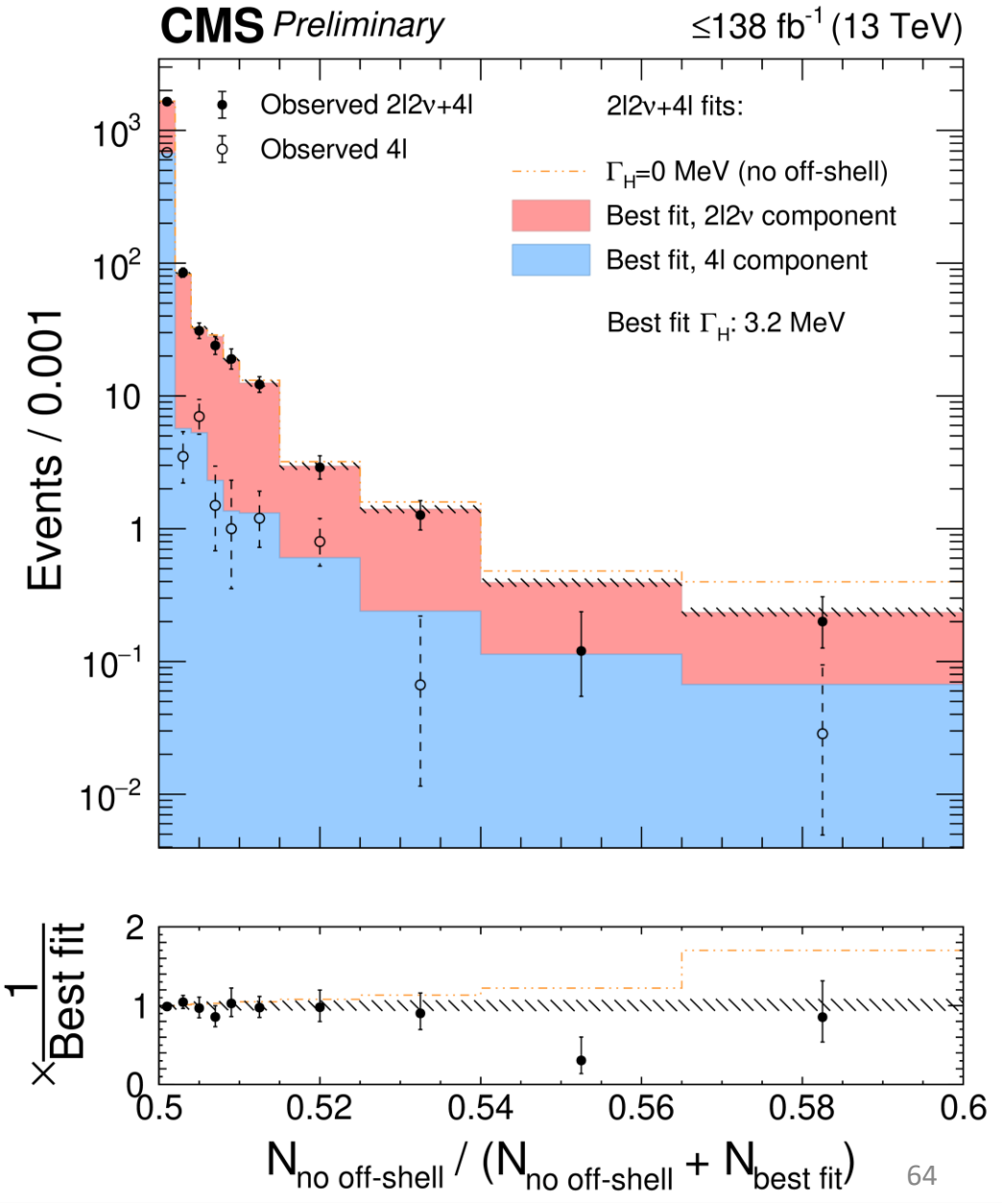

Plotted is a bin-by-bin ratio over the histograms of all observables and categories.

Evidence for off-shell from $2\ell 2\nu + 4\ell$

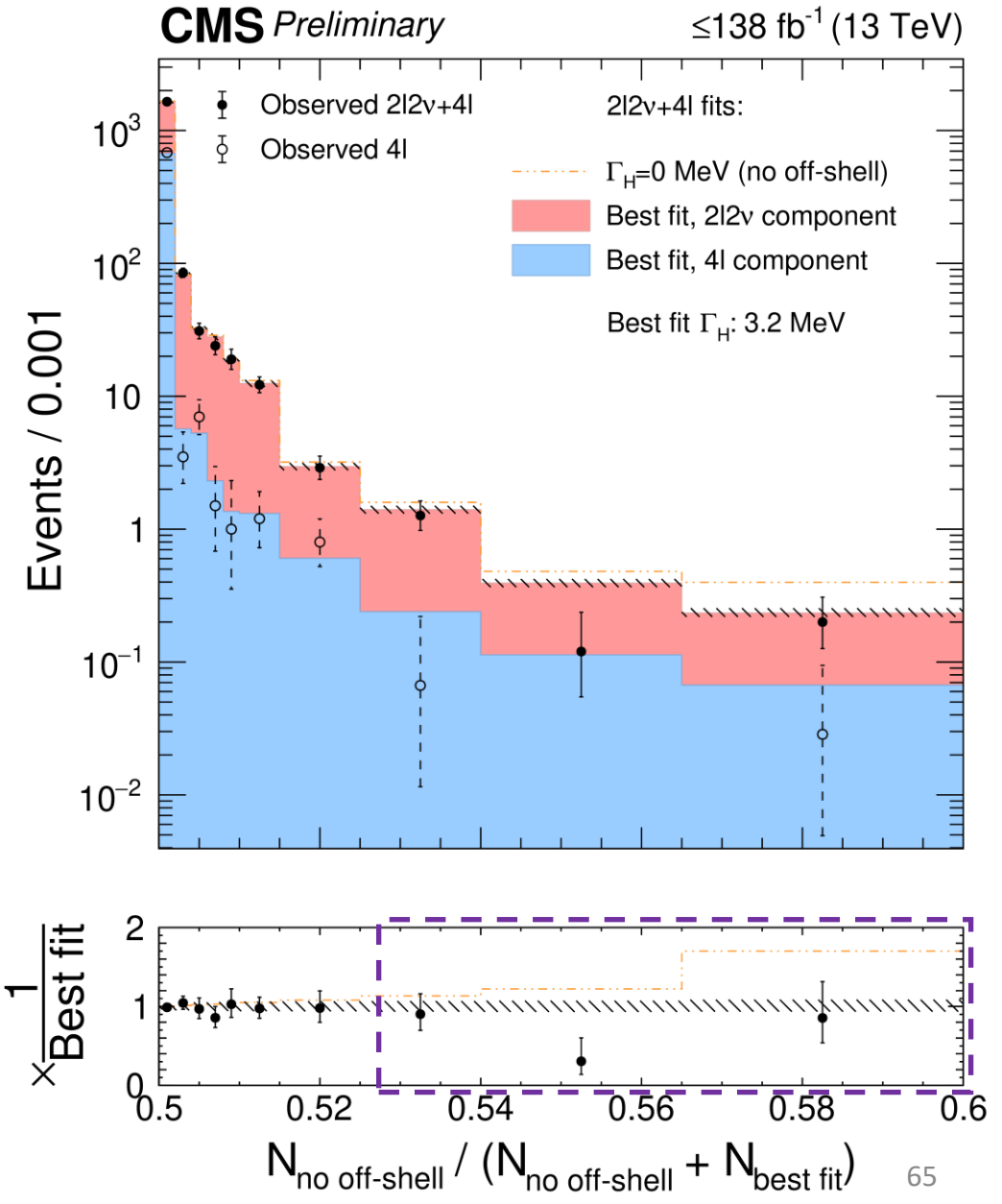

Plotted is a bin-by-bin ratio over the histograms of all observables and categories.

Once everything is considered, significance reaches 3.6 standard deviations.

Evidence for off-shell from $2\ell 2\nu + 4\ell$

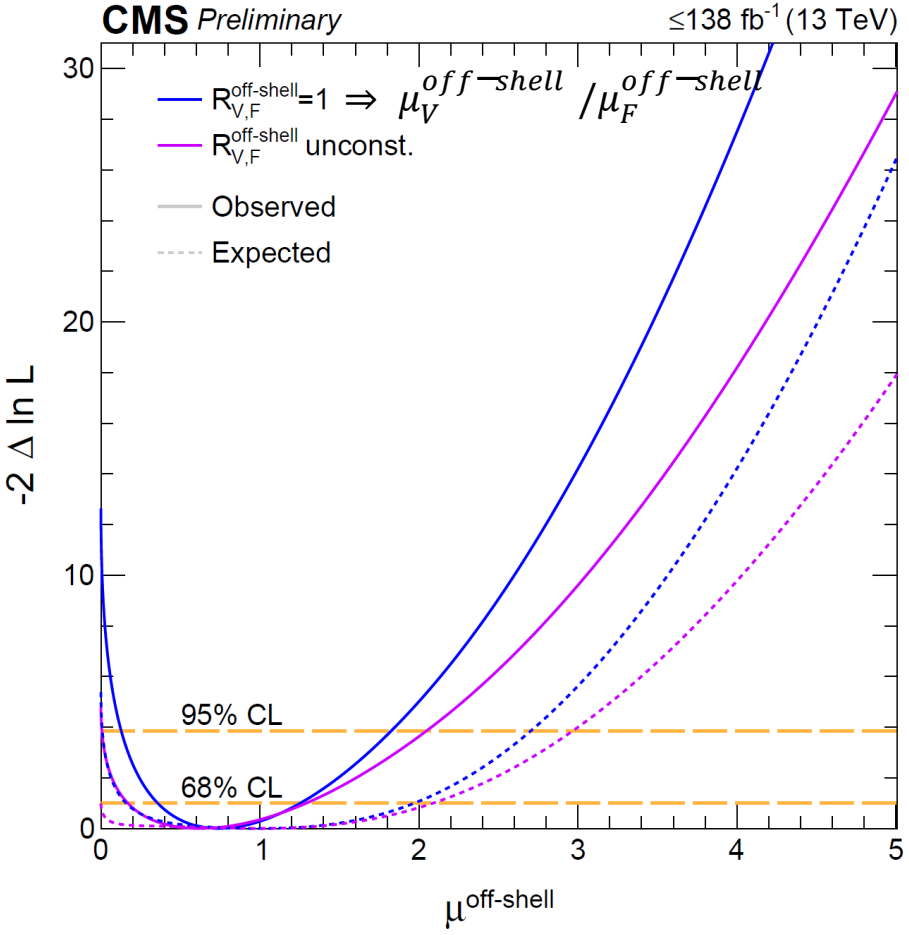

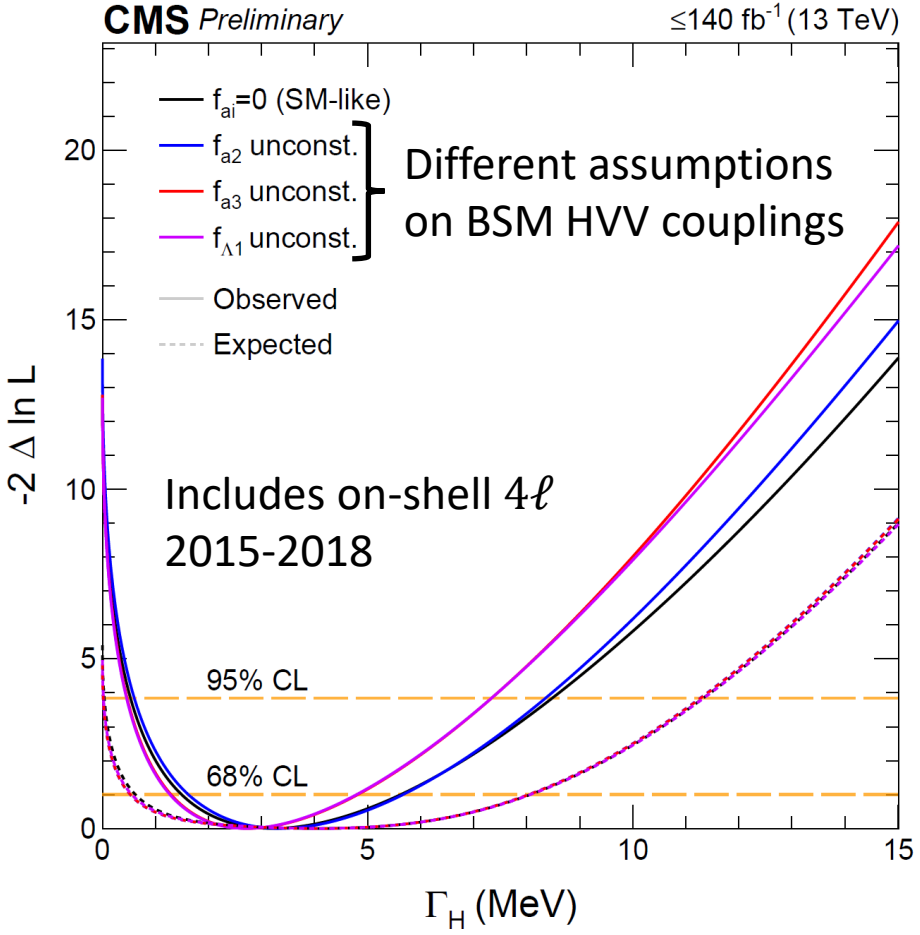

No – off-shell scenario ($\mu^{off-shell} = 0$) is excluded by more than 99.9% confidence

Observed $\Gamma_H = 3.2^{+2.4}_{-1.7}$ MeV
[0.53, 8.5] MeV @ 95% CL

Evidence for off-shell from $2\ell 2\nu + 4\ell$

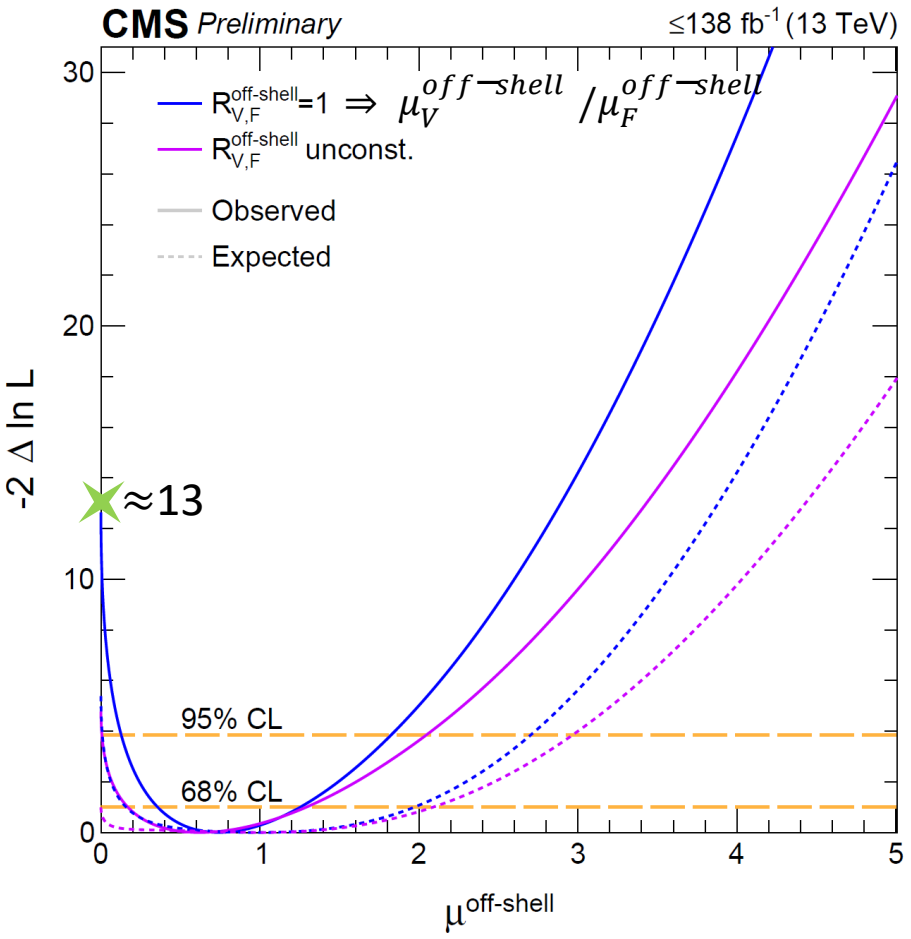

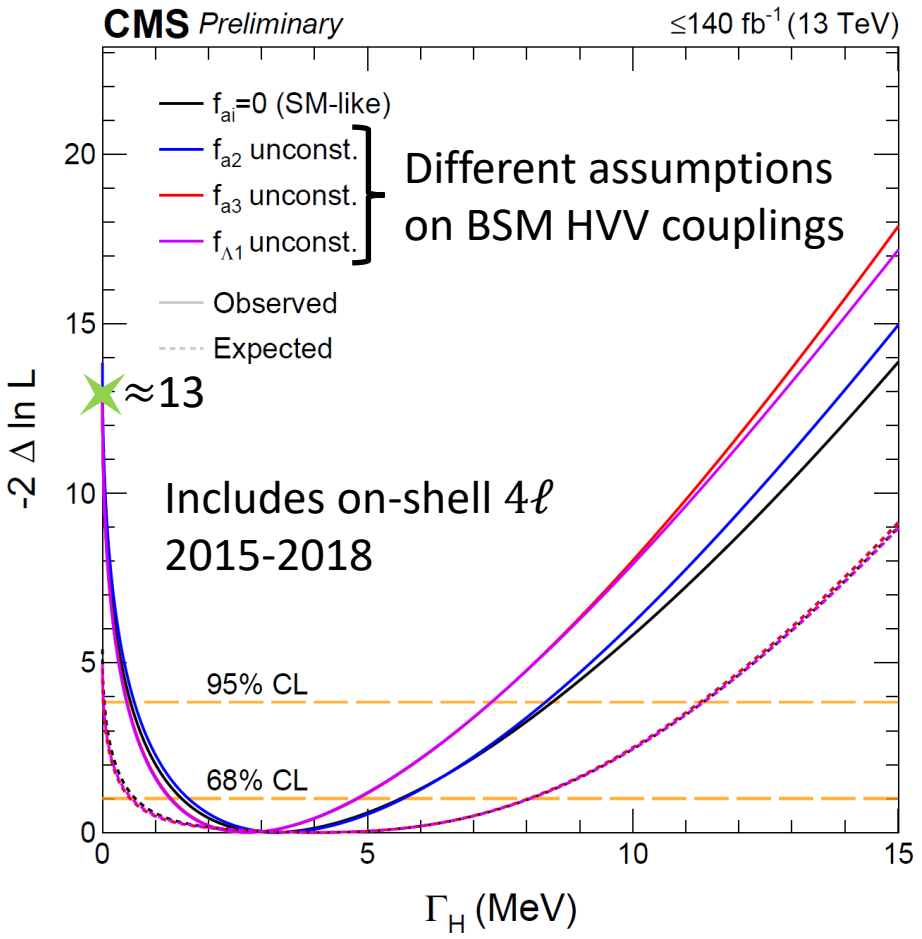

No – off-shell scenario ($\mu^{off-shell} = 0$) is excluded by more than 99.9% confidence (3.6 standard deviations)

Observed $\Gamma_H = 3.2^{+2.4}_{-1.7}$ MeV
[0.53, 8.5] MeV @ 95% CL

Evidence for off-shell from $2\ell 2\nu + 4\ell$

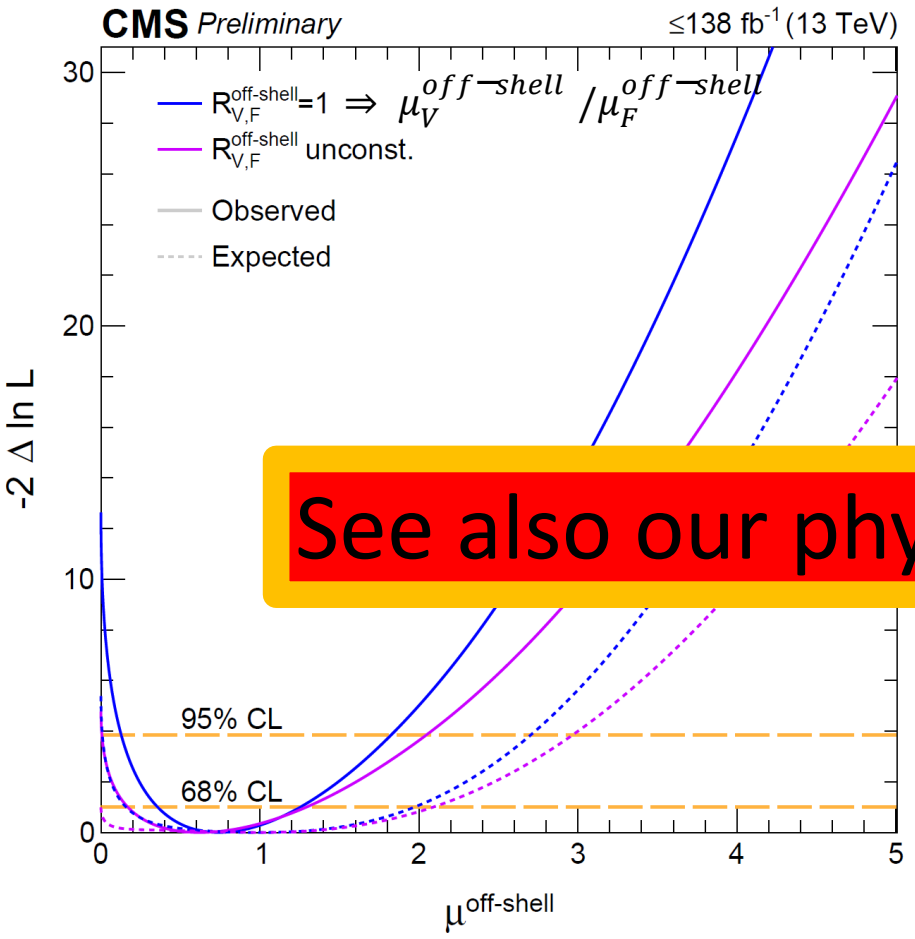

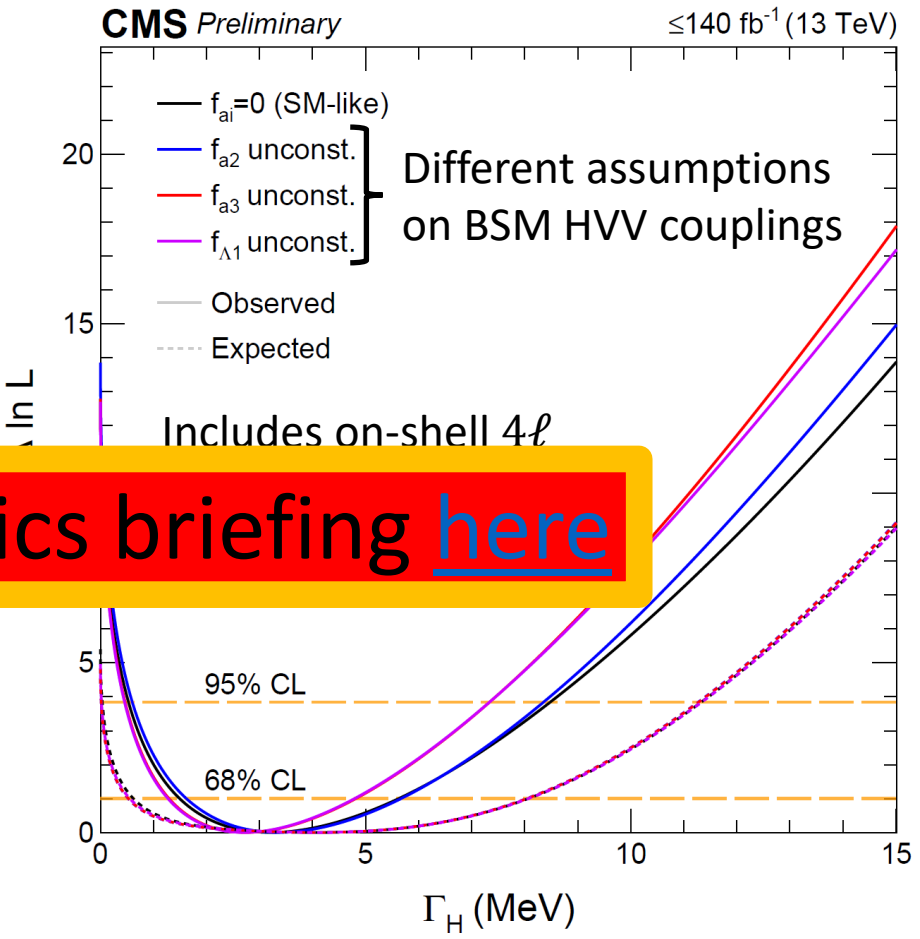

See also our physics briefing here

No – off-shell scenario ($\mu^{off-shell} = 0$) is excluded by more than 99.9% confidence (3.6 standard deviations)

Observed $\Gamma_H = 3.2^{+2.4}_{-1.7}$ MeV
[0.53, 8.5] MeV @ 95% CL

Off-shell combination: $\mu_F^{off-shell}, \mu_V^{off-shell}$

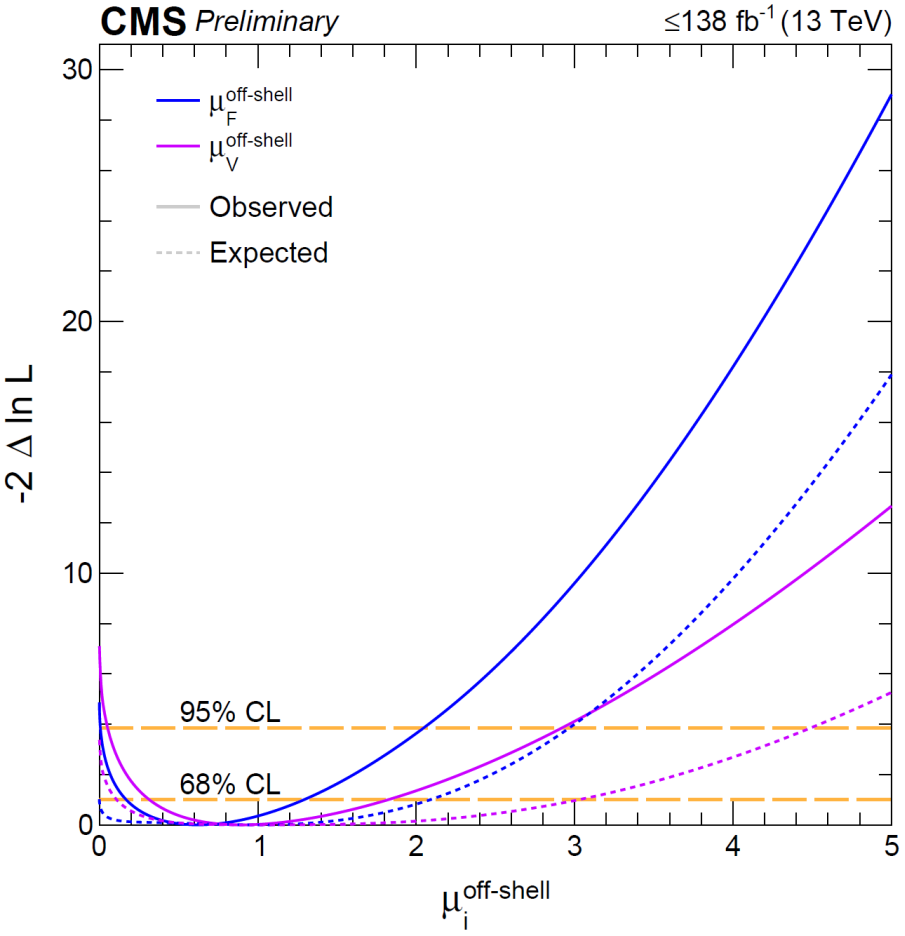

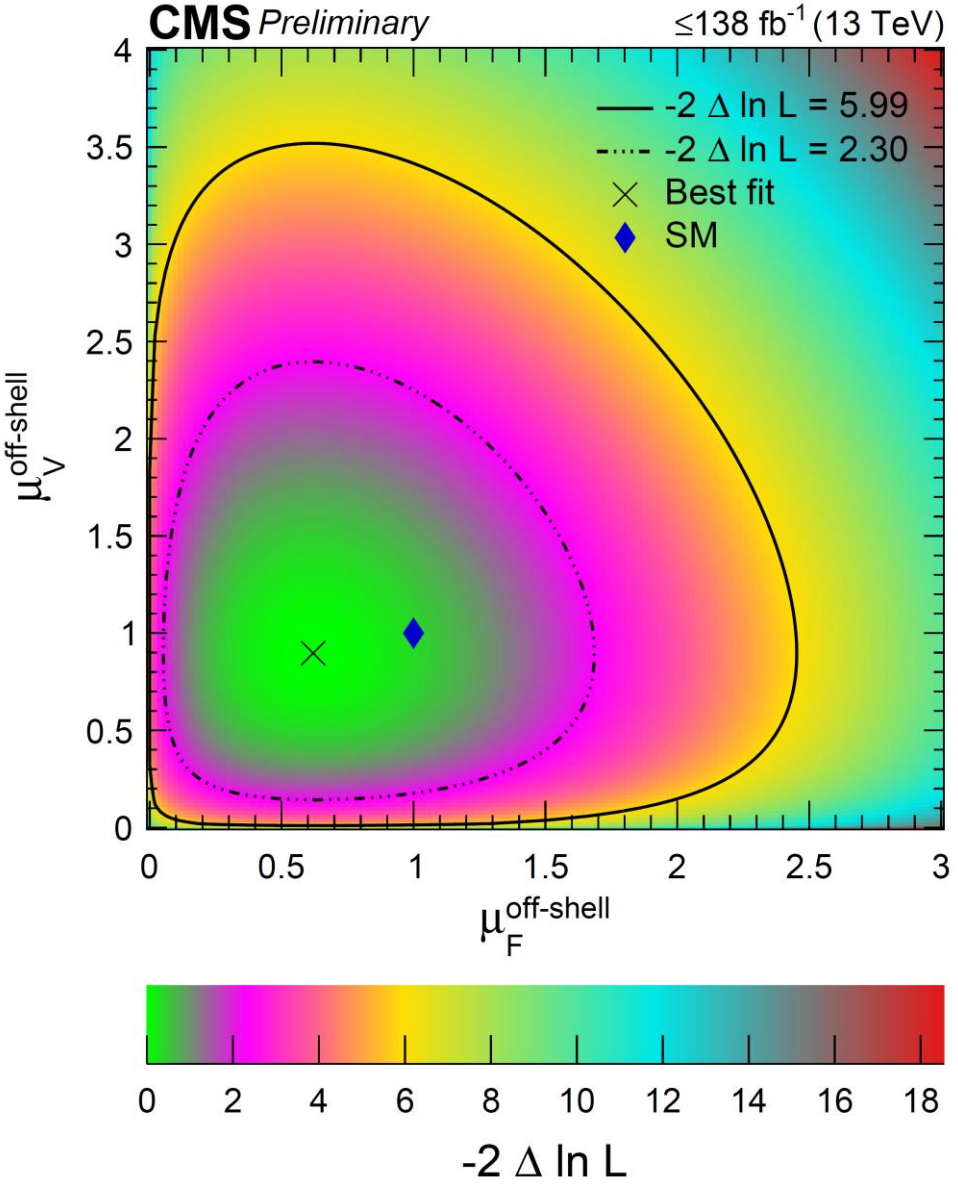

Joint constraints on
$\mu_F^{off-shell}$ (gg production) and
$\mu_V^{off-shell}$ (EW production)

Off-shell combination: $\mu_F^{off-shell}, \mu_V^{off-shell}$

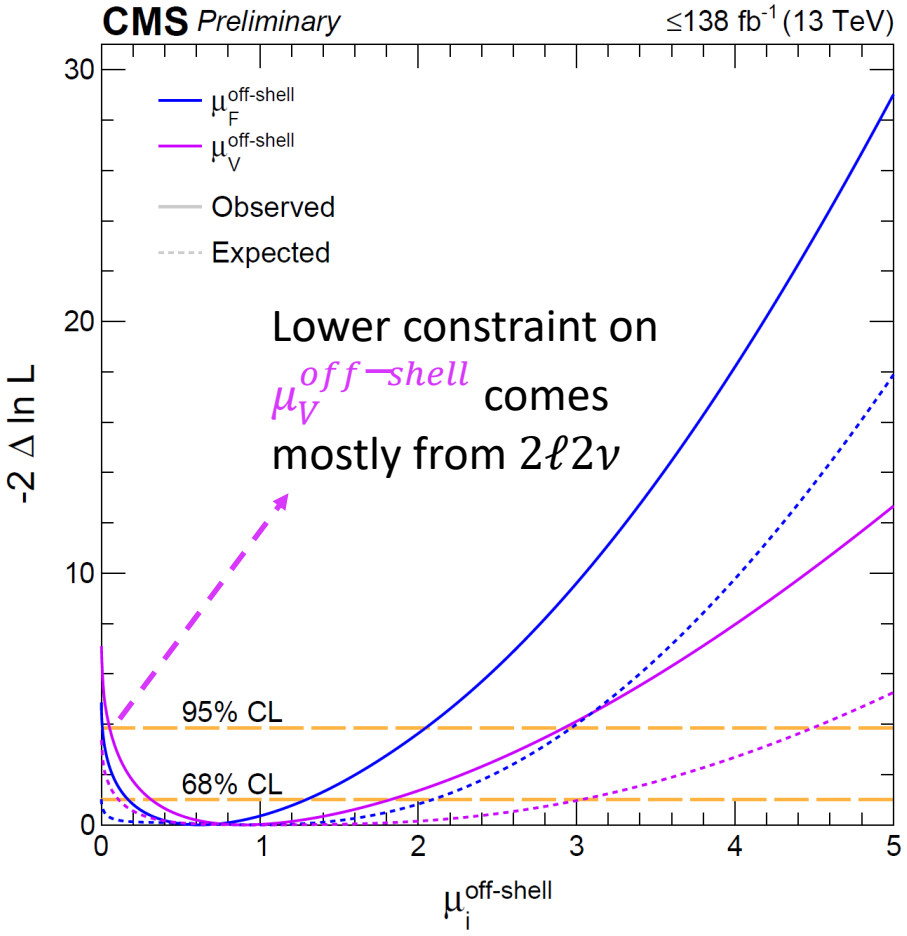

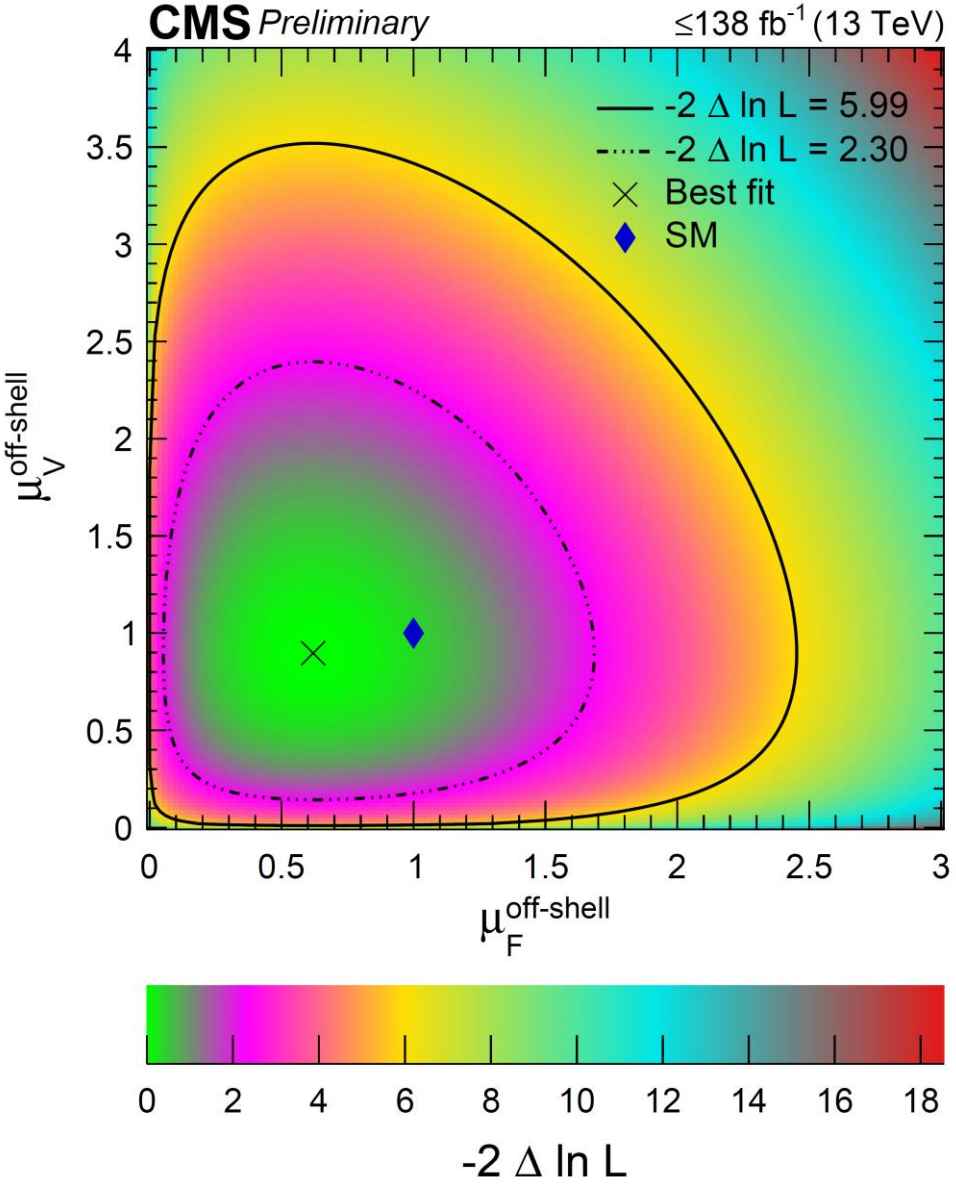

Joint constraints on
$\mu_F^{off-shell}$ (gg production) and
$\mu_V^{off-shell}$ (EW production)

Anomalous HVV couplings from off-shell

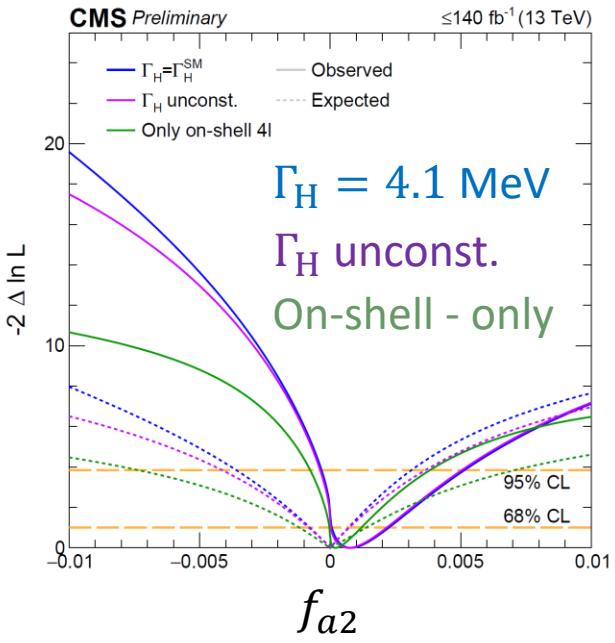

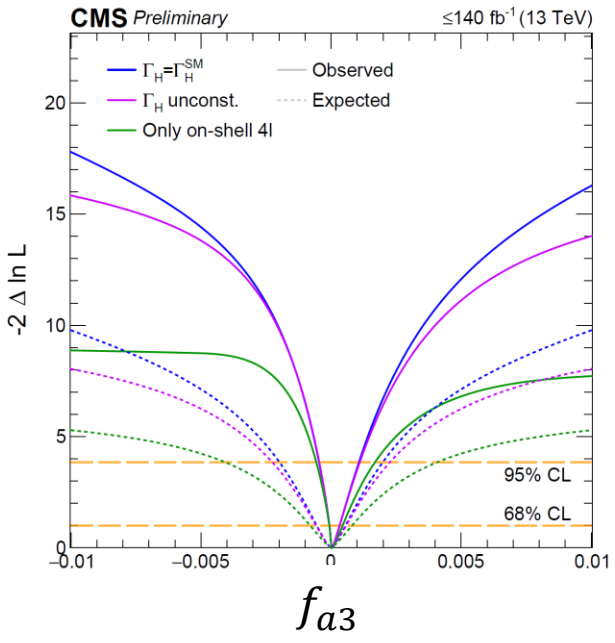

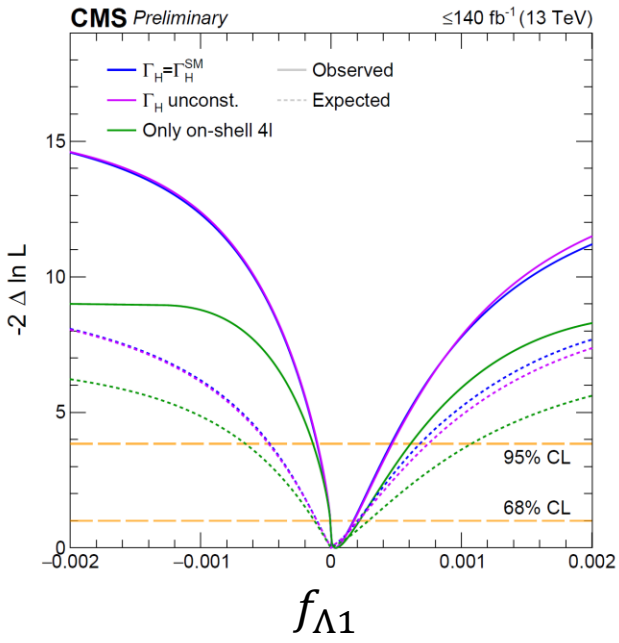

On-shell constraints (from CMS-HIG-19-009):

	f_{a3}	f_{a2}	$f_{\Lambda 1}$
best fit	0.00004	0.00020	0.00004
68% CL	$[-0.00007, 0.00044]$	$[-0.00010, 0.00109]$	$[-0.00002, 0.00022]$
95% CL	$[-0.00055, 0.00168]$	$[-0.00078, 0.00368]$	$[-0.00014, 0.00060]$

$O(10^{-5}-10^{-3})$ constraints on fractional on-shell contributions

O(10%) improvement at 95% CL from adding off-shell information

Comparison to on-shell $4\ell + \tau\tau$

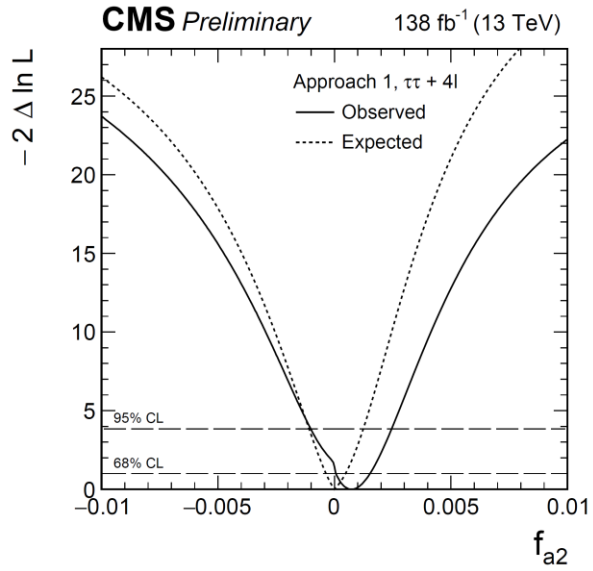

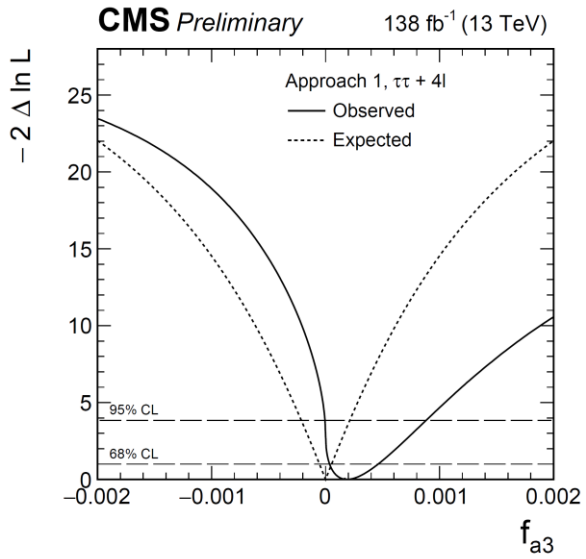

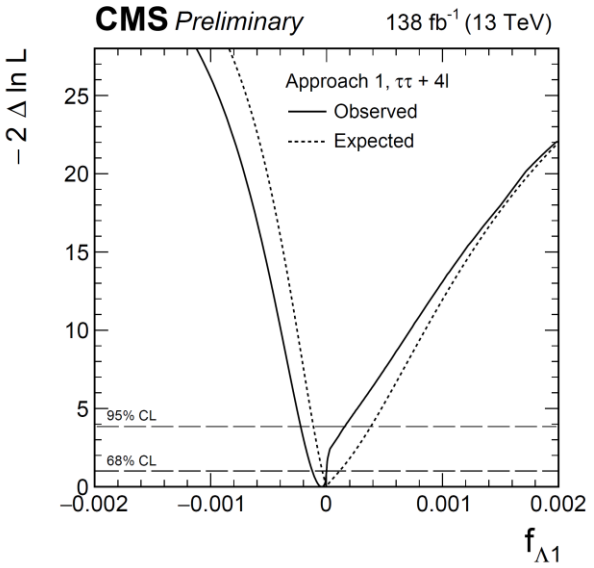

[CMS-PAS-HIG-20-007]

Parameter	Observed / (10^{-3})		Expected / (10^{-3})	
	68% CL	95% CL	68% CL	95% CL
f_{a3}	$0.20^{+0.26}_{-0.16}$	$[-0.01, 0.88]$	0.00 ± 0.05	$[-0.21, 0.21]$
f_{a2}	$0.7^{+0.8}_{-0.6}$	$[-1.0, 2.5]$	$0.0^{+0.5}_{-0.4}$	$[-1.1, 1.2]$
$f_{\Lambda 1}$	$-0.04^{+0.04}_{-0.08}$	$[-0.22, 0.16]$	$0.00^{+0.11}_{-0.04}$	$[-0.11, 0.38]$

On-shell 4ℓ
+ on-shell (VBF) $H \to \tau\tau$
improves constraints by ~ 2
compared to on-shell 4ℓ-only
→ VBF production more sensitive than decay
→ Significant enough VBF signal

On-shell $4\ell + \tau\tau$ $[+t\bar{t}H(\rightarrow \gamma\gamma)]$

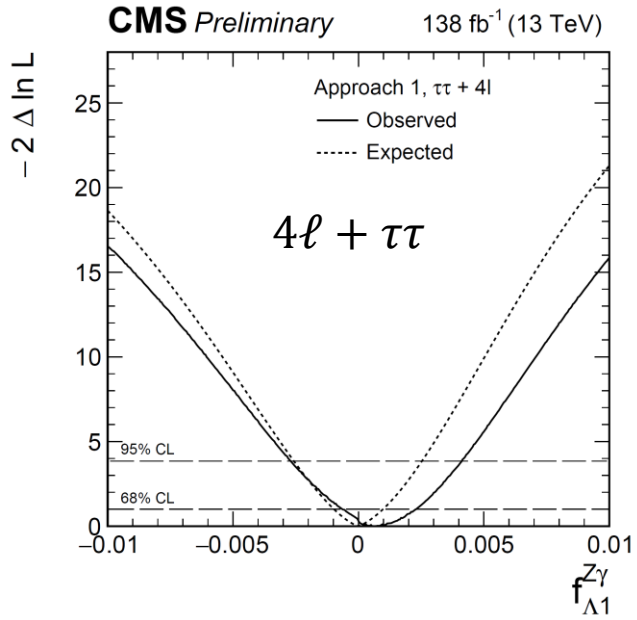

Extra term in the HVV amplitude $\propto -\frac{q_\gamma^2}{\Lambda_1^2} m_Z^2 \epsilon_Z^* \epsilon_\gamma^*$ only accessible on-shell

On-shell $4\ell + \tau\tau$ $[+t\bar{t}H(\rightarrow \gamma\gamma)]$

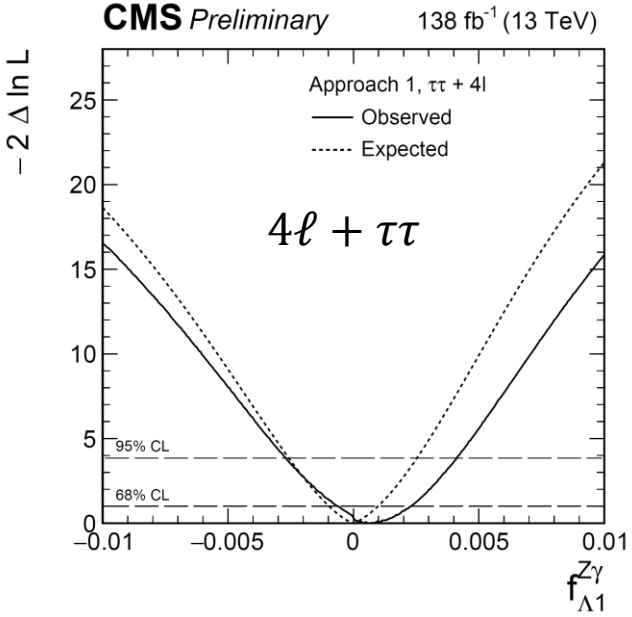

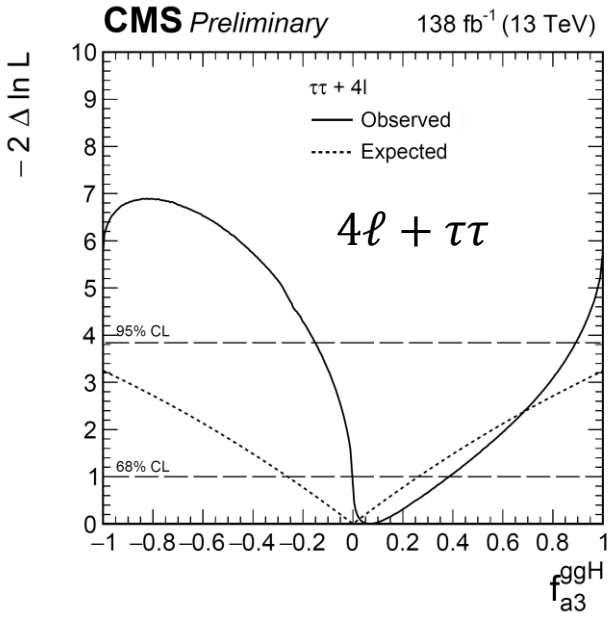

Extra term in the HVV amplitude $\propto -\frac{q_\gamma^2}{\Lambda_1^2} m_Z^2 \epsilon_Z^* \epsilon_\gamma^*$ only accessible on-shell

Also constrain pseudoscalar couplings of the Higgs to gluons (EFT, a_3^{ggH})

On-shell $4\ell + \tau\tau$ $[+t\bar{t}H(\rightarrow \gamma\gamma)]$

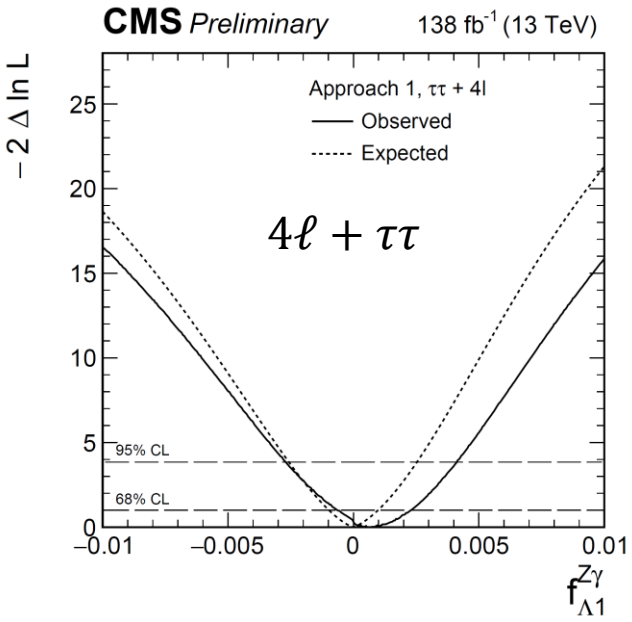

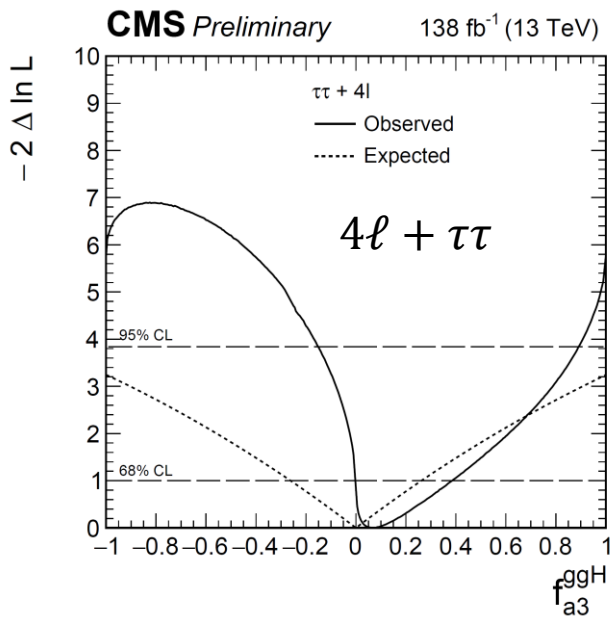

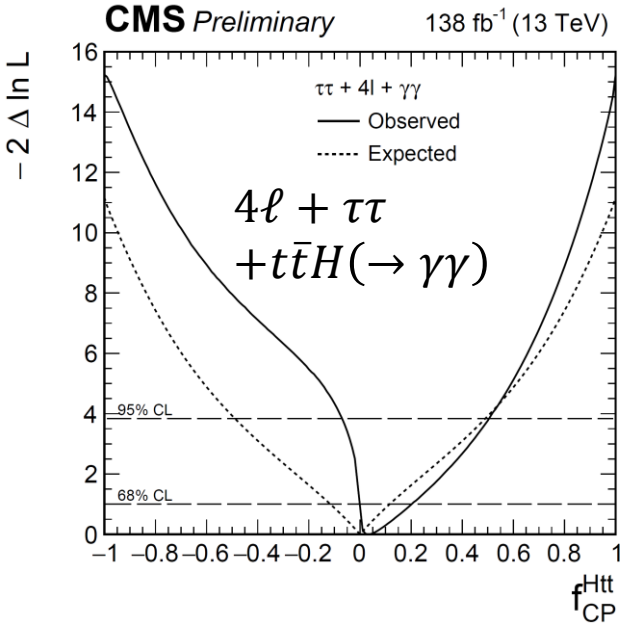

Extra term in the HVV amplitude $\propto -\frac{q_\gamma^2}{\Lambda_1^2} m_Z^2 \epsilon_Z^* \epsilon_\gamma^*$ only accessible on-shell

Also constrain pseudoscalar couplings of the Higgs to gluons (EFT, a_3^{ggH}) or tops (direct Htt)

$$\mathcal{A}(\mathrm{Hff}) = -\frac{m_f}{v}\bar{\psi}_f \left(\kappa_\mathrm{f} + \mathrm{i}\,\tilde{\kappa}_\mathrm{f}\gamma_5\right)\psi_f$$

SM PS

So far, we have covered:

So far, we have covered:

→ Visible decay modes are mostly consistent with the SM, but O(10%) discrepancy is possible.

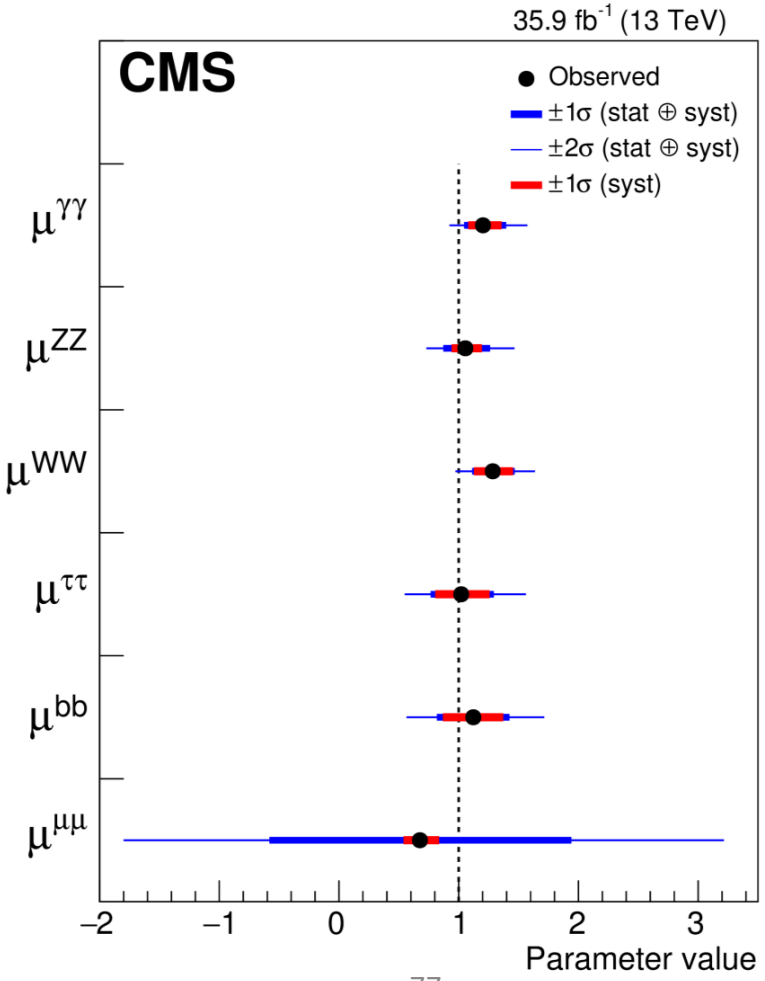

So far, we have covered:

→ Visible decay modes are mostly consistent with the SM, but O(10%) discrepancy is possible.

→ Measured Higgs width seems to be close to what the SM predicts.

→ Value can still be $\times \sim 2$ wrt. the prediction according to this measurement.

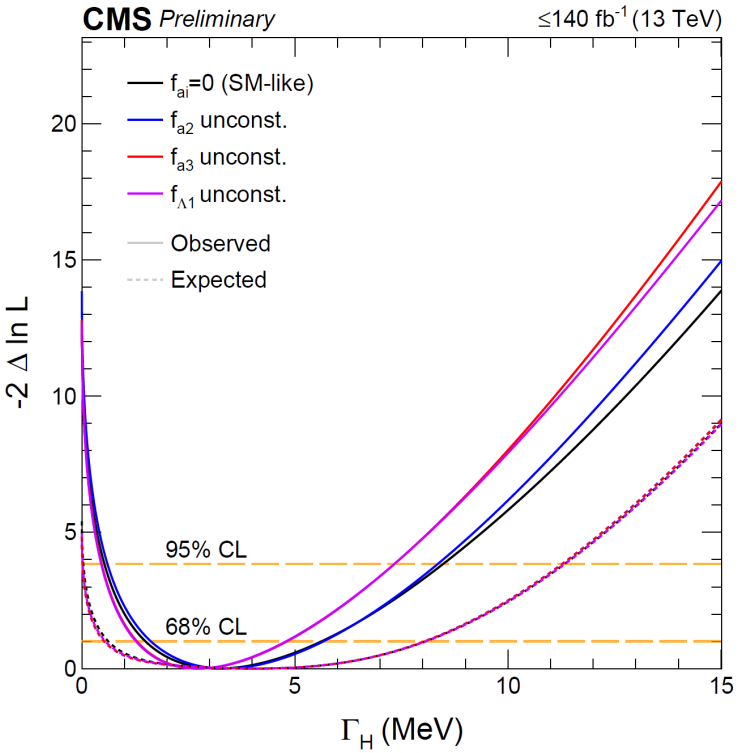

So far, we have covered:

→ Visible decay modes are mostly consistent with the SM, but O(10%) discrepancy is possible.

→ Measured Higgs width seems to be close to what the SM predicts.

→ Value can still be $\times \sim 2$ wrt. the prediction according to this measurement.

→ Anomalous couplings of the Higgs are not observed yet to deviate significantly from null.

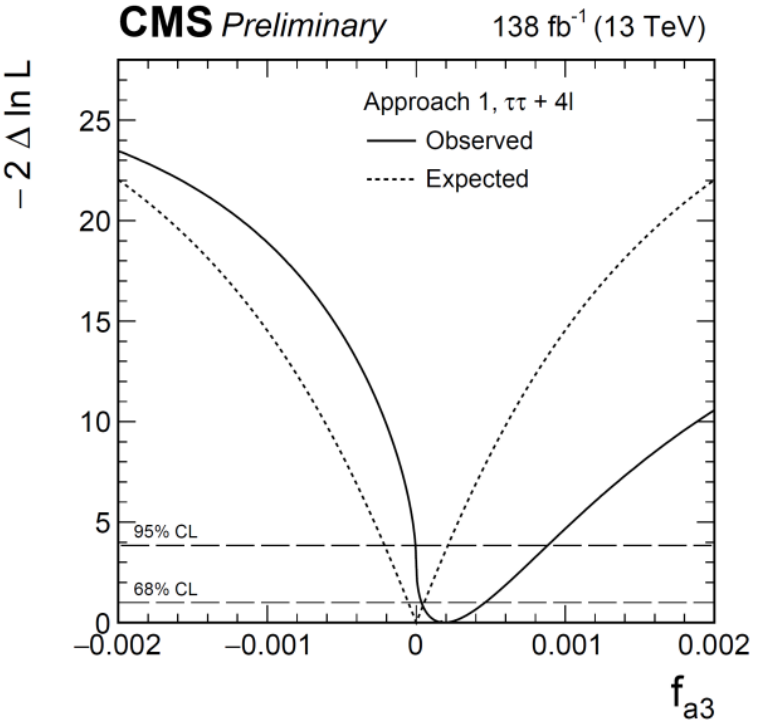

So far, we have covered:

→ Visible decay modes are mostly consistent with the SM, but O(10%) discrepancy is possible.

→ Measured Higgs width seems to be close to what the SM predicts.

→ Value can still be $\times \sim 2$ wrt. the prediction according to this measurement.

→ Anomalous couplings of the Higgs are not observed yet to deviate significantly from null.

What about decay modes that escape detection?

Invisible Higgs decays

CMS-PAS-HIG-20-003:
Analysis of the $H \rightarrow$ invisible

Includes data from 2017 and 2018, and combines with the 2016 analysis

Events are categorized as
- "Missing momentum-triggered" (MTR)
  $p_{\mathrm{T}}^{\mathrm{miss}} > 250$ GeV
- "VBF-jets triggered" (VTR)
  Mainly 250 GeV $> p_{\mathrm{T}}^{\mathrm{miss}} > 160$ GeV

Targets VBF production signature at high m_{jj}:
- MTR: $m_{jj} > 200$ GeV
- VTR: $m_{jj} > 900$ GeV

Fits performed with m_{jj} as the observable

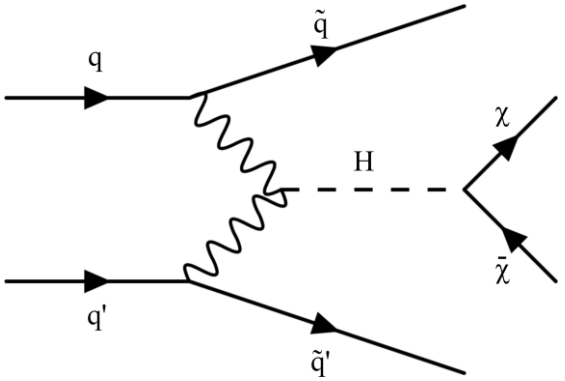

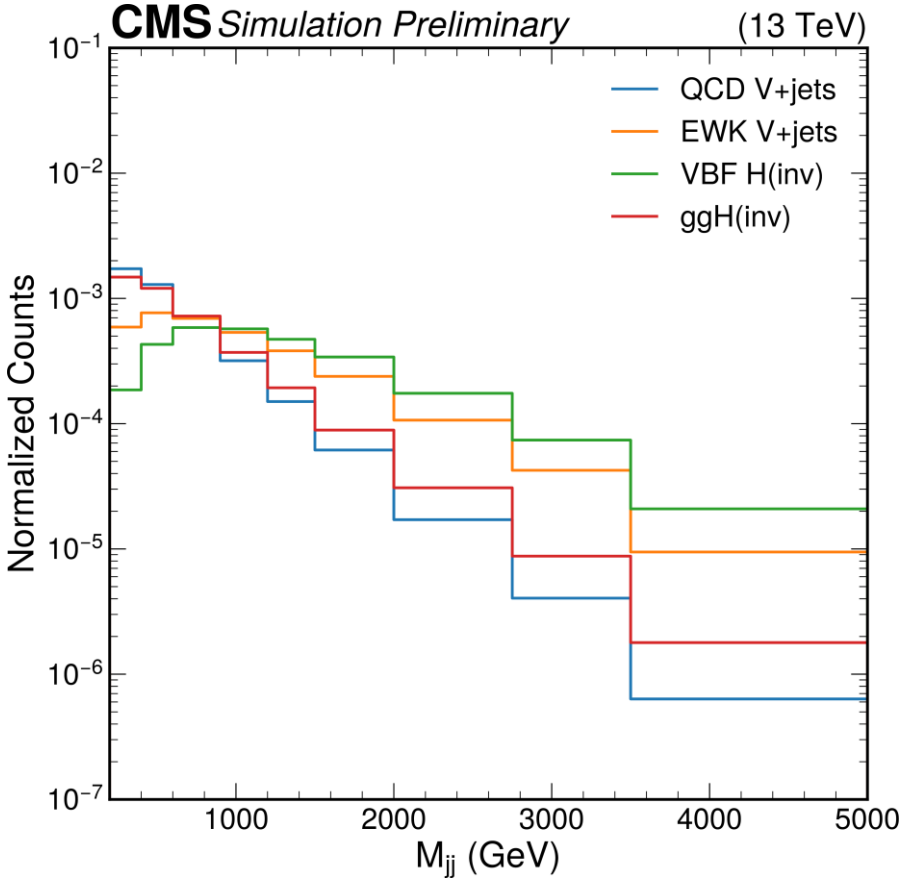

VBF $H \rightarrow$ invisible: Backgrounds

$Z \rightarrow \nu\nu$:

→ Estimated using $Z \rightarrow \ell\ell$ and γ+jets

(MTR only) control samples

VBF $H \rightarrow$ invisible: Backgrounds

$Z \rightarrow \nu\nu$:
→ Estimated using $Z \rightarrow \ell\ell$ and γ+jets
(MTR only) control samples

$W \rightarrow \ell\nu$ with a lost lepton:
→ Estimated using single lepton control samples

VBF $H \rightarrow$ invisible: Backgrounds

$Z \rightarrow \nu\nu$:
→ Estimated using $Z \rightarrow \ell\ell$ and γ+jets
(MTR only) control samples

$W \rightarrow \ell\nu$ with a lost lepton:
→ Estimated using single lepton control samples

HF noise:
→ Analysis already applied HF noise removal
→ Invert to obtain a control sample, apply data-driven weights based on rejection rate

VBF $H \rightarrow$ invisible: Backgrounds

$Z \rightarrow \nu\nu$:
→ Estimated using $Z \rightarrow \ell\ell$ and γ+jets (MTR only) control samples

$W \rightarrow \ell\nu$ with a lost lepton:
→ Estimated using single lepton control samples

HF noise:
→ Analysis already applied HF noise removal
→ Invert to obtain a control sample, apply data-driven weights based on rejection rate

QCD multijet:
→ Enters as a result of mismeasured jets
→ Estimated through a parametrization of the $\min \Delta\phi$ between jets and $\vec{p}_{\mathrm{T}}^{\,\mathrm{miss}}$ from data

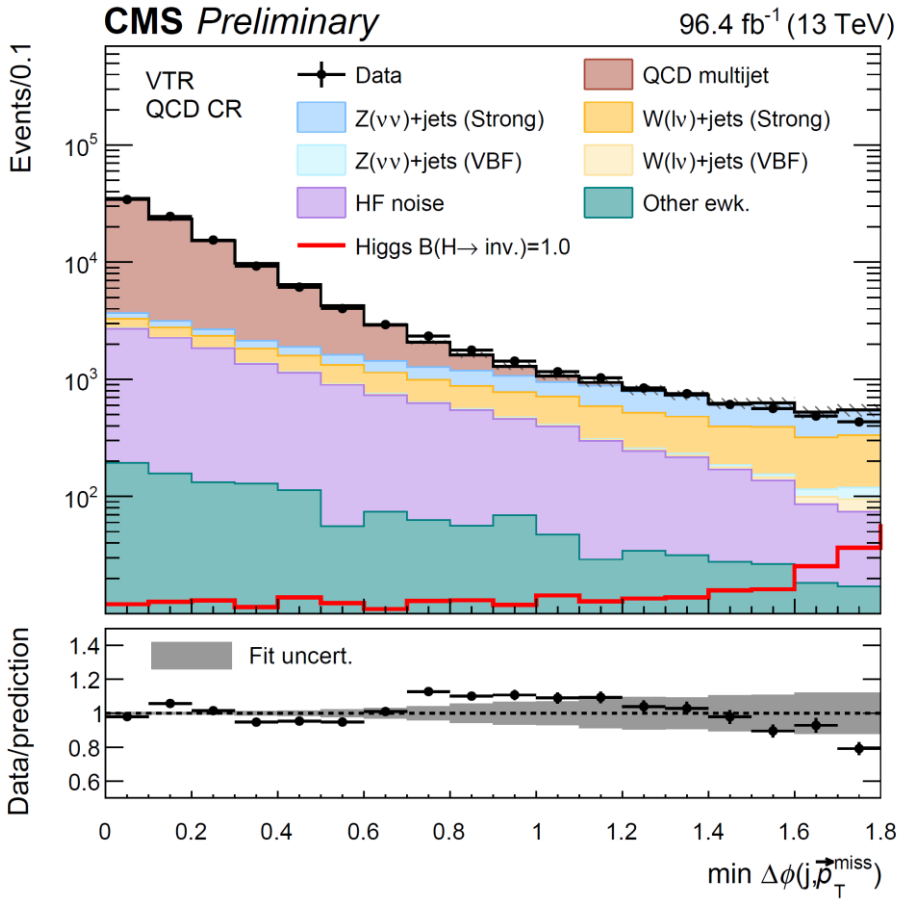

VBF $H \rightarrow$ invisible: Backgrounds

$Z \rightarrow \nu\nu$:
→ Estimated using $Z \rightarrow \ell\ell$ and γ+jets (MTR only) control samples

$W \rightarrow \ell\nu$ with a lost lepton:
→ Estimated using single lepton control samples

HF noise:
→ Analysis already applied HF noise removal
→ Invert to obtain a control sample, apply data-driven weights based on rejection rate

QCD multijet:
→ Enters as a result of mismeasured jets
→ Estimated through a parametrization of the $\min \Delta\phi$ between jets and $\vec{p}_{\mathrm{T}}^{\,\mathrm{miss}}$ from data

All others are small, estimated from simulation

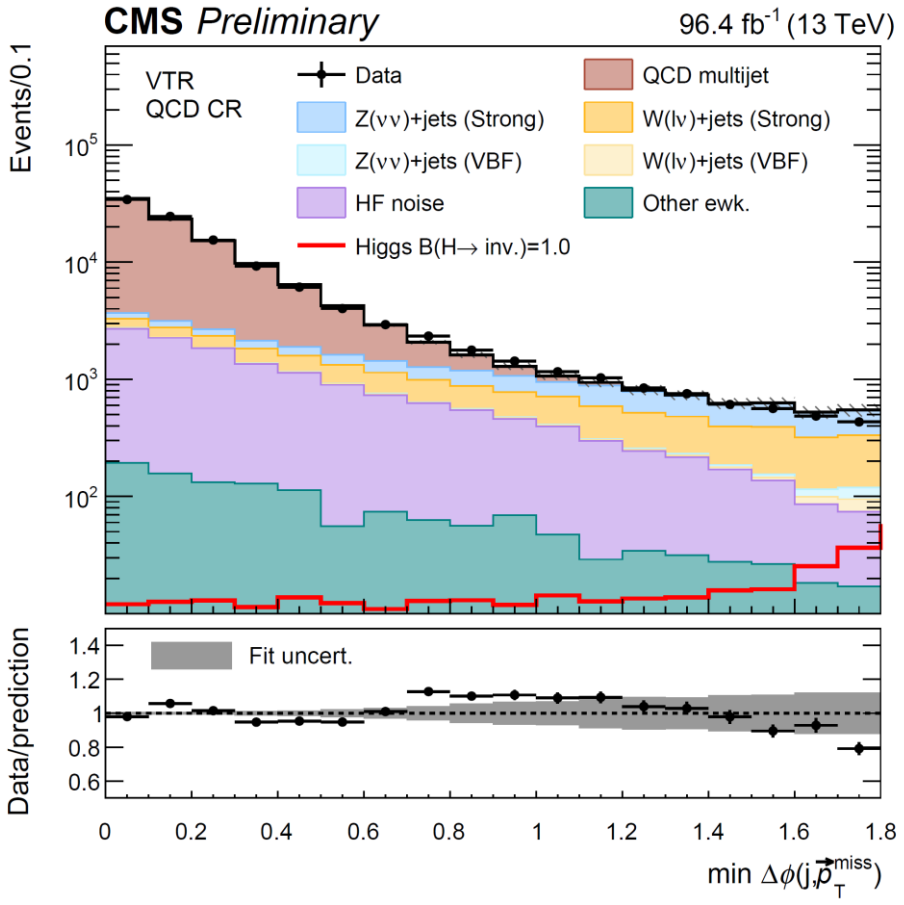

VBF $H \rightarrow$ invisible: Event distributions

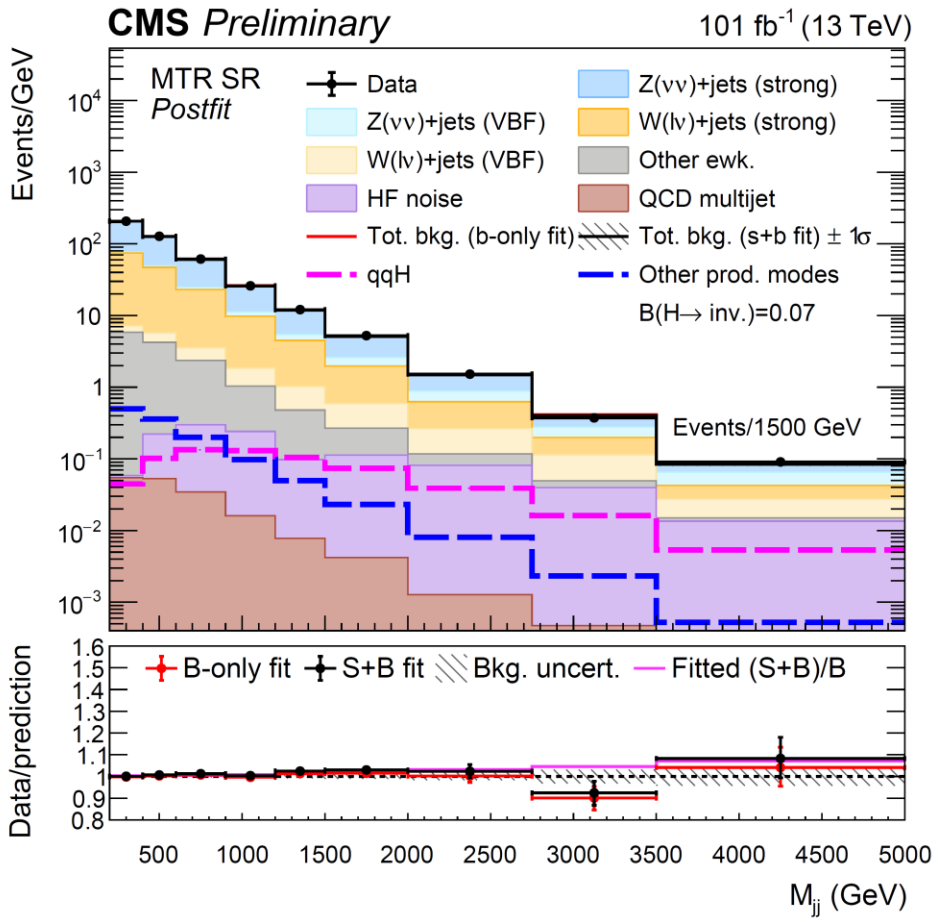

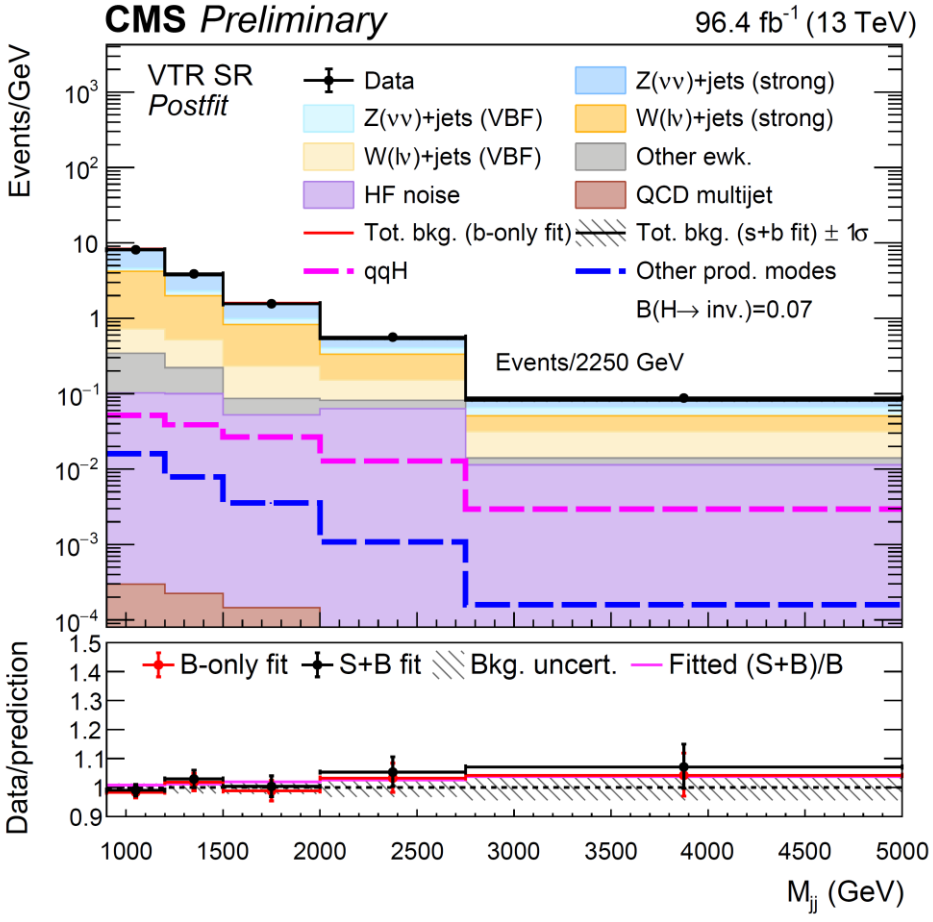

VBF (qqH on the figures) vs non-VBF Higgs production ratios are fixed to those predicted in the SM

→ Displayed signals are adjusted to the fitted branching ratio in data (= 0.07).

$H \rightarrow$ invisible limits

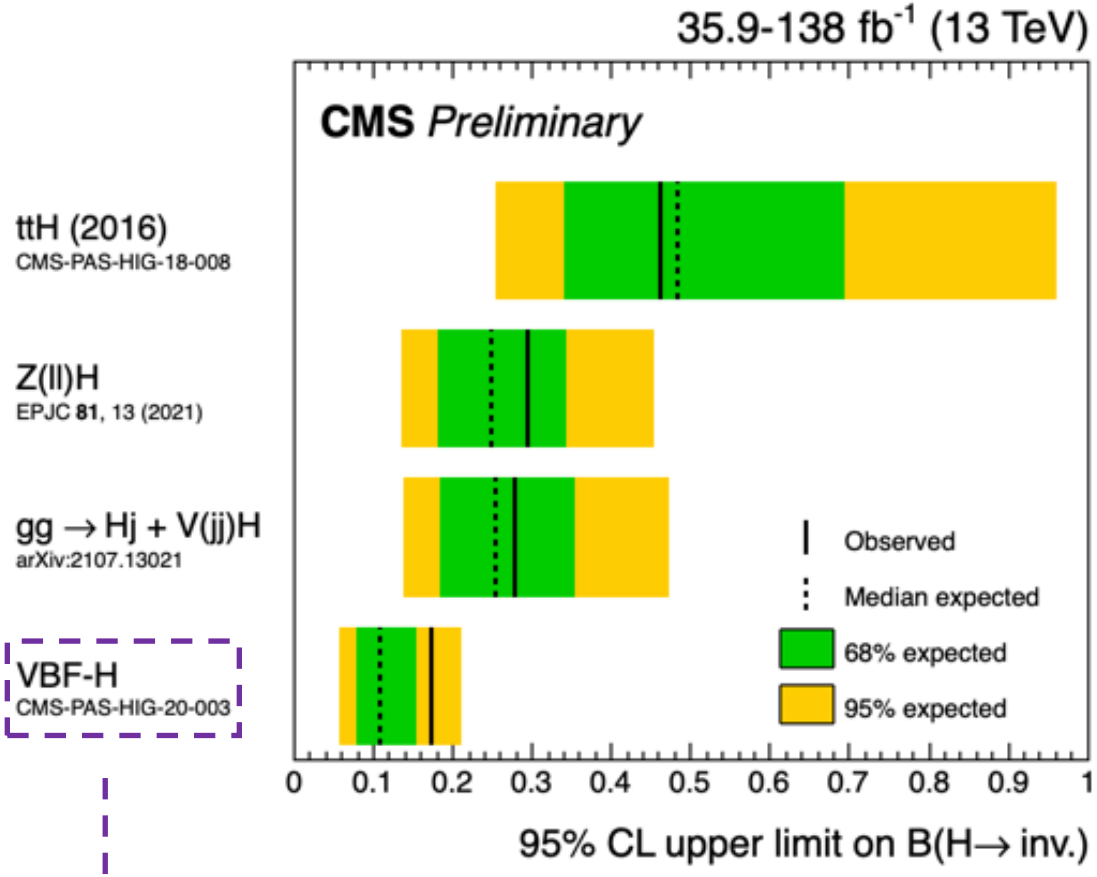

Observed	Expected	1-σ interval	2-σ interval
0.17	0.11	[0.08 – 0.15]	[0.06 – 0.21]

Most stringent CMS limit $B(H \rightarrow \text{inv.}) < 0.17$.

Other $H \rightarrow$ inv. interpretations as follows:

CMS-PAS-HIG-18-008: $t\bar{t}H$

CMS-EXO-19-003: $Z(\rightarrow \ell\ell)H$

CMS-EXO-20-004: $gg \rightarrow Hj, V(\rightarrow jj)H$

$H \rightarrow$ invisible limits

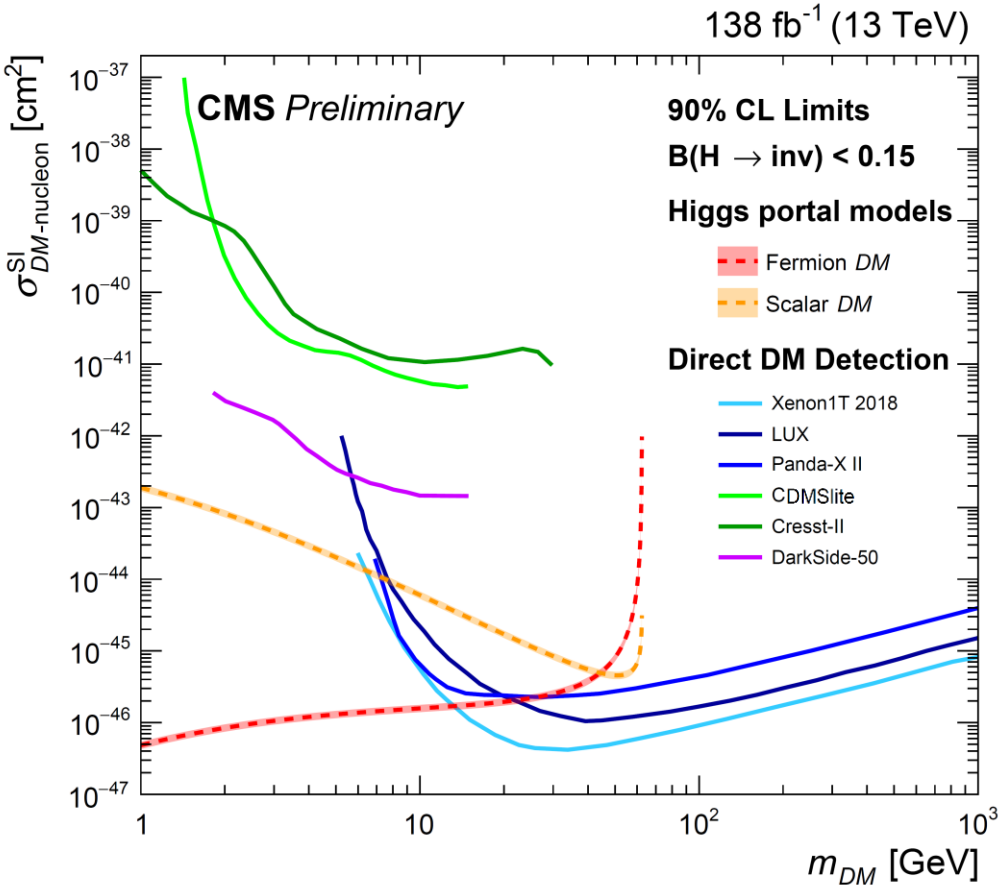

The limits can be interpreted in terms of Higgs portal models with $m_{DM} < m_{\mathrm{H}}/2$, where a dark matter scatters off a nucleus via Higgs boson exchange.

See also Refs. [1,2] for an extensive discussion of the relevant models.

Summary

Presented searches for new physics utilizing the Higgs boson

Particular focus on constraints utilizing the width/lifetime and related measurements:
→ Overview of direct measurements of Higgs branching ratios, width and lifetime
→ First off-shell production evidence from CMS-PAS-HIG-21-013 using $4\ell + 2\ell 2\nu$
→ Constraints on anomalous HVV couplings
  → Using off-shell information, or
  → On-shell $4\ell +$ from CMS-PAS-HIG-20-007
    Also includes results on Hgg and Htt couplings after adding $t\bar{t}H(\rightarrow \gamma\gamma)$
→ Limits on the $H \rightarrow$ invisible branching ratio from CMS-PAS-HIG-20-003 using VBF-like events
  → Interpretation as dark matter-nucleon scattering via Higgs boson exchange

Stay tuned for more exciting results as we continue to collect data in Run 3 and develop analysis methods further!

Back-up

Full table of observables for off-shell 4ℓ

Category	VBF-tagged	VH-tagged	Untagged
Selection	$\mathcal{D}_{\text{2jet}}^{\text{VBF}}$ or $\mathcal{D}_{\text{2jet}}^{\text{VBF,BSM}} > 0.5$	$\mathcal{D}_{\text{2jet}}^{\text{WH}}$ or $\mathcal{D}_{\text{2jet}}^{\text{WH,BSM}}$, or $\mathcal{D}_{\text{2jet}}^{\text{ZH}}$ or $\mathcal{D}_{\text{2jet}}^{\text{ZH,BSM}} > 0.5$	Rest of events
SM obs.	$m_{4\ell}$, $\mathcal{D}_{\text{bkg}}^{\text{VBF+dec}}$, $\mathcal{D}_{\text{bsi}}^{\text{VBF+dec}}$	$m_{4\ell}$, $\mathcal{D}_{\text{bkg}}^{\text{VH+dec}}$, $\mathcal{D}_{\text{bsi}}^{\text{VH+dec}}$	$m_{4\ell}$, $\mathcal{D}_{\text{bkg}}^{\text{kin}}$, $\mathcal{D}_{\text{bsi}}^{\text{gg,dec}}$
a_3 obs.	$m_{4\ell}$, $\mathcal{D}_{\text{bkg}}^{\text{VBF+dec}}$, $\mathcal{D}_{0-}^{\text{VBF+dec}}$	$m_{4\ell}$, $\mathcal{D}_{\text{bkg}}^{\text{VH+dec}}$, $\mathcal{D}_{0-}^{\text{VH+dec}}$	$m_{4\ell}$, $\mathcal{D}_{\text{bkg}}^{\text{kin}}$, $\mathcal{D}_{0-}^{\text{dec}}$
a_2 obs.	$m_{4\ell}$, $\mathcal{D}_{\text{bkg}}^{\text{VBF+dec}}$, $\mathcal{D}_{0h+}^{\text{VBF+dec}}$	$m_{4\ell}$, $\mathcal{D}_{\text{bkg}}^{\text{VH+dec}}$, $\mathcal{D}_{0h+}^{\text{VH+dec}}$	$m_{4\ell}$, $\mathcal{D}_{\text{bkg}}^{\text{kin}}$, $\mathcal{D}_{0h+}^{\text{dec}}$
Λ_1 obs.	$m_{4\ell}$, $\mathcal{D}_{\text{bkg}}^{\text{VBF+dec}}$, $\mathcal{D}_{\Lambda 1}^{\text{VBF+dec}}$	$m_{4\ell}$, $\mathcal{D}_{\text{bkg}}^{\text{VH+dec}}$, $\mathcal{D}_{\Lambda 1}^{\text{VH+dec}}$	$m_{4\ell}$, $\mathcal{D}_{\text{bkg}}^{\text{kin}}$, $\mathcal{D}_{\Lambda 1}^{\text{dec}}$

Full table of observables for on-shell 4ℓ

2016-2018 categorization follows the order
- VBF-2 jet
- VH-hadronic
- VH-leptonic (1 lepton or an $\ell^+\ell^-$ pair)
- VBF-1 jet
- Boosted
- Untagged

Category	Selection	Observables $\vec{x}$ for fitting
Boosted	$p_{\mathrm{T}}^{4\ell} > 120\,\mathrm{GeV}$	$\mathcal{D}_{\mathrm{bkg}}, p_{\mathrm{T}}^{4\ell}$
VBF-1jet	$\mathcal{D}_{1\mathrm{jet}}^{\mathrm{VBF}} > 0.7$	$\mathcal{D}_{\mathrm{bkg}}, p_{\mathrm{T}}^{4\ell}$
VBF-2jet	$\mathcal{D}_{2\mathrm{jet}}^{\mathrm{VBF}} > 0.5$	$\mathcal{D}_{\mathrm{bkg}}^{\mathrm{EW}}, \mathcal{D}_{0\mathrm{h}+}^{\mathrm{VBF+dec}}, \mathcal{D}_{0-}^{\mathrm{VBF+dec}}, \mathcal{D}_{\Lambda 1}^{\mathrm{VBF+dec}}, \mathcal{D}_{\Lambda 1}^{\mathrm{Z}\gamma,\mathrm{VBF+dec}}, \mathcal{D}_{\mathrm{int}}^{\mathrm{VBF}}, \mathcal{D}_{CP}^{\mathrm{VBF}}$
VH-hadronic	$\mathcal{D}_{2\mathrm{jet}}^{\mathrm{VH}} > 0.5$	$\mathcal{D}_{\mathrm{bkg}}^{\mathrm{EW}}, \mathcal{D}_{0\mathrm{h}+}^{\mathrm{VH+dec}}, \mathcal{D}_{0-}^{\mathrm{VH+dec}}, \mathcal{D}_{\Lambda 1}^{\mathrm{VH+dec}}, \mathcal{D}_{\Lambda 1}^{\mathrm{Z}\gamma,\mathrm{VH+dec}}, \mathcal{D}_{\mathrm{int}}^{\mathrm{VH}}, \mathcal{D}_{CP}^{\mathrm{VH}}$
VH-leptonic	see Section 3	$\mathcal{D}_{\mathrm{bkg}}, p_{\mathrm{T}}^{4\ell}$
Untagged	none of the above	$\mathcal{D}_{\mathrm{bkg}}, \mathcal{D}_{0\mathrm{h}+}^{\mathrm{dec}}, \mathcal{D}_{0-}^{\mathrm{dec}}, \mathcal{D}_{\Lambda 1}^{\mathrm{dec}}, \mathcal{D}_{\Lambda 1}^{\mathrm{Z}\gamma,\mathrm{dec}}, \mathcal{D}_{\mathrm{int}}^{\mathrm{dec}}, \mathcal{D}_{CP}^{\mathrm{dec}}$

Off-shell $2\ell 2\nu$: Event selection

Quantity	Requirement
p_{T}^{ℓ}	$p_{\mathrm{T}}^{\ell} \geq 25\,\mathrm{GeV}$ on both leptons
$\lvert\eta_{\ell}\rvert$	< 2.4 on μ, < 2.5 on e
$m_{\ell\ell}$	$\lvert m_{\ell\ell} - 91.2\rvert < 15\,\mathrm{GeV}$
$p_{\mathrm{T}}^{\ell\ell}$	$\geq 55\,\mathrm{GeV}$
N_{ℓ}	Exactly two leptons with tight isolation, no extra leptons with loose isolation and $p_{\mathrm{T}} \geq 5\,\mathrm{GeV}$
N_{trk}	No isolated tracks satisfying the selection requirements
N_{γ}	No photons with $p_{\mathrm{T}} \geq 20\,\mathrm{GeV}$, $\lvert\eta\rvert < 2.5$ satisfying the baseline selection requirements
p_{T}^{j}	$\geq 30\,\mathrm{GeV}$, used in selecting jets
$\lvert\eta_{j}\rvert$	< 4.7, used in selecting jets
N_{b}	No b-tagged jets based on the loose working point
$p_{\mathrm{T}}^{\mathrm{miss}}$	$\geq 125\,\mathrm{GeV}$ if $N_j < 2$, $\geq 140\,\mathrm{GeV}$ otherwise
$\Delta\phi_{\mathrm{miss}}^{\ell\ell}$	> 1.0 between $\vec{p}_{\mathrm{T}}^{\,\ell\ell}$ and $\vec{p}_{\mathrm{T}}^{\,\mathrm{miss}}$
$\Delta\phi_{\mathrm{miss}}^{\ell\ell+\mathrm{jets}}$	> 2.5 between $\vec{p}_{\mathrm{T}}^{\,\ell\ell} + \sum \vec{p}_{\mathrm{T}}^{\,\mathrm{j}}$ and $\vec{p}_{\mathrm{T}}^{\,\mathrm{miss}}$
$\min \Delta\phi_{\mathrm{miss}}^{\mathrm{j}}$	> 0.25 if $N_j = 1$, > 0.5 otherwise among all $\vec{p}_{\mathrm{T}}^{\,\mathrm{j}}$ and $\vec{p}_{\mathrm{T}}^{\,\mathrm{miss}}$ combinations

Requirements are mainly aimed toward reducing
- instrumental $p_{\mathrm{T}}^{\mathrm{miss}}$ smearing from Z+jets
- $t\bar{t} \rightarrow 2\ell 2\nu 2b$
- WW $\rightarrow 2\ell 2\nu$

Off-shell $2\ell 2\nu$: $q\bar{q} \to ZZ, WZ$

Quantity	Requirement
$p_{\mathrm{T}}^{\ell_{Z1}}$	$\geq 30\,\mathrm{GeV}$ on leading-p_{T} lepton forming the Z candidate
$p_{\mathrm{T}}^{\ell_{Z2}}$	$\geq 20\,\mathrm{GeV}$ on subleading-p_{T} lepton forming the Z candidate
$p_{\mathrm{T}}^{\ell_{\mathrm{W}}}$	$\geq 20\,\mathrm{GeV}$ on the remaining ℓ_{W} from the W boson
$\lvert\eta_\ell\rvert$	< 2.4 on μ, < 2.5 on e
$m_{\ell\ell}$	Use the opposite-sign, same-flavor dilepton pair with smallest $\lvert m_{\ell\ell} - 91.2\rvert < 15\,\mathrm{GeV}$ to define the Z candidate
N_ℓ	Exactly three leptons with tight isolation, no extra leptons with loose isolation and $p_{\mathrm{T}} \geq 5\,\mathrm{GeV}$
N_{trk}	No isolated tracks satisfying the selection requirements
N_γ	No photons with $p_{\mathrm{T}} \geq 20\,\mathrm{GeV}$, $\lvert\eta\rvert < 2.5$ satisfying the baseline selection requirements
p_{T}^{j}	$\geq 30\,\mathrm{GeV}$, used in selecting jets
$\lvert\eta_j\rvert$	< 4.7, used in selecting jets
N_b	No b-tagged jets based on the loose working point
$p_{\mathrm{T}}^{\mathrm{miss}}$	$\geq 20\,\mathrm{GeV}$
$m_{\mathrm{T}}^{\ell_{\mathrm{W}}}$	$\geq 20\,\mathrm{GeV}$ (10 GeV) for $\ell_{\mathrm{W}} = \mu$ ($\ell_{\mathrm{W}} = \mathrm{e}$), where $m_{\mathrm{T}}^{\ell_{\mathrm{W}}} = \sqrt{2 p_{\mathrm{T}}^{\ell_{\mathrm{W}}} p_{\mathrm{T}}^{\mathrm{miss}} \left(1 - \cos\Delta\phi_{\mathrm{miss}}^{\ell_{\mathrm{W}}}\right)}$ is the transverse mass between $\vec{p}_{\mathrm{T}}^{\,\ell_{\mathrm{W}}}$ and $\vec{p}_{\mathrm{T}}^{\,\mathrm{miss}}$
$\mathrm{A} \times m_{\mathrm{T}}^{\ell_{\mathrm{W}}} + p_{\mathrm{T}}^{\mathrm{miss}} \geq 120\,\mathrm{GeV}$, with A = 1.6 (4/3) for $\ell_{\mathrm{W}} = \mu$ (e)	
$\Delta\phi_{\mathrm{miss}}^{\mathrm{Z}}$	> 1.0 between $\vec{p}_{\mathrm{T}}^{\,\mathrm{Z}}$ and $\vec{p}_{\mathrm{T}}^{\,\mathrm{miss}}$
$\Delta\phi_{\mathrm{miss}}^{3\ell+\mathrm{jets}}$	> 2.5 between $\vec{p}_{\mathrm{T}}^{\,3\ell} + \sum \vec{p}_{\mathrm{T}}^{\,\mathrm{j}}$ and $\vec{p}_{\mathrm{T}}^{\,\mathrm{miss}}$
$\min \Delta\phi_{\mathrm{miss}}^{\mathrm{j}}$	> 0.25 among all $\vec{p}_{\mathrm{T}}^{\,\mathrm{j}}$ and $\vec{p}_{\mathrm{T}}^{\,\mathrm{miss}}$ combinations

Estimated using POWHEG simulation at NLO in QCD

→ Additional K-factors for NLO EW and NNLO QCD corrections are applied.

→ A joint fit with a 3ℓ WZ CR is done with common nuisance parameters and m_{T}^{WZ} as the only observable:

$$m_{\mathrm{T}}^{\mathrm{WZ}2} = \left[\sqrt{{p_{\mathrm{T}}^{\ell\ell}}^2 + {m_{\ell\ell}}^2} + \sqrt{\left|\vec{p}_{\mathrm{T}}^{\,\mathrm{miss}} + \vec{p}_{\mathrm{T}}^{\,\ell_{\mathrm{W}}}\right|^2 + {m_{\mathrm{W}}}^2}\right]^2 - \left|\vec{p}_{\mathrm{T}}^{\,\ell\ell} + \vec{p}_{\mathrm{T}}^{\,\ell_{\mathrm{W}}}\right|^2$$

→ Events in the CR are categorized for the same N_j bins, and $\ell_W = e, \mu$.

Off-shell $2\ell 2\nu$: Instrumental $p_{\mathrm{T}}^{\mathrm{miss}}$

Simulation cannot estimate instrumental $p_{\mathrm{T}}^{\mathrm{miss}}$ accurately.
Estimated from a single-photon CR instead:

→ Single, isolated photons from γ+jets are expected to have kinematics similar to Z+jets.

→ $\gamma \rightarrow Z$ transfer factors are extracted from $p_{\mathrm{T}}^{\mathrm{miss}} < 125$ GeV, enriched in γ/Z+jets.

→ Real-$p_{\mathrm{T}}^{\mathrm{miss}}$ contributions ($Z(\rightarrow \nu\nu)\gamma$, W+jets, $W\gamma$, and $t\gamma + X$) are subtracted afterward.

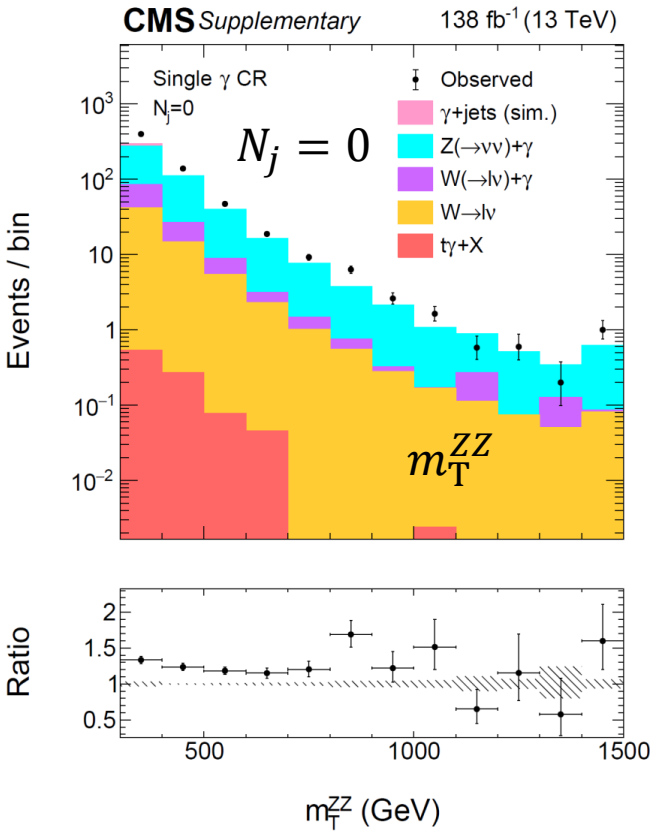

Distributions are reweighted with the $p_{\mathrm{T}}^{\mathrm{miss}} < 125$ GeV transfer factors.

We are estimating the size of the instrumental $p_{\mathrm{T}}^{\mathrm{miss}}$ contribution in data instead of what is shown from simulation in pink.

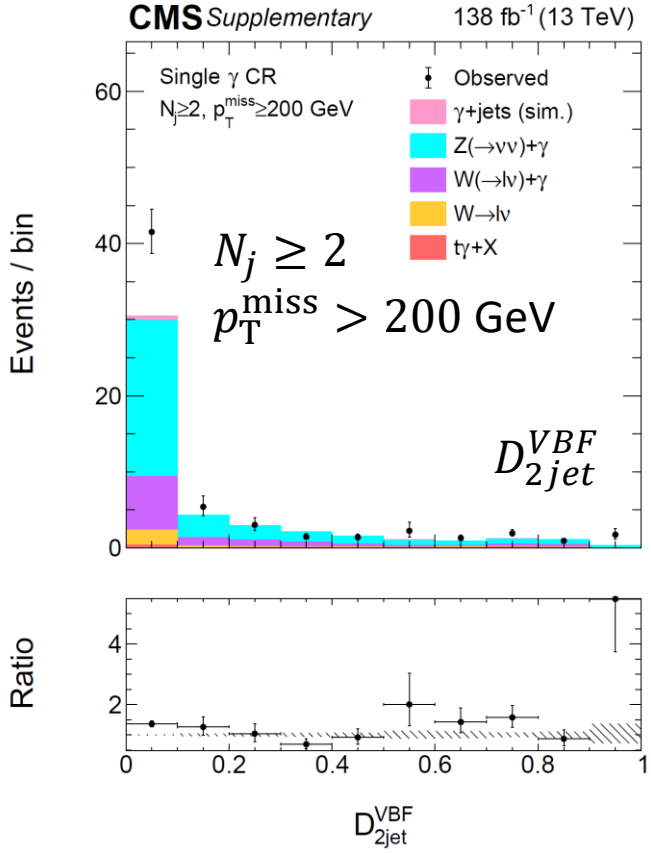

Off-shell $2\ell 2\nu$ observables: m_{T}^{ZZ}

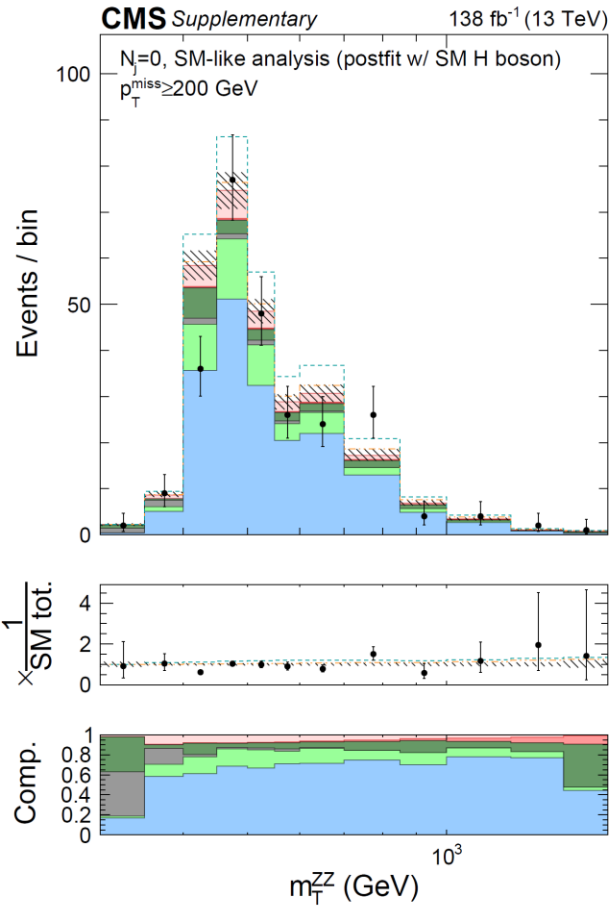

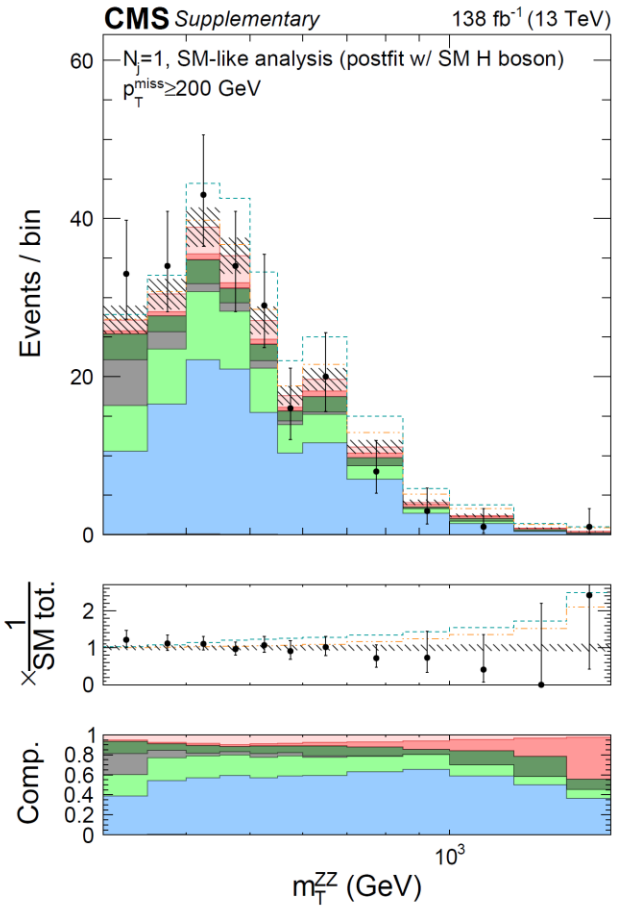

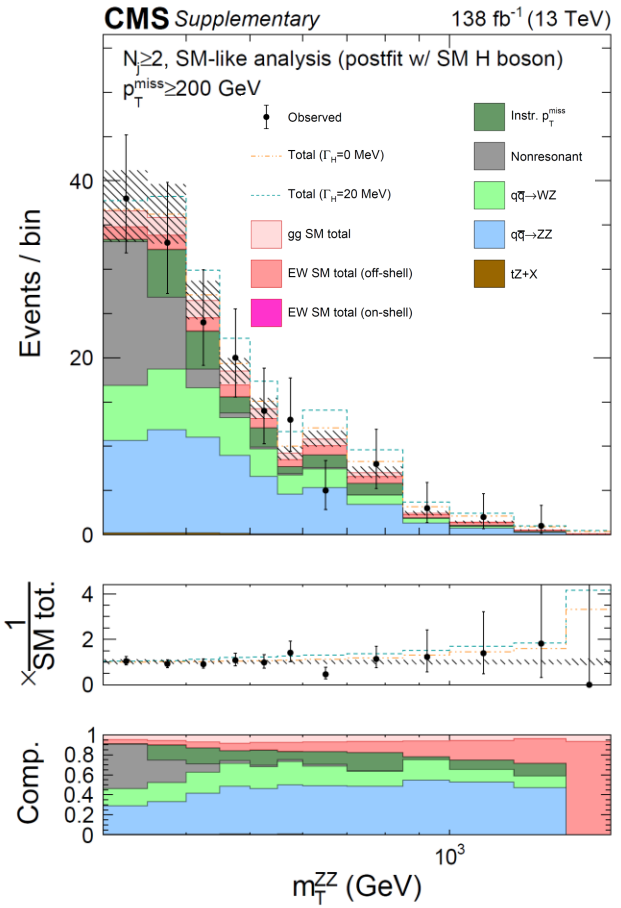

Off-shell $2\ell 2\nu$ observables: $p_{\mathrm{T}}^{\mathrm{miss}}$

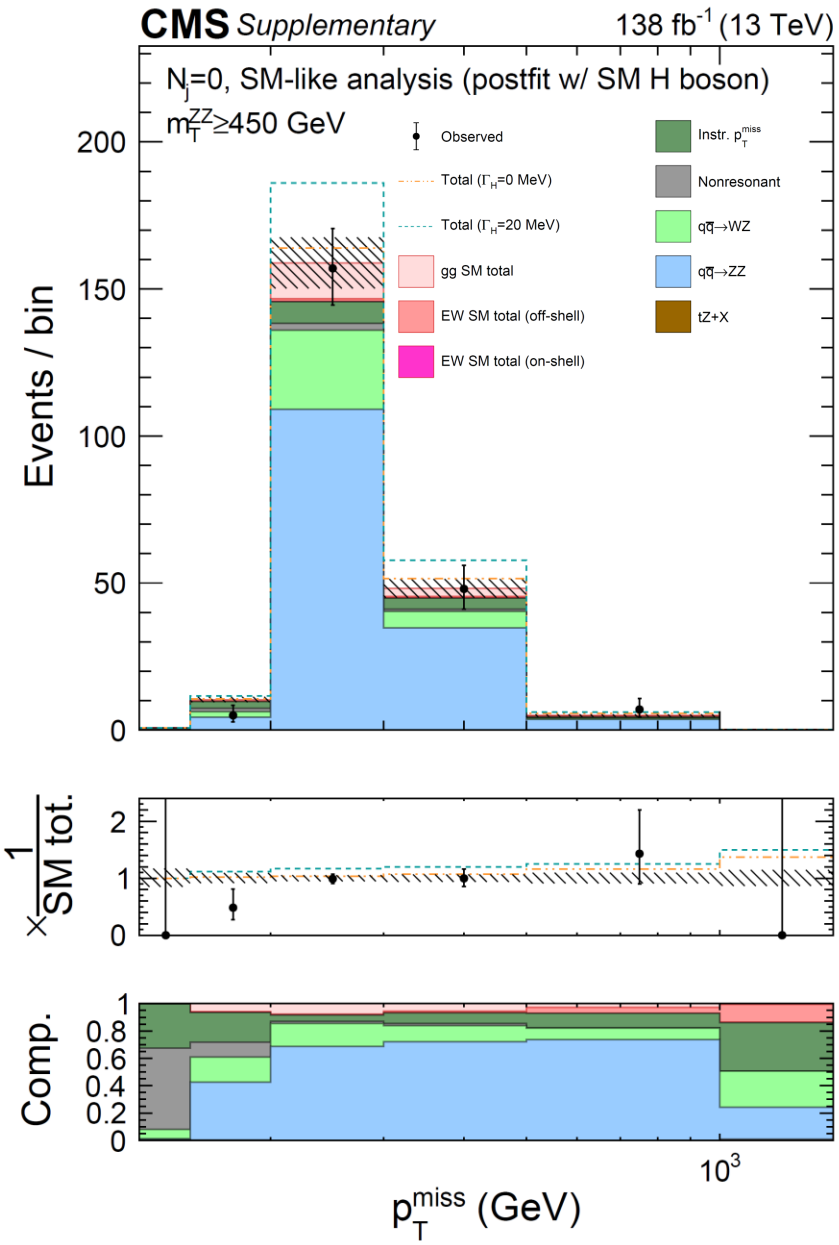

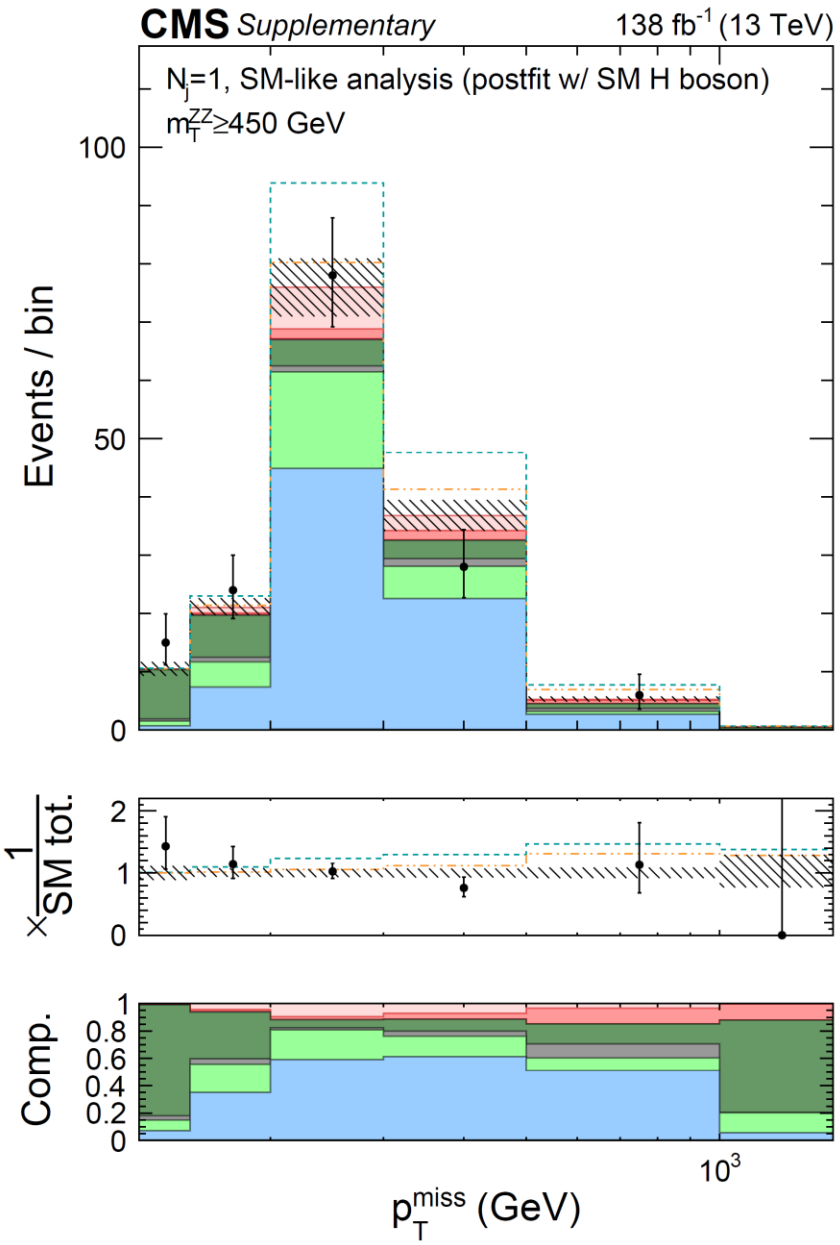

Off-shell $2\ell 2\nu$ observables: D_{2jet}^{VBF}

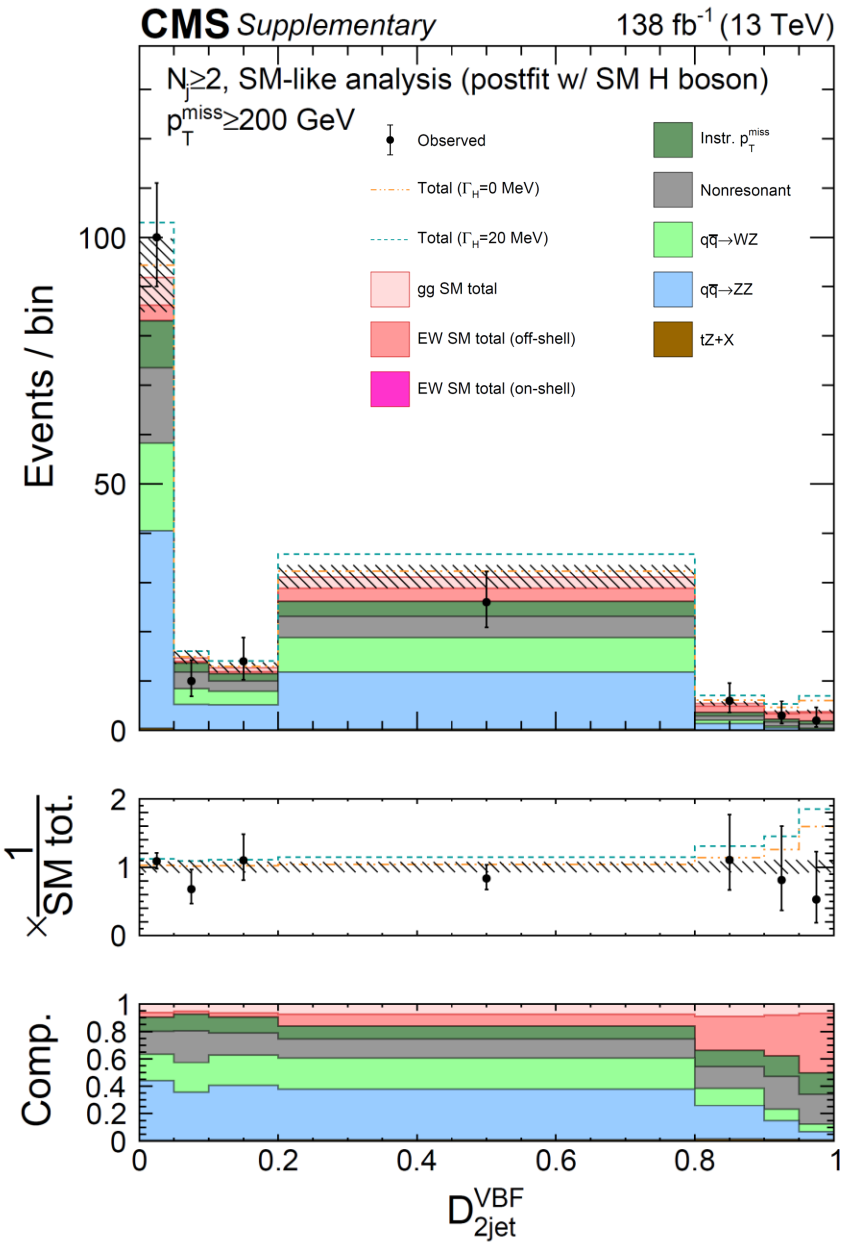

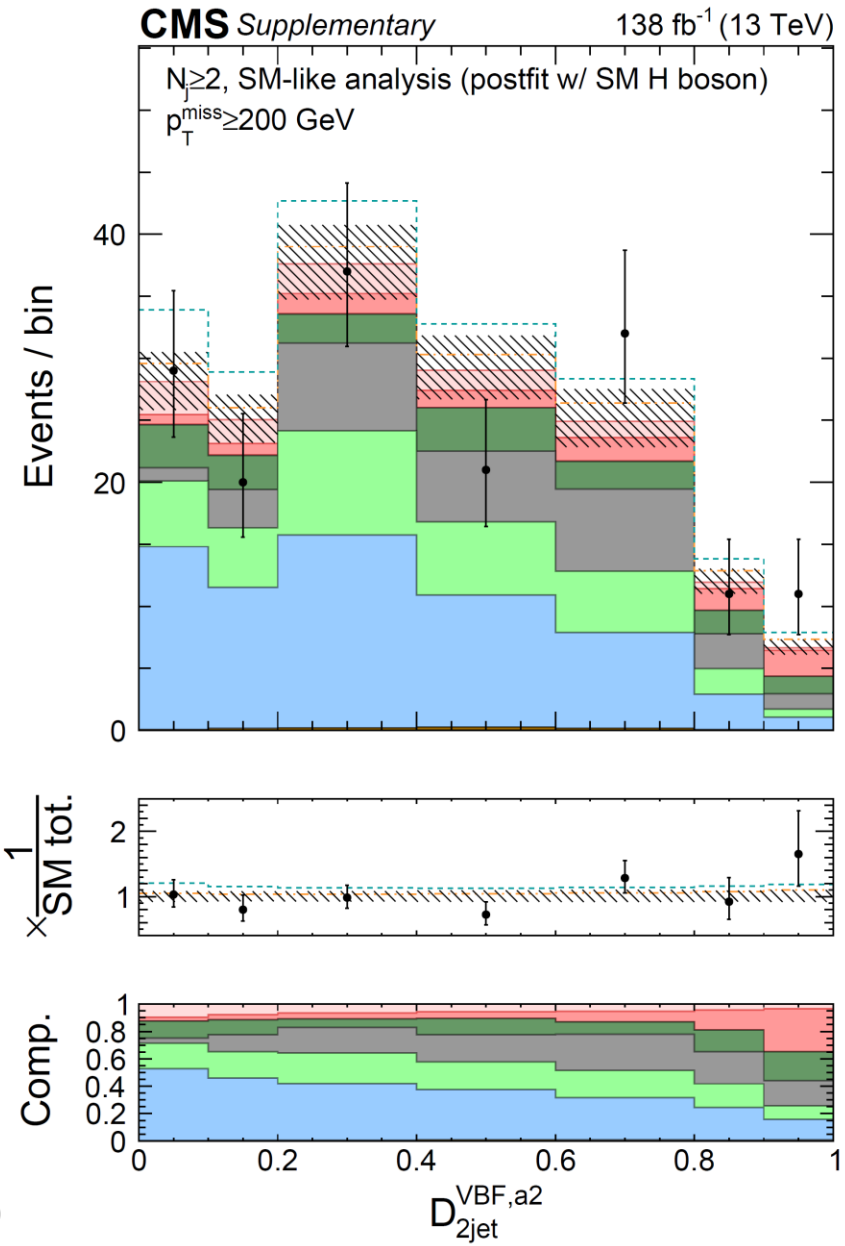

Off-shell combination: Summary

Param.	Cond.	Observed		Expected
		c.v.	68% | 95% CL	68% | 95% CL
$\mu_{\mathrm{F}}^{\mathrm{off.}}$	$\mu_{\mathrm{V}}^{\mathrm{off.}}$ (u)	0.62	$[0.17, 1.3] \mid [0.0060, 2.0]$	$[2 \cdot 10^{-5}, 2.1] \mid < 3.0$
$\mu_{\mathrm{V}}^{\mathrm{off.}}$	$\mu_{\mathrm{F}}^{\mathrm{off.}}$ (u)	0.90	$[0.31, 1.8] \mid [0.051, 2.9]$	$[0.11, 3.0] \mid < 4.5$
$\mu^{\mathrm{off.}}$	$R_{\mathrm{V,F}}^{\mathrm{off.}} = 1$	0.74	$[0.36, 1.3] \mid [0.13, 1.8]$	$[0.16, 2.0] \mid [0.0086, 2.7]$
	$R_{\mathrm{V,F}}^{\mathrm{off.}}$ (u)	0.62	$[0.17, 1.3] \mid [0.0061, 2.0]$	$[4 \cdot 10^{-5}, 2.1] \mid [1 \cdot 10^{-5}, 3.0]$
Γ_{H}	SM-like	3.2	$[1.5, 5.6] \mid [0.53, 8.5]$	$[0.62, 8.1] \mid [0.035, 11.3]$
Γ_{H}	f_{a2} (u)	3.4	$[1.6, 5.7] \mid [0.60, 8.4]$	$[0.52, 8.0] \mid [0.015, 11.3]$
Γ_{H}	f_{a3} (u)	2.7	$[1.3, 4.8] \mid [0.47, 7.3]$	$[0.53, 8.0] \mid [0.015, 11.3]$
Γ_{H}	$f_{\Lambda 1}$ (u)	2.7	$[1.3, 4.8] \mid [0.46, 7.2]$	$[0.55, 8.1] \mid [0.019, 11.3]$

On-shell $4\ell + \tau\tau\ [+t\bar{t}H(\rightarrow \gamma\gamma)]$

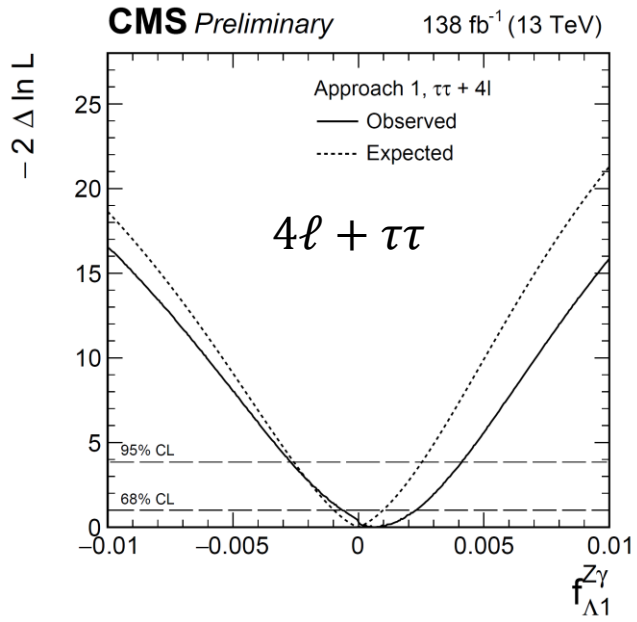

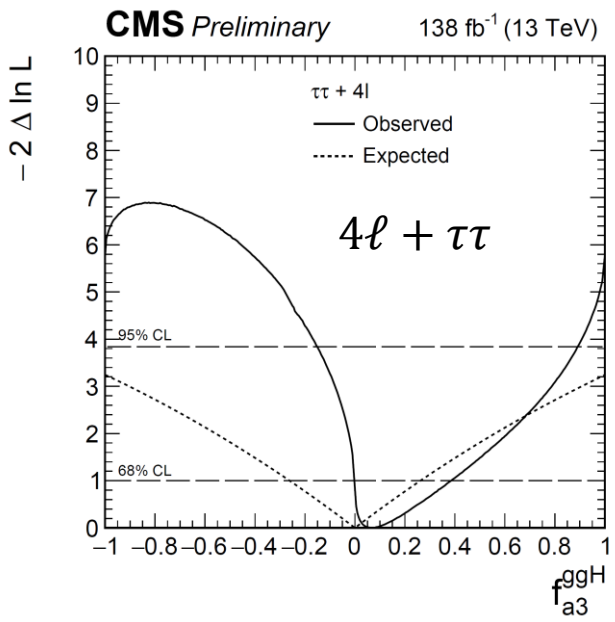

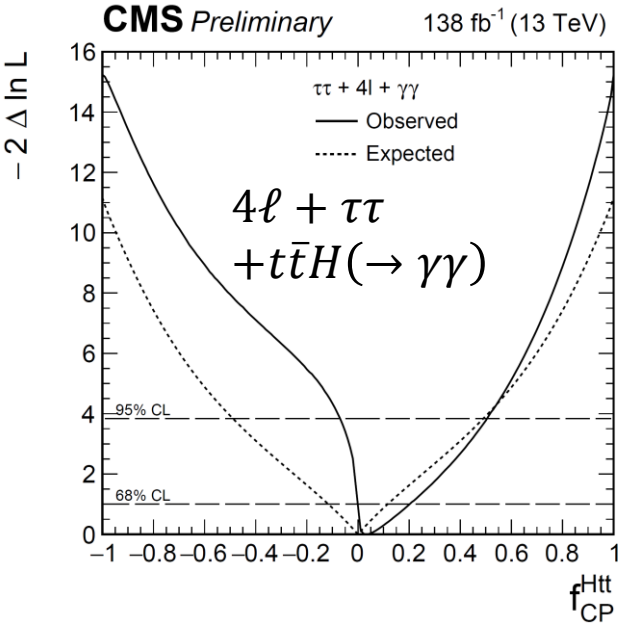

Parameter	Observed / (10^{-3})		Expected / (10^{-3})	
	68% CL	95% CL	68% CL	95% CL
$f_{\Lambda 1}^{Z\gamma}$	$0.7^{+1.6}_{-1.3}$	$[-2.7, 4.1]$	$0.0^{+1.0}_{-1.0}$	$[-2.6, 2.5]$

Parameter	Observed		Expected	
	68% CL	95% CL	68% CL	95% CL
f_{a3}^{ggH}	$0.07^{+0.32}_{-0.07}$	$[-0.15, 0.89]$	0.00 ± 0.26	-
f_{CP}^{Htt}	$0.03^{+0.17}_{-0.03}$	$[-0.07, 0.51]$	0.00 ± 0.12	$[-0.49, 0.49]$

Invisible Higgs decays: VBF $H \rightarrow$ invisible

CMS-PAS-HIG-20-003: Analysis of the $H \rightarrow$ invisible signature at high m_{jj} (VBF-like events)

→ Includes data from 2017 and 2018, and combines with the 2016 analysis

→ Events are categorized into the "missing momentum-triggered" (MTR, $> 90\%$ efficiency for $p_{\mathrm{T}}^{\mathrm{miss}} > 250$ GeV) and "VBF-jets triggered" (VTR, $> 85\%$ efficiency for $p_{\mathrm{T}}^{\mathrm{miss}} > 160$ GeV, $m_{jj} > 900$ GeV, $p_T^{j1(j2)} > 140\ (70)$ GeV) categories.

→ Fits are perfomed with m_{jj} as the observable.

→ Event selection requirements are as follows:

Observable	MTR	VTR
Choice of pair	leading-p_{T}	leading-M_{jj}
Leading (subleading) jet	$p_{\mathrm{T}} > 80\ (40)$ GeV, $\lvert\eta\rvert < 4.7$	$p_{\mathrm{T}} > 140\ (70)$ GeV, $\lvert\eta\rvert < 4.7$
$p_{\mathrm{T}}^{\mathrm{miss}}$	> 250 GeV	$160 < p_{\mathrm{T}}^{\mathrm{miss}} \leq 250$
$\min\Delta\phi(\vec{p}_{\mathrm{T}}^{\mathrm{miss}}, \vec{p}_{\mathrm{T}}^{\mathrm{jet}})$	> 0.5 rad	> 1.8 rad
$\lvert\Delta\phi_{\mathrm{jj}}\rvert$	< 1.5 rad	< 1.8 rad
M_{jj}	> 200 GeV	> 900 GeV
$\lvert p_{\mathrm{T}}^{\mathrm{miss}} - \mathrm{calo}p_{\mathrm{T}}^{\mathrm{miss}}\rvert / p_{\mathrm{T}}^{\mathrm{miss}}$	< 0.5	
Leading/subleading jets $\lvert\eta\rvert < 2.5$	NHEF < 0.8, CHEF > 0.1	
HF-noise jet candidates	0 (see Table 1)	
τ_{h} candidates	$\mathrm{N}_{\tau_{\mathrm{h}}} = 0$ with $p_{\mathrm{T}} > 20$ GeV, $\lvert\eta\rvert < 2.3$	
b quark jet	$\mathrm{N}_{\mathrm{jet}} = 0$ with $p_{\mathrm{T}} > 20$ GeV, DeepCSV Medium	
$\eta_{\mathrm{j1}} \times \eta_{\mathrm{j2}}$	< 0	
$\lvert\Delta\eta_{\mathrm{jj}}\rvert$	> 1	
Muons (electrons)	$\mathrm{N}_{\mu,\mathrm{e}} = 0$ with $p_{\mathrm{T}} > 10$ GeV, $\lvert\eta\rvert < 2.4\ (2.5)$	
Photons	$\mathrm{N}_{\gamma} = 0$ with $p_{\mathrm{T}} > 15$ GeV, $\lvert\eta\rvert < 2.5$	

⇒ calorimeter noise cleanup